Cir 319
AN/181

A Unified Framework for Collision Risk Modelling in Support of the ***Manual on Airspace Planning Methodology for the Determination of Separation Minima*** (Doc 9689)

Approved by the Secretary General and published under his authority

International Civil Aviation Organization

Cir 319
AN/181

A Unified Framework for Collision Risk Modelling in Support of the *Manual on Airspace Planning Methodology for the Determination of Separation Minima* (Doc 9689)

Approved by the Secretary General and published under his authority

International Civil Aviation Organization

Published in separate English, French, Russian and Spanish editions by
the INTERNATIONAL CIVIL AVIATION ORGANIZATION
999 University Street, Montréal, Quebec, Canada H3C 5H7

For ordering information and for a complete listing of sales agents
and booksellers, please go to the ICAO website at www.icao.int

ICAO Cir 319, *A Unified Framework for Collision Risk Modelling in Support of the* Manual on Airspace Planning Methodology for the Determination of Separation Minima *(Doc 9869)*
Order Number: CIR319
ISBN 978-92-9231-428-6

TABLE OF CONTENTS

Page

———————

ABSTRACT

1. This circular provides guidance to safety experts who have a background in probability and who want to acquire some expertise in the field of collision risk modelling applied to the determination of separation minima.

2. This circular contains a theoretical introduction to all the collision risk models (CRMs) used in the *Manual on Airspace Planning Methodology for the Determination of Separation Minima* (Doc 9689) and the *Manual on Implementation of a 300 m (1 000 ft) Vertical Separation Minimum Between FL 290 and FL 410 Inclusive* (Doc 9574) and also provides further applications.

3. To help the reader acquire a comprehensive understanding of all these CRMs, a unified derivation of these models, based on a general framework, is presented. It appears that all the CRMs in ICAO guidance material can be derived from the same fundamental equation, known as the Rice Formula, so that the main differences between the different models lie in the assumptions and approximations made for each of them. Understanding the assumptions and the simplifying approximations made in deriving a collision risk model is essential in order to assess whether the model is applicable to the airspace that one intends to study.

4. An important criterion for a model to be applicable is its conservativeness; the application of collision risk models in safety assessment must be conservative. For example, when the risk estimate is compared with a threshold, the objective of the safety assessment is to ensure, with a specified level of confidence, that the actual risk is below the threshold. Therefore, it is essential, when applying a collision risk model, to check that the assumptions and approximations made in the modelling do not lead to an underestimation of the risk. In this circular particular attention has been paid to this point by clearly introducing all the assumptions and approximations made in the derivation of the different models.

5. It is foreseen that in the future ICAO will publish real examples from States or Organizations where the use of the general framework outlined herein was adjusted in order to apply the generic design to particular operational environments. These examples will give users additional perspectives and solutions to particular problems found by other stakeholders using collision risk modelling.

Chapter 1

INTRODUCTION

1.1 The collision risk models (CRMs) covered in this circular are those presented in the *Manual on Airspace Planning Methodology for the Determination of Separation Minima* (Doc 9689) and the *Manual on Implementation of a 300 m (1 000 ft) Vertical Separation Minimum Between FL 290 and FL 410 Inclusive* (Doc 9574). This circular introduces a unified framework which enables an analytical derivation of all these collision risk models. The reason why it is possible to derive them under the same framework is that these CRMs share similar modelling assumptions.

1.2 Chapter 2 introduces the appropriate nomenclature. Chapter 3 reviews the modelling of the uncertainty associated with aircraft location and examines some extensions to current CRMs. It appears that, from a controller's viewpoint, the modelling of uncertainties described in Chapter 3 is inadequate in environments with a high update rate of aircraft positions. Actually, all CRMs presented in Docs 9689 and 9574 apply to environments with a low update rate. Possible methods for modelling uncertainties in environments with a high update rate are suggested in Chapter 3, 3.6.

1.3 Chapter 4 introduces a key formula, called the Rice Formula, which plays a major part in the derivation of CRMs. Derivation of CRMs using the Rice Formula is presented in Chapters 5 to 7.

1.4 Chapters 8 and 9 present a generic CRM which applies to any operational scenario involving a pair of aircraft, either for same/opposite directions (Chapter 8) or for crossing routes (Chapter 9). Since this CRM is particularly interesting for the risk assessment of predetermined operational hazards, it is presented in a more general form first, followed by an important application of this CRM in an ADS-C environment.

1.5 Finally, Chapter 10 provides a list of recommended reading and reference material.

———————————

Chapter 2

BACKGROUND

2.1 CONSERVATIVE RISK ASSESSMENT

2.1.1 As specified in Doc 9689, Chapters 5 and 6, when a safety assessment is performed on a proposed system's separation minimum, there are two basic methods for determining whether the system is acceptably safe:

a) comparison with a reference system; or

b) evaluation of the system risk against a threshold.

2.1.2 The comparison methodology is applied if the reference system is proven to be safe (historically or theoretically) and if the assessed system is very similar to the reference in the risk-related aspects. Collision risk modelling is one possible tool for comparing the reference system versus the assessed one, but it is not the only one. One example of a comparison study which does not rely on collision risk modelling is the radar comparison in Doc 9689, Appendix 6.

2.1.3 The threshold in the second method is usually referred to as the target level of safety (TLS) and is expressed in terms of the expected number of fatal accidents per aircraft flying hour. This is the usual metric for societal risk, which is defined as the "average risk, in terms of fatalities, of groups of people (e.g. airport employees, crew or even society at large) exposed to an accident scenario". By using this metric it is possible to compare the risk between different activities (e.g. road transportation versus air transportation).

2.1.4 In order to ensure with a predetermined level of confidence that the real risk is below the TLS, it is necessary that each of the calculation steps in a risk assessment lead to an exact or conservative value.

2.2 FEATURES COMMON TO THE CRMS USED IN ICAO DOCUMENTATION

2.2.1 The purpose of collision risk models in the context of the determination of separation minima is to model the chain of events leading a pair of initially separated aircraft to a collision. The causation may or may not involve the responsibility of the air traffic controller, depending on whether the surveillance enables the controller to detect the loss of separation and possibly prevent the collision. These two configurations share common features.

2.2.2 The first configuration occurs when the surveillance does not provide the air traffic controller with any means to detect the loss of separation and prevent the collision. In the lateral dimension, an example is a pair of aircraft on parallel routes, laterally separated. If the airspace uses procedural separation and if an aircraft starts to laterally deviate due to, for instance, a waypoint insertion error, the air traffic controller has no means to detect the deviation and, in the worst case, prevent a collision. Similarly, in the vertical dimension, a significant error in the altimetry system of an aircraft may result in the aircraft flying at an incorrect flight level and, if under procedural separation, this deviation would also go uncorrected. For all situations where the controller has no means to detect and prevent the loss of separation, the risk of collision is modelled according to the following assumptions:

a) Deviations of aircraft from their assigned routes/flight levels are modelled by probability density functions in the lateral and vertical dimensions.

b) For an individual aircraft, deviations in the lateral and vertical dimensions are assumed to be independent.

c) In the lateral and vertical dimensions, aircraft are assumed to have been flying long enough along their routes so that the probability density function of the lateral and vertical deviations are stationary, i.e. independent of time.

d) As a consequence of c), the modelling of scenarios of atypical errors (such as waypoint insertion errors in lateral risk) may be done by adding a "tail" component to the probability distribution of the deviation in the corresponding dimension.

Points c) and d) will be developed in further detail in Chapter 3.

2.2.3 The second configuration occurs when surveillance regularly informs air traffic controllers of aircraft position so that they can detect a loss of separation and possibly prevent a collision. ADS-C surveillance provides an example of this for lateral and longitudinal separation in procedural airspace. The features common to the CRMs for this configuration are:

a) Deviations of aircraft from their assigned routes/flight levels are modelled by probability density functions in the lateral and vertical dimensions.

b) For an individual aircraft, deviations in the lateral and vertical dimensions are assumed to be independent.

c) Position reports provided by surveillance show that a pair of aircraft is separated and that, on the basis of the extrapolated positions from the initial speeds, the pair will remain separated in the future, at least until the next position update.

d) However, in the course of time, navigational deviations (in terms of position and speed)**,** communication delays or surveillance errors may lead the pair of aircraft to lose separation, possibly leading to a collision, in spite of ATC surveillance.

e) At the next position update, the air traffic controller detects the loss of separation but may not have enough time to prevent a collision.

For this second configuration, an implicit assumption is that the update period for position reporting is sufficiently long to allow the two aircraft to lose their separation until they eventually collide.

2.2.4 When the position update rate is high and contradicts this implicit assumption (as in radar surveillance), it is necessary to refine the chain of causation leading an air traffic controller to miss a loss of separation that is visible on a display. This requires, for instance, inclusion in the modelling of potential misunderstandings between pilots and controllers or heavy controller workload. This is discussed further in Chapter 3, 3.6.

2.3 ROUTE NETWORKS

The most convenient way to describe route networks is to assume that they are made up of linear segments organized into a variety of track geometries. These geometries generally simplify to the following scenarios:

a) aircraft on two parallel tracks separated by a distance S_y. The distance S_y is usually referred to as the lateral separation minimum (standard) between the tracks. The direction of the traffic may be the same or opposite;

b) aircraft on multiple (near-) parallel tracks as in the North Atlantic Organized Track System. Again, the aircraft may be flying in the same or opposite direction;

c) aircraft flying in the same direction on the same flight level of the same track;

d) aircraft on different flight levels of the same track, flying in the same or opposite direction;

e) aircraft flying on the same flight level of intersecting tracks;

f) aircraft flying on different flight levels of intersecting tracks.

2.4 REPRESENTATION OF AIRCRAFT

2.4.1 It would be impossible to model a collision between aircraft using complex aircraft shapes and collision geometries. Complex aircraft shapes therefore are modelled by simpler shapes like boxes or cylinders enveloping the real shapes as in Figure 2-1. The choice between a box or a cylinder is optional, in principle, but any subsequent calculations are greatly simplified if the box is used for parallel tracks and aircraft on the same track, and the cylinder for aircraft on intersecting tracks. A collision between two aircraft corresponds to an intersection of the corresponding volumes.

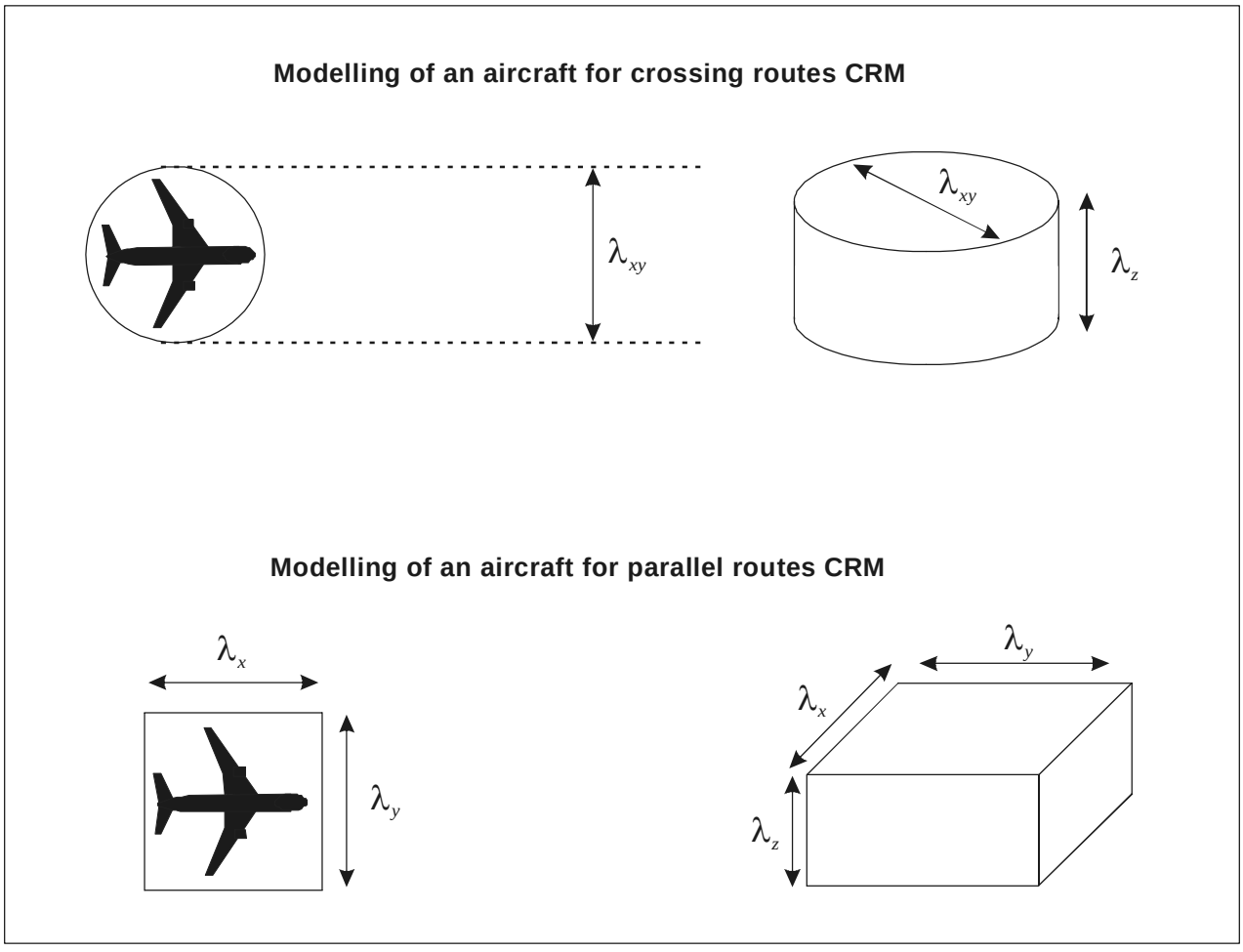

Figure 2-1. Modelling of aircraft shapes

2.4.2 Modelling a collision in terms of the intersection of volumes has an equivalent representation if a double-size volume is associated to one of the aircraft and a "zero-size" volume to the other aircraft. This is illustrated in Figure 2-2 (for crossing routes) and in Figure 2-3 (for parallel routes), where aircraft A_1 has a double-size volume and aircraft A_2 is reduced to a point. For this equivalent representation, a collision can be seen as a particle entering a given volume. This representation will be the one used for the different collision risk models. The previous modelling can be easily extended to different aircraft sizes, where one aircraft would have a "sum-of-aircraft size" volume and the other aircraft would have a "zero-size" volume.

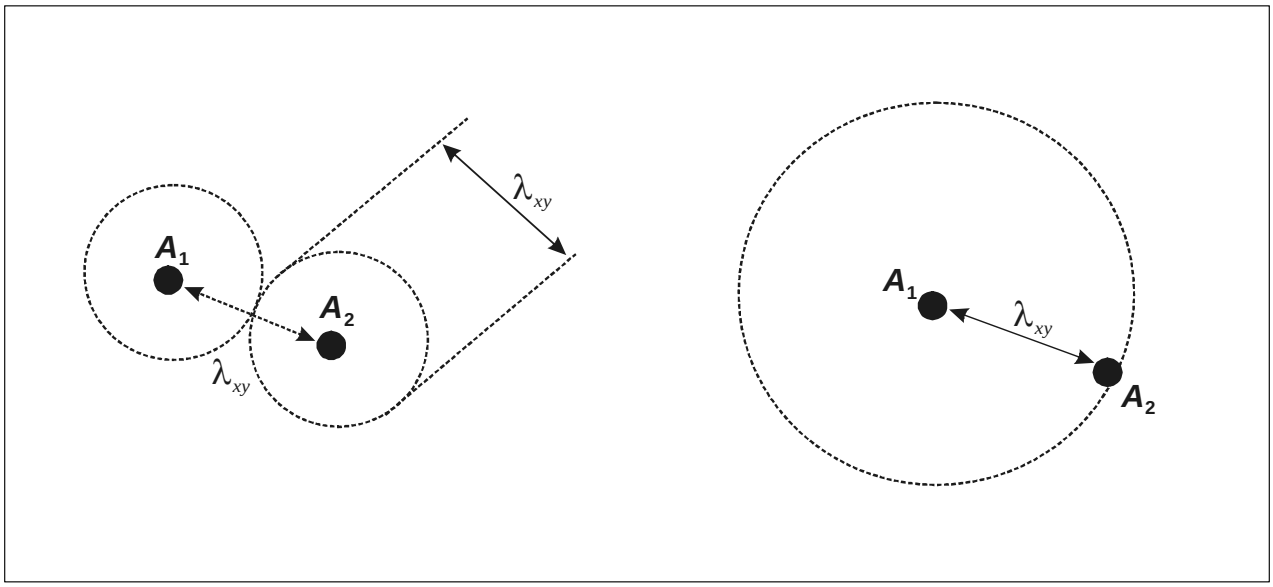

Figure 2-2. Modelling a collision in terms of the intersection of volumes for crossing routes

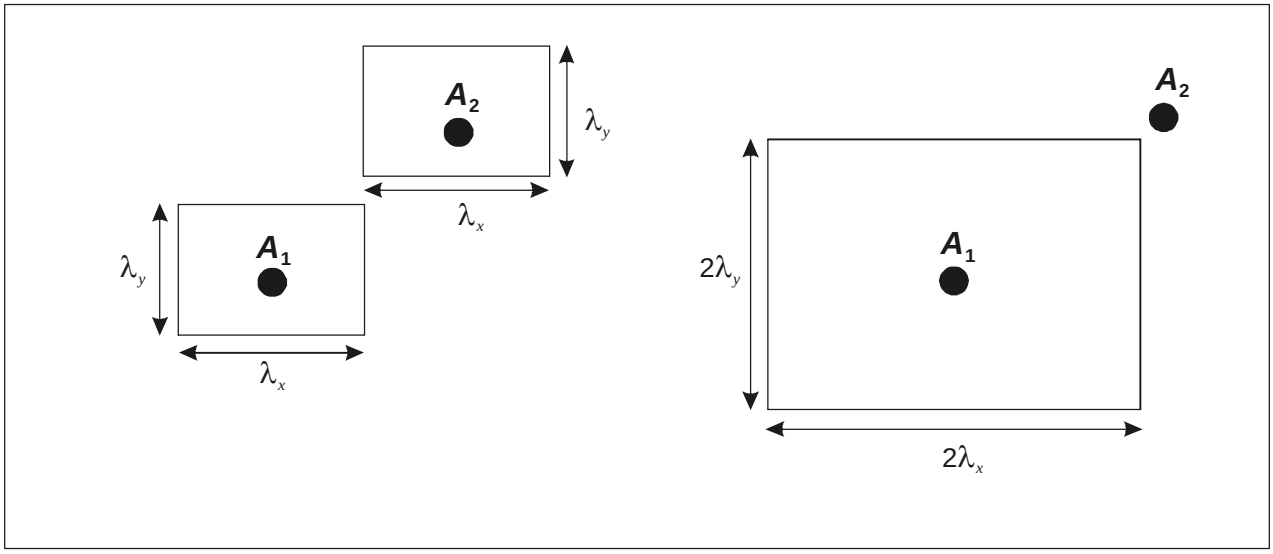

Figure 2-3. Modelling a collision in terms of the intersection of volumes for parallel routes

2.5 SEPARATION CRITERIA

2.5.1 The unit for a separation minimum (standard) is either a time duration (usually in minutes) or a distance (in NM for the horizontal and in feet for the vertical).

2.5.2 Separation minima expressed in units of time usually apply to procedural airspace, where aircraft are required to report when they arrive at predetermined spatial locations. The air traffic controller must ensure that the temporal separation Δt between two co-altitude aircraft arriving at the same spatial location is greater than or equal to a predetermined separation minimum, i.e. $\Delta t \geq S_{time\text{–}\min}$.

2.5.3 Separation minima expressed in units of distance are either vertical or horizontal. For distance-based separation, aircraft positions may be displayed at regular time intervals on the controller's screen. These positions are either sent by the aircraft (as in ADS-C or ADS-B) or measured by ground equipment (as in radar surveillance). The air traffic controller must ensure that at all times, and for all pairs of aircraft, either the horizontal or the vertical separation is greater than the corresponding separation minima.

———————

Chapter 3

MODELLING OF THE UNCERTAINTY ASSOCIATED WITH AIRCRAFT LOCATION

3.1 INTRODUCTION

3.1.1 "Uncertainty associated with aircraft location" is the difference between the actual aircraft location and the location where an air traffic controller believes the aircraft to be.

3.1.2 As seen in Chapter 2, 2.4, a collision between aircraft can be seen as one "zero volume" aircraft entering a "double volume" centred on the other aircraft. A collision has occurred if both aircraft are inside the double-size cylinder in Chapter 2, Figure 2-2, or the double-size box in Figure 2-3.

3.1.3 The relative position of one aircraft with respect to the other is represented by X or the triple (x, y, z). For aircraft moving in the same or opposite direction, x denotes the relative position of the aircraft in the longitudinal dimension, and y, z are the relative positions in the lateral and vertical dimensions.

3.1.4 For two aircraft on crossing routes, (x, y) denotes the relative position in the horizontal plane, and z denotes the relative position in the vertical dimension. Relative velocity is represented by putting a dot over a relative position. For example, $\dot{z}$ represents the relative vertical velocity and $(\dot{x}, \dot{y})$ represents the relative horizontal velocities for a crossing-routes case. In what follows, a velocity component will often be referred to as a speed when the context is clear. It is understood then that the speed could be negative. Finally, when a symbol depends on time, an index t will be added to it. This convention also applies to density functions. The possible time-dependence of position and speed deviations is discussed in 3.2.

3.2 STATIONARY AND NON-STATIONARY CASES

3.2.1 Figure 3-1 represents a set of individual aircraft trajectories on a given route. Assuming that the aircraft have been flying sufficiently long on the route to have reached a kind of "steady state", it can be concluded that the density function of the lateral deviations from the assigned route at a given time, t, $f_t(y)$, is the same for all t. In that case, $f_t(y)$ no longer depends on t, so that the t index can be dropped. The density is said to be stationary if it is independent of t. Strictly speaking, it is the underlying stochastic process which is stationary.

3.2.2 By contrast, consider an aircraft that is assumed to be flying at some indicated constant speed or Mach number on a route. If this indicated speed is subject to some small uncertainty or technical tolerance, this will induce a position error for the aircraft $\Delta x = t\ (v_{indicated} - v_{actual})$, where t is the flying time of the aircraft since its last position report (see Figure 3-2). In that case the longitudinal deviation increases linearly with time. Therefore the associated density is not stationary.

3.2.3 This concludes the introduction to the modelling of the evolution of aircraft deviations in the course of time. Discussion will now focus on the modelling of deviations when they are assumed to be independent of time. This applies essentially in the lateral and vertical dimensions.

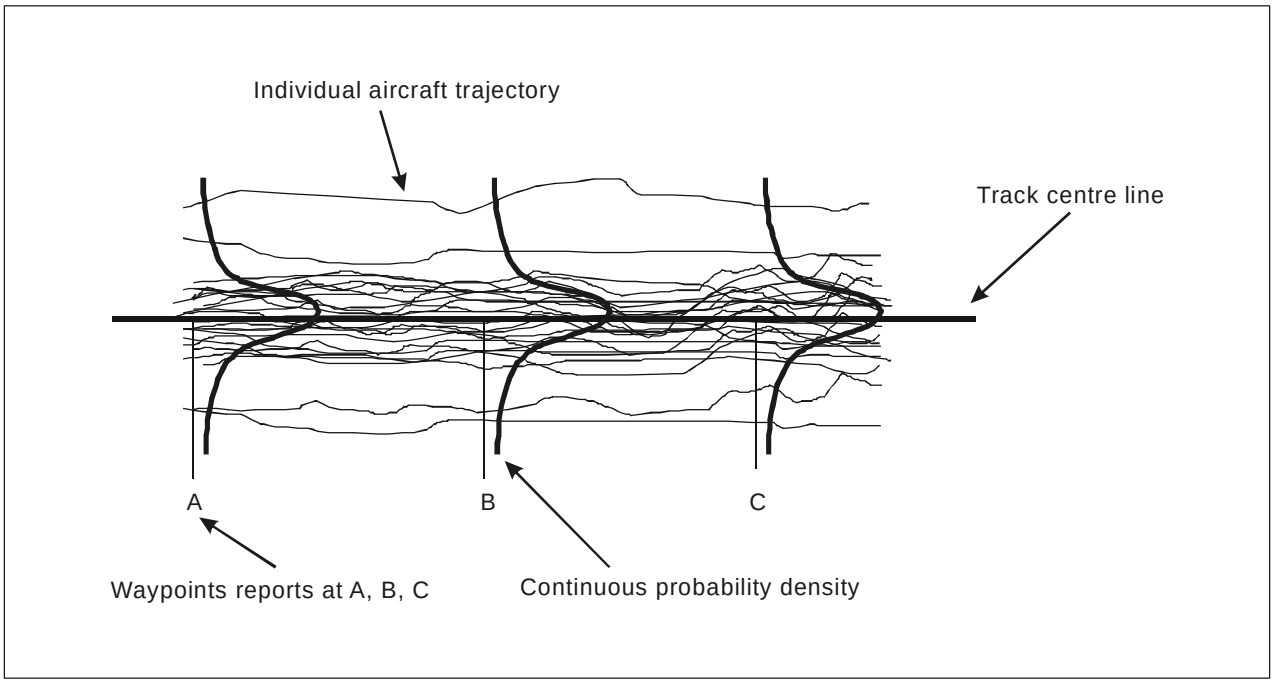

Figure 3-1. A set of individual aircraft trajectories on a given route

3.3 APPLICATION OF EXTREME VALUE THEORY TO THE MODELLING OF ATYPICAL LARGE DEVIATIONS

3.3.1 In current ICAO documentation, the modelling of large deviations does not rely on extreme value theory, but rather on various empirical considerations. However, extreme value theory provides a rigorous frame for the justification of this empirical modelling, which is why some key results from extreme value theory will be introduced before discussing how atypical deviations are currently modelled in ICAO documentation.

3.3.2 First two key results will be introduced and then it will be shown how these results enable, in practice, the modelling of the tail distribution from a collected data sample $X_1, X_2, \ldots, X_n$ of aircraft deviations, assumed to be independent and identically distributed.

3.3.3 Consideration is given to n independent random variables $X_1, X_2, \ldots, X_n$, with distribution F. M_n denotes the maximum of $X_1, X_2, \ldots, X_n$. Distribution F is said to be extremal if it is possible to find two sequences a_n and b_n such that the affine transformed maximum $\frac{M_n - b_n}{a_n}$ converges in distribution towards a distribution G. This is equivalent to saying that $\lim_{n\to\infty} F^n\left(a_n x + b_n\right) = G\left(x\right)$ for all x. If this is the case, then G is defined up to a certain scaling and shifting factor. This means that if it is possible to find two sequences a_n and b_n such that $F^n\left(a_n x + b_n\right)$ converges to $G(x)$, and two other sequences c_n and d_n such that $F^n\left(c_n x + d_n\right)$ converges to another function $H(x)$, then there exists scaling and shifting constants α and β such that $G\left(x\right) = H\left(\alpha x + \beta\right)$ (see Chapter 10, Reference 4, Theorem 14.2). The first fundamental result from extreme value theory (the so-called Fischer-Tippet Theorem, see Chapter 10, Reference 4, Theorem 14.3) is that, if F is extremal, there are only three possible choices for the kind of limit distribution $G(x)$ (up to the scaling and shifting factors previously mentioned):

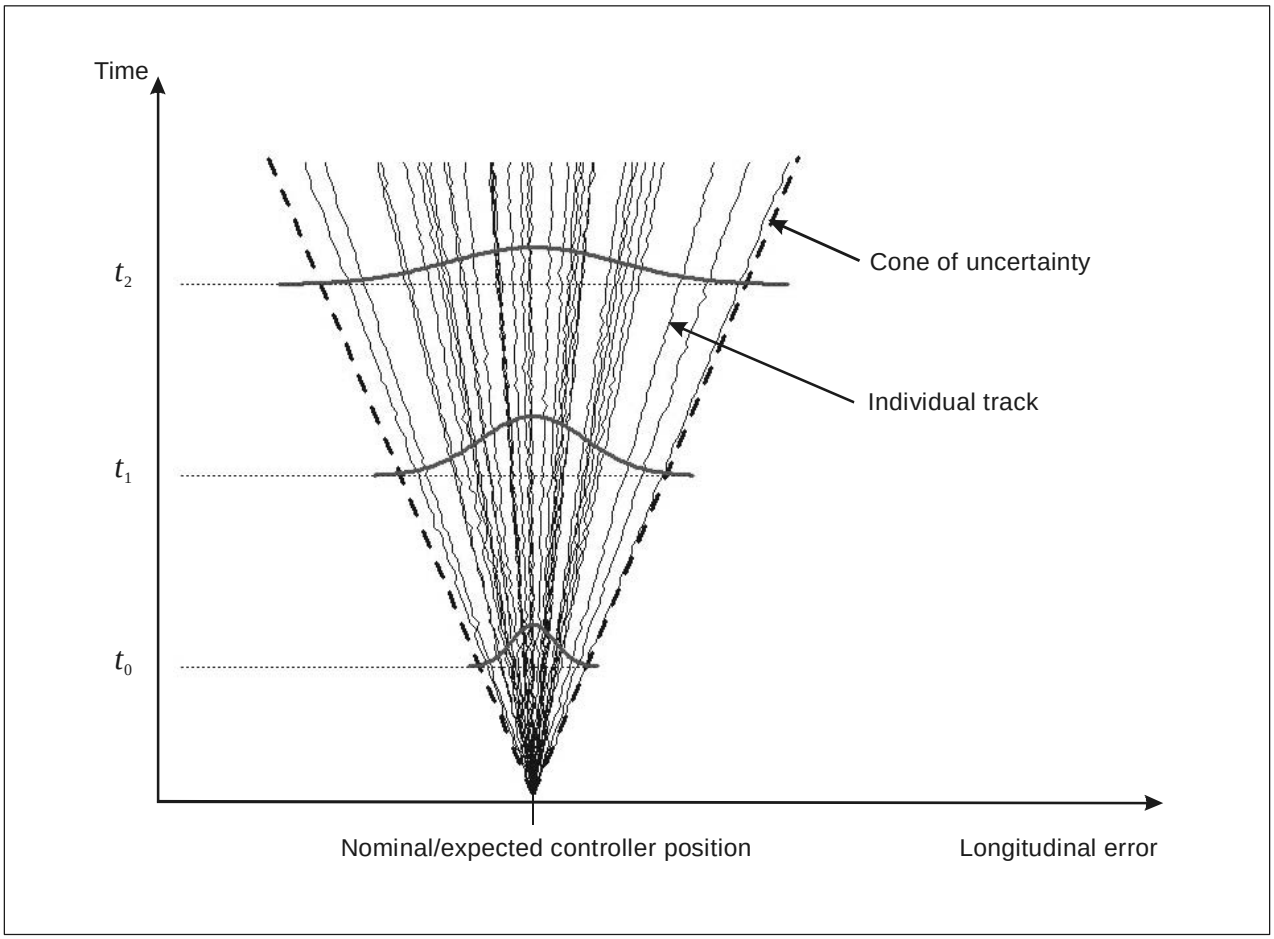

Figure 3-2. Longitudinal deviation and time

Frechet: $\Phi_\alpha(x) = \begin{cases} 0, & x \le 0 \\ \exp(-x^{-\alpha}), & x > 0 \end{cases} \qquad \alpha > 0.$

Weibull: $\Psi_\alpha(x) = \begin{cases} \exp(-(-x)^{\alpha}), & x \le 0 \\ 1, & x > 0 \end{cases} \qquad \alpha > 0.$

Gumbel: $\Lambda(x) = \exp(-e^{-x})$.

3.3.4 The three families of distributions above are gathered into one, namely H_ξ, defined by:

$$H_\xi = \begin{cases} \Phi_{1/\xi} & \text{if } \xi > 0 \\ \Lambda & \text{if } \xi = 0 \\ \Psi_{-1/\xi} & \text{if } \xi < 0. \end{cases}$$

3.3.5 Another formulation for extremal distributions is to say that F is attracted by G, where G is any of the Frechet, the Weibull or the Gumbel distributions. $MDA(H_\xi)$ (maximum domain of attraction) denotes the class of all distributions F which are attracted by the distribution (H_ξ). A criterion for checking if a given distribution F belongs to $MDA(H_\xi)$ is provided by the so-called von Mises conditions (see subsection 3.3 of Chapter 10, Reference 6). It turns out that all families of distributions fall within the maximum domain of attraction of one of the three limit distributions in 3.3.3.

3.3.6 This first fundamental result has been mentioned in order to introduce the key concept of MDA. Now, if a given distribution F is known to belong to $MDA(H_\xi)$, it is possible to approximate the tail distribution of F by using a generalized pareto distribution (GPD). This is the second fundamental result that will now be explained.

3.3.7 Generalized pareto distribution (GPD) (G_ξ) is defined by:

$$G_\xi(x) = \begin{cases} 1-(1+\xi x)^{-1/\xi}, & \text{if } \xi \neq 0 \\ 1-\exp(-x), & \text{if } \xi = 0. \end{cases} \tag{3-1}$$

If ξ is positive, then $G_\xi(x)$ is defined for positive x. If ξ is negative, then $G_\xi(x)$ is defined for $0 \leq x \leq -1/\xi$. Similarly, the scaled GPD, $G_{\xi;\beta}(x)$, is defined by replacing the argument x above by x/β. The support has to be adjusted accordingly. If X is a random variable with distribution F, then for a fixed positive threshold, u, the excess distribution over the threshold u, F_u, is defined as:

$$F_u(x) = \Pr\{X - u \leq x | X > u\}.$$

3.3.8 Then the second fundamental result (see Theorem 3.4.13 in Chapter 10, Reference 6) claims that, if F belongs to $MDA(H_\xi)$, then for sufficiently large positive values of u, $F_u(x)$ can be approximated by a scaled GPD $G_{\xi;\beta(u)}(x)$, where $\beta(u)$ is a positive function of u.

3.3.9 In practice, this result is used as follows. Given a collected data sample $X_1, X_2, \ldots, X_n$ of independent random variables with distribution F, extreme value theory provides several methods for estimating the three unknown parameters:

a) the value of the threshold $\hat{u}$;

b) the shape parameters $\hat{\xi}$ for which F belongs to $MDA(H_{\hat{\xi}})$, and the scaling parameter $\hat{\beta}$, which provide the best approximation $F_{\hat{u}}(x) \approx G_{\hat{\xi};\hat{\beta}}(x)$ for $x \geq \hat{u}$.

3.3.10 Once $\hat{\xi}$, $\hat{u}$ and $\hat{\beta}$ have been estimated, from the equality $F_u(x) = F(u + x)/(1 - F(u))$ one obtains:

$$\begin{aligned} 1-F(x) &\approx (1-F(\hat{u}))\left(1-G_{\hat{\xi};\hat{\beta}}(x-\hat{u})\right) \\ &\approx \frac{k}{n}\left(1-G_{\hat{\xi};\hat{\beta}}(x-\hat{u})\right) \end{aligned} \quad \text{for } x \geq \hat{u} \tag{3-2}$$

where k is the number of items greater than $\hat{u}$ in the collected data sample $X_1, X_2, \ldots, X_n$.

3.3.11 The modelling of the tail distribution of Equation (3-2) is illustrated using a data sample of 500 000 randomly simulated normal variables with mean zero and standard deviation 1, where only the positive values (around 250 000) have been retained. Figure 3-3 shows the diagram $\Pr\{X > x\}$ as a function of x, where the vertical axis is in logarithmic scale. Extreme value theory claims (see Equation (3.40) of Chapter 10, Reference 6) that normal distributions belong to $MDA(H_0)$, so that the shape parameter $\hat{\xi}$ should be close to zero. For $\xi = 0$, Equations (3-1) and (3-2) show that the tail distribution $1 - F(x)$ is approximated by $\frac{k}{n}\exp(\frac{x-\hat{u}}{\hat{\beta}})$, which should appear in Figure 3-3 as a

straight line, due to the logarithmic scale. For a threshold value $\hat{u} = 3.2$, the parameters $\hat{\xi} = -0.089$ and $\hat{\beta} = 0.31$ have been estimated by applying a maximum likelihood technique, and the approximated tail distribution is shown in the left diagram of Figure 3-3. Also added, as a dashed line, is the straight line which corresponds to the "theoretical" case $\hat{\xi} = 0$.

3.3.12 To help the reader appreciate the effect of the shape parameter ξ on the modelling of the tail distribution, represented on the right diagram of Figure 3-3 is a GPD tail distribution for the three different values $\xi = -0.2$, $\xi = 0$ and $\xi = 0.2$.

3.3.13 In current ICAO documentation, the use of an exponential distribution for the modelling of distribution tails is often seen, without justification. In this section it can be seen that this choice is justified for all distributions which belong to $MDA(H_0)$; Chapter 10, Reference 6 gives numerous examples of distributions in $MDA(H_0)$, such as:

a) the normal and the log-normal distributions;

b) exponential distributions;

c) Weibull distributions;

d) Erlang distributions.

3.3.14 As previously indicated, the modelling of distribution tails in current ICAO documentation is based on empirical considerations that will now be explained.

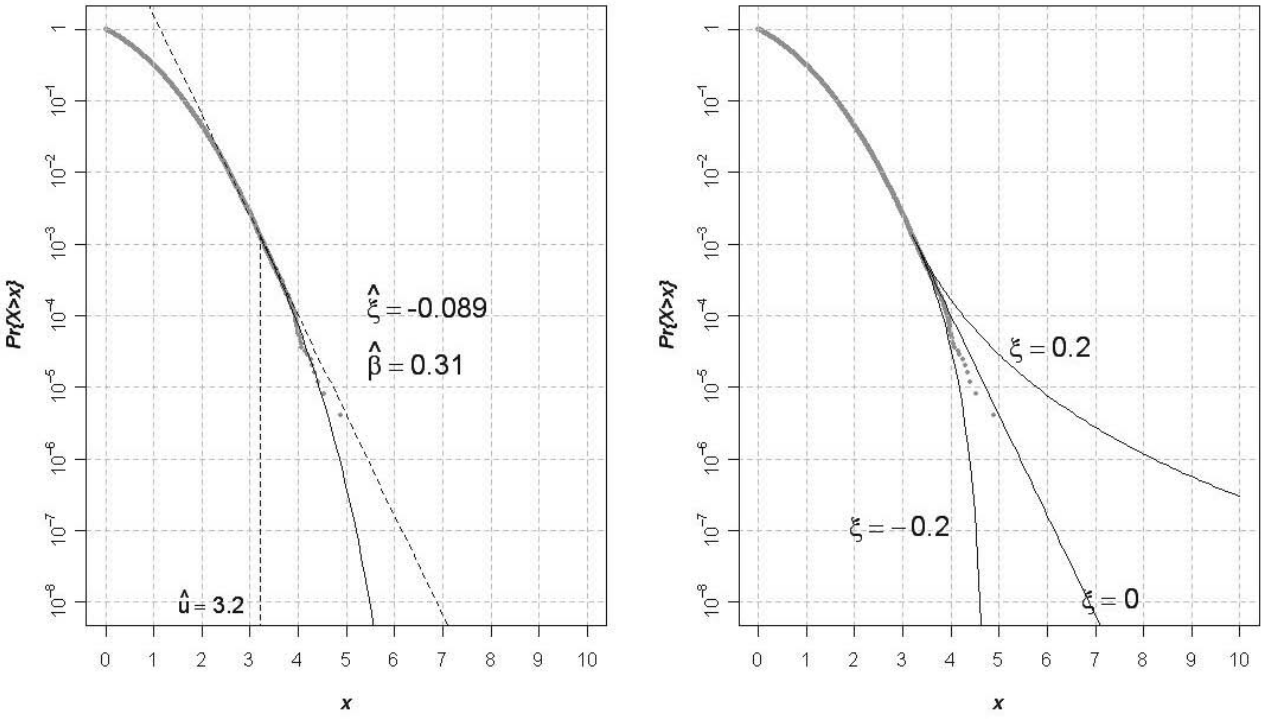

Figure 3-3. Modelling of tail distributions

3.4 DISTINCTION BETWEEN TYPICAL AND ATYPICAL DEVIATIONS IN CURRENT ICAO DOCUMENTATION

3.4.1 Typical deviations correspond to deviations observed in routine practice. They can be modelled by collecting a data sample and estimating the underlying distribution. In practice, the estimation is parametric in the sense that one first chooses a distribution family and then estimates the parameters of the distribution using one of the many existing methods (maximum likelihood, method of moments, etc.). The choice of the family of distributions relies either on some knowledge of the distribution of the deviation (for GPS, deviations are often taken to be Gaussian) or on some conservative criteria.

3.4.2 On the other hand, atypical deviations happen in exceptional circumstances and are impossible to model from a collected data sample due to the size of the sample necessary to observe them. For example, a collected data sample might cover one week of traffic, whereas an atypical deviation that could possibly result in a collision might happen only once in one or more years.

3.4.3 Assume that density functions for typical and atypical deviations, $f_{core}(x)$ and $f_{tail}(x)$ respectively, have been determined. Then the overall density function of the deviations is modelled by the mixture $f(x) = (1 - \alpha)\, f_{core}(x) + \alpha\, f_{tail}(x)$, where α is the rate of atypical deviations. Notice that this modelling differs from extreme value theory, since the $f_{tail}(x)$ component applies to the whole domain of the distribution, whereas in extreme value theory the approximated tail distribution provided by Equation (3-2) holds only when x is greater than a certain threshold for $\hat{u}$.

3.5 DETERMINATION OF THE DISTRIBUTION OF ATYPICAL ERRORS

3.5.1 As previously stated, the choice of a double exponential (DE) distribution for the distribution $f_{tail}(x)$ of atypical deviations is often seen. It can also be used for the distribution $f_{core}(x)$ of typical errors, in order to add conservativeness. Recall that the density f_{DE} associated with a DE distribution is given by:

$$f_{DE}(y) = \frac{1}{2\lambda} e^{-\frac{|y|}{\lambda}} \text{ for } -\infty < y < \infty. \tag{3-3}$$

3.5.2 For example, deviations for RNP k (k = 10 for instance) aircraft could be modelled as:

$$f(y) = \frac{1}{2\lambda} e^{-\frac{|y|}{\lambda}} \text{ with } \lambda = -\frac{k}{\ln(0.05)}. \tag{3-4}$$

The parameter λ is chosen to satisfy the requirement $\int_{-k}^{k} f(y)\, dy = 0.95$, which states that RNP k aircraft are expected to have position errors less than k NM in magnitude during 95% of their flight time.

3.5.3 Linear combinations of DE distributions have been used to avoid underestimating the probability of large deviations due to atypical lateral errors in the safety assessment performed for the implementation of 50 NM lateral separation in an RNP 10 environment (see Chapter 10, Reference 6). The overall density function of lateral deviations was chosen as $f(y) = (1 - \alpha)\, f_{core}(y) + \alpha\, f_{tail}(y)$, where $f_{core}(y)$ is the density function of lateral deviations for an RNP aircraft, given by Equation (3-4). $f_{tail}(y)$ is the density function of atypical lateral deviations and α is the probability that an aircraft's lateral deviation at an arbitrarily chosen instant is due (at least partly) to an atypical error. It was decided in the safety assessment to model $f_{tail}(y)$ as a DE density function. For each level of occupancy, the parameter α was chosen to have the maximum acceptable value that it could assume when the lateral overlap probability attained its maximum acceptable value (for that occupancy level). The λ parameter of f_{tail} was conservatively assumed to equal S_y.

3.5.4 Figure 3-4 shows a pair of aircraft on two parallel routes separated by S_y, where the lateral deviations are denoted by y_1 and y_2. Representing the two aircraft as boxes with width λ_y (see Chapter 2, Figure 2-3), it can be seen that the two aircraft are in lateral overlap if the lateral deviation of the second aircraft, y_2, belongs to the interval $\left[S_y - y_1 - \lambda_y, S_y - y_1 + \lambda_y\right]$. The probability for the two aircraft to be in lateral overlap is then given by:

$$P_y(S_y) = \int_{-\infty}^{\infty} f(y_1)\left(\int_{S_y - y_1 - \lambda_y}^{S_y - y_1 + \lambda_y} f(y_2)dy_2\right)dy_1 = \int_{S_y - \lambda_y}^{S_y + \lambda_y}\left(\int_{-\infty}^{\infty} f(y_1)\, f(y - y_1)dy_1\right)dy.$$

Notice that the two aircraft are assumed to have the same probability density function $f(y)$. The value of the λ parameter associated with $f_{\text{tail}}(y)$, which maximizes the probability of lateral overlap, is approximately equal to the lateral separation minimum, S_y. Accordingly, the probability density function associated with the lateral errors was taken as:

$$\begin{cases} (1-\alpha)DE(\lambda_{\text{core}}) + \alpha\ DE(\lambda_{\text{tail}}) \\ \lambda_{\text{core}} = -\dfrac{k}{\ln(0.05)} \quad \text{(for an RNP k)} \\ \lambda_{\text{tail}} = S_y = 50 \text{ NM.} \end{cases} \tag{3-5}$$

This concludes the discussion on modelling of the uncertainty associated with aircraft position. Discussion will now focus on the limitations of this modelling, particularly for the case of operational errors in environments with frequent position updating.

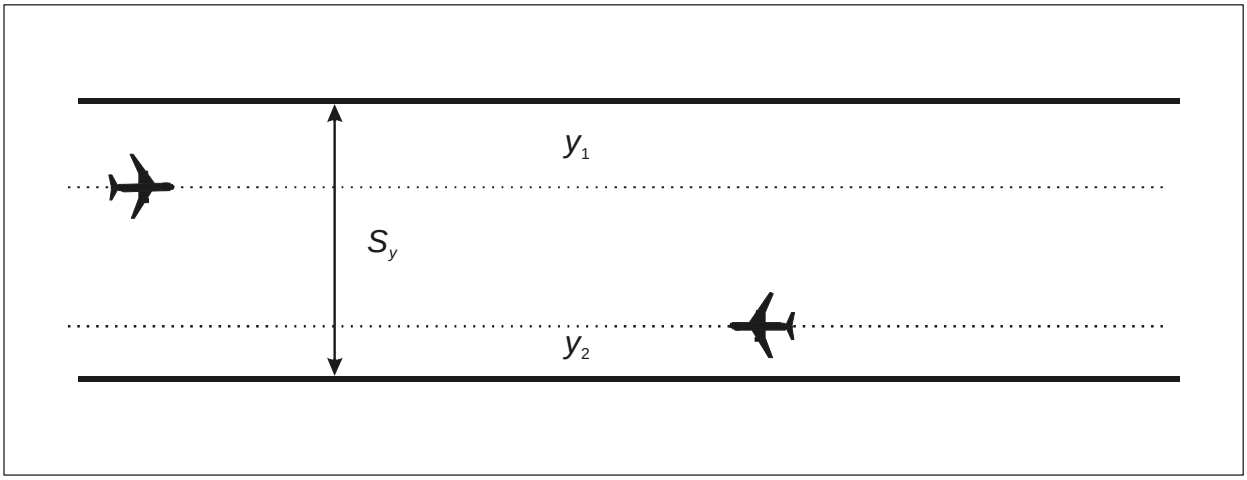

Figure 3-4. A pair of aircraft on two parallel routes separated by S_y, where the lateral deviations are denoted by y_1 and y_2

3.6 EXTENDING THE MODELLING OF OPERATIONAL RISK — FROM THE AIR TRAFFIC CONTROLLER'S VIEWPOINT

3.6.1 As set out in Chapter 2, 2.2, the models in the *Manual on Airspace Planning Methodology for the Determination of Separation Minima* (Doc 9689) and the *Manual on Implementation of a 300 m (1 000 ft) Vertical Separation Minimum Between FL 290 and FL 410 Inclusive* (Doc 9574) support essentially procedural separation. The pertinent lateral and vertical models do not account for any air traffic controller intervention. The longitudinal distance-based models do, but the current modelling is valid only for low update rates. In addition, the longitudinal separation minimum is sufficiently large to allow successful intervention.

3.6.2 In this section, the modelling of aircraft navigation deviations, from the viewpoint of an air traffic controller, is examined. Recall that "aircraft navigation deviation" represents the difference between the actual location of the aircraft and where the air traffic controller believes the aircraft to be. A deviation d_t at time t may be modelled, for example, by a density $f_t(\bullet)$. The time dependence refers to the uncertainty, at time t, associated with the position of the aircraft from the controller's viewpoint. At first sight, it is reasonable to model this uncertainty as a function of time when aircraft positions are updated at regular intervals. At the time of the update the controller "knows" where the aircraft is with an uncertainty associated with the position estimate, and this uncertainty is likely to increase in the course of time due to possible navigational errors.

3.6.3 For example, if the update rate is once every 30 minutes, then 15 minutes after a position update the air traffic controller cannot be certain that the aircraft has not deviated from its schedule for any reason. Therefore, it makes sense to model the possible location of the aircraft at time t as a random quantity, whose density $f_t(\bullet)$ depends on time.

3.6.4 However, if the update rate increases to an update every couple of seconds, as in radar surveillance, the previous modelling is no longer adequate for modelling a deviation from the assigned route. The reason is that the time duration between consecutive position updates is so short that the deviation has to be very small and cannot account for a risk of collision. In other words, the air traffic controller has no reason to believe that the succession of position updates for an aircraft does not correspond to the route followed by that aircraft. Even if one or two position updates have a large error, the air traffic controller can predict the aircraft position from the previous position updates and correct the large errors. It is only for consecutive large errors that the air traffic controller will not be able to detect and correct the errors. Therefore, the previous modelling applies provided that, in the modelling, one has added the occurrence of consecutive large errors.

3.6.5 There are a number of alternative ways to model the uncertainty associated with aircraft position, from a controller's viewpoint. A first possibility is to include latency terms in the modelling. Latency represents the "age" of the position displayed on a controller's screen, and it is the sum of all time delays between the elaboration of the position and its final display. If the latency is constant, then it is impossible for the air traffic controller to detect it, and in that case the controller sees aircraft backward from their actual position. Latency terms induce a time uncertainty, rather than a position uncertainty, in the sense that the position displayed on the controller's screen actually corresponds to the aircraft's position, but at a previous time. Another form of time uncertainty is due to the delay of the tracking system in detecting aircraft manoeuvres. For example, an aircraft may appear on the controller's screen as flying in a straight line whereas it has already started turning. As a consequence the controller will have an incorrect interpretation of the aircraft's profile.

3.6.6 In addition to the above technical sources of uncertainty, cognitive factors in a controller's mind may play a part. For example, when a controller expects an aircraft to perform a manoeuvre, the controller cannot be certain that the aircraft has performed that manoeuvre until it can be seen on the controller's screen. If the aircraft does not carry out the expected manoeuvre, the detection of the operational error by the controller will not be instantaneous, particularly if the controller is busy, or in the case of a technical time delay.

3.6.7 Figure 3-5 shows an example of the latter in the vertical dimension, where one aircraft is climbing and is expected (by the air traffic controller) to level off, while the other one is steady at the next flight level. Notice also that

the deviating trajectory shown in Figure 3-5 is essentially deterministic, in the sense that it corresponds to an extrapolation from the climbing phase. Elements that are not deterministic and have to be modelled in probabilistic terms are related to the following:

a) What if the arrival time of the steady aircraft at the "vertical colliding point" had been slightly different?

b) How long would it take the controller to detect this operational error?

c) What would be the chance of the controller solving the operational error before a collision?

Scenarios of operational error, such as the one illustrated in Figure 3-5, play a significant part in the operational risk in the terminal control area where climbing aircraft are often requested to level off.

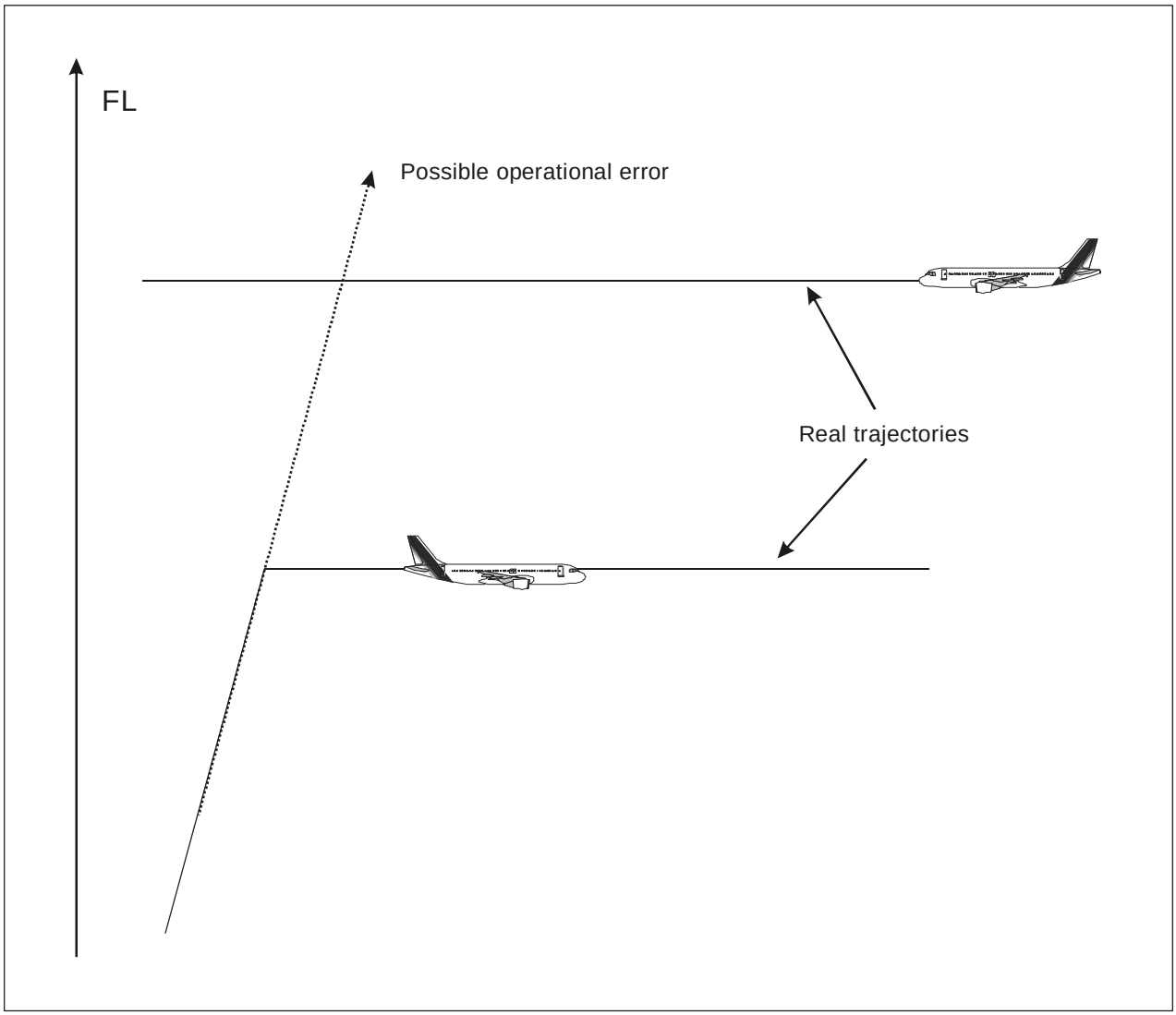

Figure 3-5. Possible operational error scenario

3.6.8 More generally, scenarios involving a misunderstanding of the aircraft's route by the air traffic controller can often be modelled by deterministic trajectories, in the sense that it is possible to infer without ambiguity what will be the "unexpected" future trajectory of the aircraft. Such a case has been discussed for the vertical dimension, but the same also holds for the horizontal plane when the air traffic controller expects an aircraft to turn but it keeps going in a straight line. It even holds in the "speed dimension," for instance when an air traffic controller requests an aircraft to increase its speed (due to trailing aircraft) and the aircraft does not follow the instruction. In all these cases, there is no gain in modelling a deviation in terms of a random variable d_t distributed according to a density $f_t(d)$, since the deviating trajectory is essentially deterministic.

3.6.9 This unified framework does not intend to cover the high surveillance update rate aspect of collision risk modelling for operational errors. This aspect has just been mentioned to emphasize that the framework applies only to collision risk models in Docs 9689 and 9574 and that none of them address the modelling of operational errors in radar surveillance.

3.6.10 The reader who is interested in the modelling of operational errors in terms of deterministic trajectories is referred to Chapter 10, Reference 4, where several operational errors in the vertical dimension have been modelled that way for the safety assessment of reduced vertical separation minimum (RVSM) in the United Kingdom.

———————

Chapter 4

THE RICE FORMULA

4.1 INTRODUCTION

4.1.1 As was seen in Chapter 3, a collision between aircraft can be modelled as a particle (representing the relative position of the centre of one aircraft) entering a volume around a second aircraft. Furthermore, each aircraft deviates "at random" from its assigned route so that the particle also follows a random path.

4.1.2 There are several ways to determine analytically the probability for a particle, following a random trajectory, to enter a volume. In order to illustrate this probability in an intuitive way, a derivation based on fluid dynamics has been chosen. The benefit of this derivation is that the equation obtained has a very intuitive interpretation.

4.1.3 First some preliminary concepts drawn from fluid dynamics will be introduced, and then these concepts will be used to determine the probability for a particle to enter a volume.

4.2 PRELIMINARY CONCEPTS

4.2.1 The area of a trapezium, having height *h* and width *x*, is given by the product *h x*. The area of a trapezium formed by two vectors is then calculated using the formalism of the dot product, a type of inner product. The dot product can be expressed as the product of the lengths of the vectors times the cosine of the angle between the two vectors. If $\vec{n}$ is the vector normal to the width and having unit length, and $\vec{L}$ is the vector directed along the side of the trapezium then, as can be seen in Figure 4-1, the height, *h*, is given by the dot product of $\vec{n}$ and $\vec{L}$, denoted by $\vec{L} \bullet \vec{n}$. The area of the trapezium is given by $x\left(\vec{L} \bullet \vec{n}\right)$.

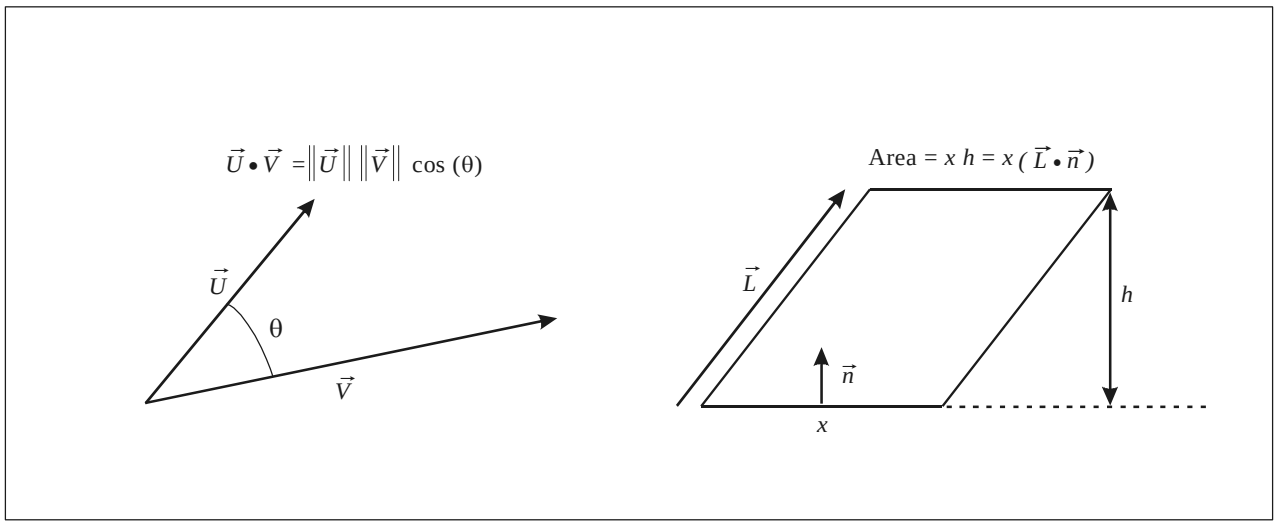

Figure 4-1. Area of a trapezium formed by two vectors

4.2.2 Consider the following problem:

A fluid is flowing in the plane, and it is assumed that at each point (x, y) of the plane the two-dimensional velocity vector, denoted by $\vec{v}(x, y)$, is known. A portion of the space denoted by Ω and delimited by a boundary denoted by $\partial\Omega$ will also be considered. What is the flow rate entering Ω?

4.2.3 Figure 4-2 illustrates the problem. The fluid velocity at each point is represented by a two-dimensional vector, and an infinitesimal portion of the boundary of Ω, having length *dx* and inner normal vector $\vec{n}$, has been magnified. Incoming flow rate means the amount of fluid entering Ω per unit time. ρ denotes the fluid surface density, so that the amount of fluid in a surface element, *ds*, is given by $\rho\, dS$.

4.2.4 An infinitesimal time interval, δt, is considered in trying to find the amount of fluid entering into Ω through an infinitesimal element of the boundary of Ω having width *dx* and unit normal vector $\vec{n}$ (see Figure 4-2). As illustrated in Chapter 3, Figure 3-3, it can be seen that the amount of fluid entering Ω through *dx* during δt is contained in the trapezium whose width has length *dx* and inner normal $\vec{n}$, and whose side corresponds to $\vec{v}\,\delta t$. The main approximation is that the velocity $\vec{v}$ is constant inside this trapezium. This approximation holds since, by letting δt tend towards zero, the trapezium collapses to *dx*. The area of the trapezium is given by $(\vec{n} \bullet (\vec{v}\,\delta t))dx$. Since it is the fluid entering Ω that is of interest, the focus will be on the parts of the boundary where the dot product $\vec{n} \bullet \vec{v}$ is positive. For any quantity *q*, q^+ denotes the positive part of *q*. That is:

$$q^+ = \begin{cases} q & \text{if } q > 0 \\ 0 & \text{otherwise.} \end{cases}$$

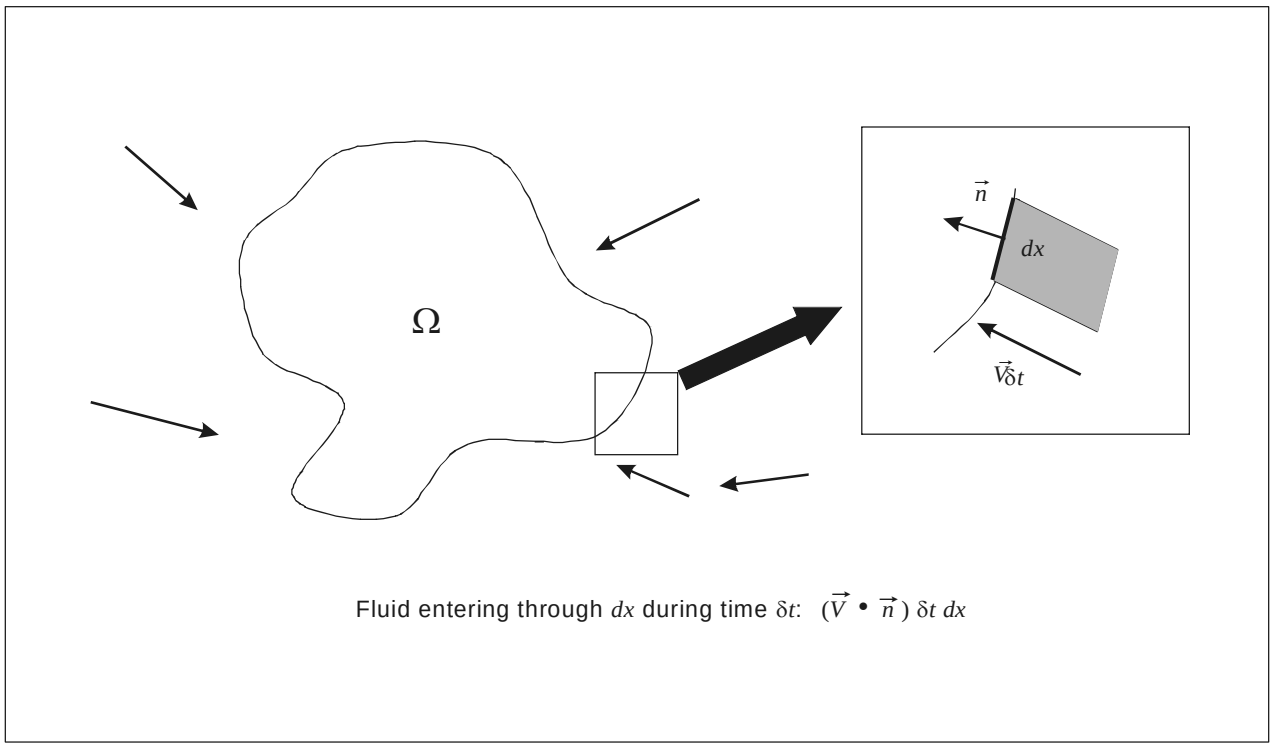

Figure 4-2. Determining the flow rate entering Ω

The negative part is defined similarly:

$$q^{-} = \begin{cases} -q & \text{if } q < 0 \\ 0 & \text{otherwise.} \end{cases}$$

4.2.5 Notice that both the negative and the positive part are always positive. The amount of fluid entering Ω during the time interval δt can now be expressed as equal to the product of the incoming flow rate $\varphi_{incoming}$ and the infinitesimal time interval δt with

$$\begin{aligned} \varphi_{incoming}\,\delta t &= \int_{\partial\Omega} \rho\left(\vec{n} \bullet \vec{v}\delta t\right)^{+} dx \\ &= \delta t \int_{\partial\Omega} \rho\left(\vec{n} \bullet \vec{v}\right)^{+} dx. \end{aligned} \tag{4-1}$$

Therefore the incoming flow rate is given by:

$$\varphi_{incoming} = \int_{\partial\Omega} \rho\left(\vec{n} \bullet \vec{v}\right)^{+} dx \tag{4-2}$$

where the normal vector $\vec{n}$ corresponds to the inner normal, directed towards the inside of Ω.

4.3 ILLUSTRATION OF A SIMPLE CASE

4.3.1 For clarification, consider the case of the incoming flow rate for a disk with radius r. The origin of the plane is fixed at the centre of the disk such that the boundary of the disk is represented by the one-parameter curve (see Figure 4-3).

$$\partial\Omega\text{:}\ \begin{pmatrix} r\cos\theta \\ r\sin\theta \end{pmatrix},\quad \theta \in [0, 2\pi]. \tag{4-3}$$

4.3.2 As shown in Figure 4-3, the inner unit normal at θ is given by:

$$\vec{n} = \begin{pmatrix} -\cos\theta \\ -\sin\theta \end{pmatrix},$$

and the element of boundary corresponding to $\delta\theta$ has length $r\delta\theta$. Therefore, if the velocity is given by:

$$\vec{v}(x, y) = \begin{pmatrix} v_x(x, y) \\ v_y(x, y) \end{pmatrix},$$

the flow rate into the disk is given by:

$$\begin{aligned} \varphi_{incoming} &= \int_0^{2\pi} \rho\left(\begin{pmatrix} -\cos\theta \\ -\sin\theta \end{pmatrix} \bullet \begin{pmatrix} v_x(r\cos\theta, r\sin\theta) \\ v_y(r\cos\theta, r\sin\theta) \end{pmatrix}\right)^{+} r d\theta \\ &= \int_0^{2\pi} \rho\left(-v_x(r\cos\theta, r\sin\theta)\cos\theta - v_y(r\cos\theta, r\sin\theta)\sin\theta\right)^{+} r d\theta. \end{aligned} \tag{4-4}$$

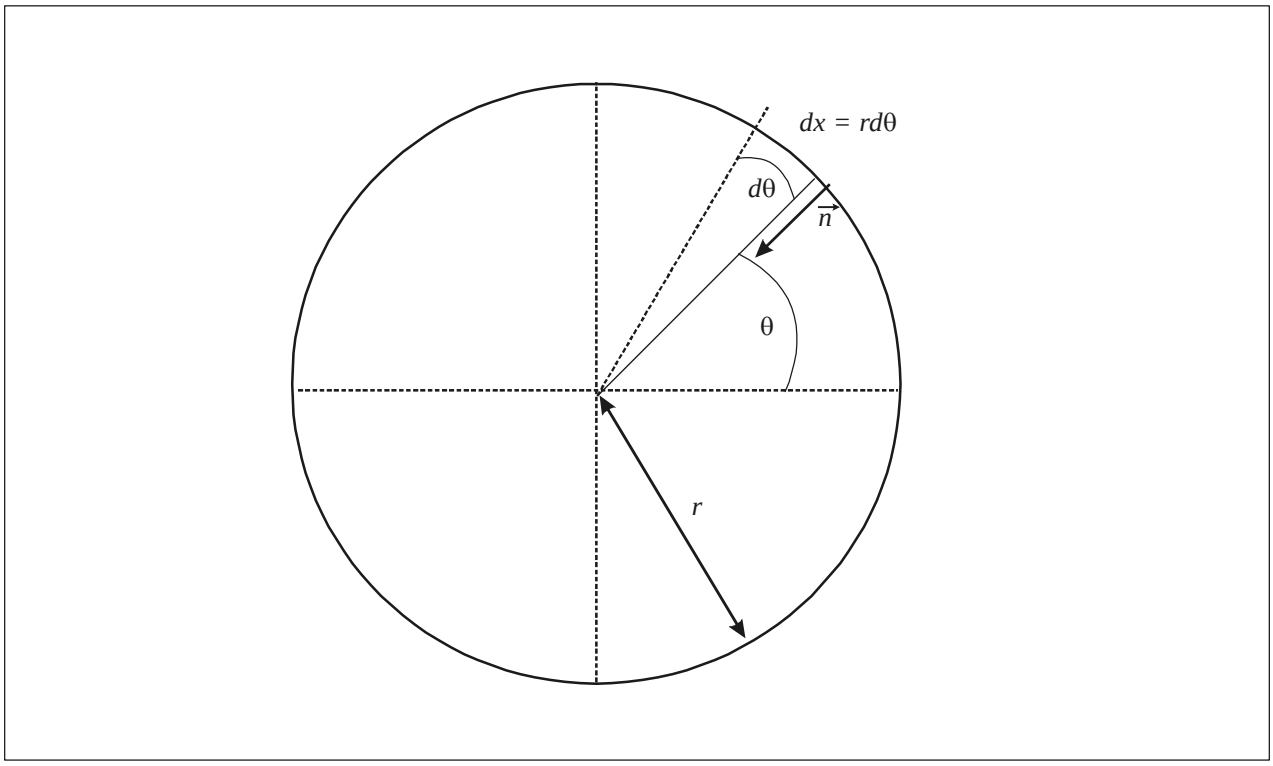

Figure 4-3. Incoming flow rate for a disk with radius *r*

4.4 GENERALIZATION TO THREE DIMENSIONS

4.4.1 The equation for the incoming flow rate generalizes to the case of a fluid in a three-dimensional space entering a three-dimensional volume. Here, the infinitesimal volume that is considered corresponds to a "tilted column" as shown in Figure 4-4, where *S* is the surface area of the base.

4.4.2 By generalizing the two-dimensional case, Equation (4-2), to three dimensions, it can be seen that the incoming flow rate for a fluid entering a three-dimensional volume Ω having boundary $\partial\Omega$ is given by:

$$\varphi_{incoming} = \iint_{\partial\Omega} \rho\left(\vec{n} \bullet \vec{v}\right)^{+} dS. \tag{4-5}$$

Here, the integral is a double integral over the boundary of the three-dimensional volume Ω, and *ds* represents a surface area infinitesimal. ρ represents the volume density such that the amount of fluid in a volume element *dV* is given by ρdV.

4.5 APPLICATION TO RANDOM PROCESSES

4.5.1 Returning to the initial problem, which involved finding the probability for a particle moving "at random" to enter a given volume, let $\left(x_t, y_t, z_t\right)$ denote the three-dimensional position at time *t* and $\left(\dot{x}_t, \dot{y}_t, \dot{z}_t\right)$ the three-dimensional velocity vector at time *t*.

4.5.2 Stochastic processes are not always continuous (some processes have "jumps") so that the speed at time *t* is not always defined. In this case, it will be assumed that for any time *t*, the state $(x_t, y_t, z_t, \dot{x}_t, \dot{y}_t, \dot{z}_t)$ is defined and that the joint probability admits a density function $f_t = f_t(x, y, z, \dot{x}, \dot{y}, \dot{z})$, where $f_t(x, y, z, \dot{x}, \dot{y}, \dot{z})\Delta x\Delta y\Delta z\Delta\dot{x}\Delta\dot{y}\Delta\dot{z} = P\{x_t \in [x, x+\Delta x], y_t \in [y, y+\Delta y], \ldots\}$.

4.5.3 To simplify the notation, capital letters will be used to denote three-dimensional positions and velocities. X_t will denote the three-dimensional position (x_t, y_t, z_t) of the particle at time *t*, and V_t the three-dimensional velocity $(\dot{x}_t, \dot{y}_t, \dot{z}_t)$ of the particle at time *t*. Similarly, *X* will denote a three-dimensional position (x, y, z), and *V* will denote a three-dimensional velocity $(\dot{x}, \dot{y}, \dot{z})$. Furthermore, when the symbol *V* appears in a dot product, an arrow will be added over it (writing it $\vec{V}$), in order to recall that it represents a vector.

4.5.4 Whenever a three-dimensional quantity is used to define a vector element, as in Figure 4-4, an arrow will be added on top of the symbol. Rather than considering the six-dimensional $(x, y, z, \dot{x}, \dot{y}, \dot{z})$, and the associated probability density function $f_t(x, y, z, \dot{x}, \dot{y}, \dot{z})$, the notation (*X*,*V*) and f_t (*X*,*V*) will be used as often as possible.

4.5.5 Figure 4-5 shows how the probability of a three-dimensional stochastic process entering a three-dimensional volume Ω can be seen in terms of the incoming rate of the trajectories. The $\vec{V}_t$ notation in Figure 4-5 is the velocity vector associated to the three-dimensional stochastic process X_t. Consider an infinitesimal boundary element of Ω located at *X* with surface area *dS* and with an inward unit normal vector $\vec{n}$. Assume that the velocity $\vec{V}_t$ of the stochastic process "around *dS*" equals $\vec{V}$. The stochastic process, outside of Ω at *t*, enters Ω through *dS* between *t* and *t* + δt if it is in the tilted cylinder having volume $\left(\vec{n} \bullet (\vec{V}\,\delta t)\right)^{+} dS$ at time *t*. The + means that if the velocity is opposite to the inner normal, there is no way for the process to enter. In other words, the probability of entering through *dS* between *t* and *t* + δt, given a velocity vector $\vec{V}$ at time *t*, is the probability to be in the small volume shown in Figure 4-5. Assuming that the tilted cylinder is small enough for the probability density function to be approximated as a constant in the infinitesimal volume element, the probability of the particle being in this small tilted cylinder is given by $f_t(X,V)\left(\vec{n} \bullet (\vec{V}\,\delta t)\right)^{+} dS$. It must be emphasized that the three-dimensional position *X* is not a random quantity but corresponds to a point on the boundary of Ω. However, the velocity vector $\vec{V}$ is allowed to vary, since the velocity is no longer deterministic. There is a need to integrate over all possible values $\vec{V}$ of the velocity $\vec{V}_t$ at time *t*.

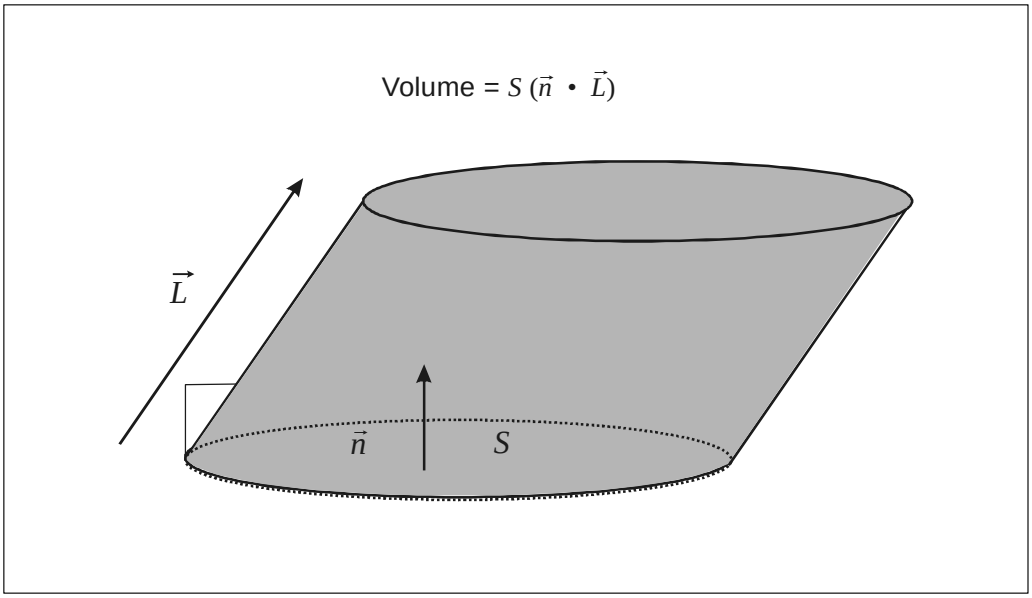

Figure 4-4. Defining a vector element

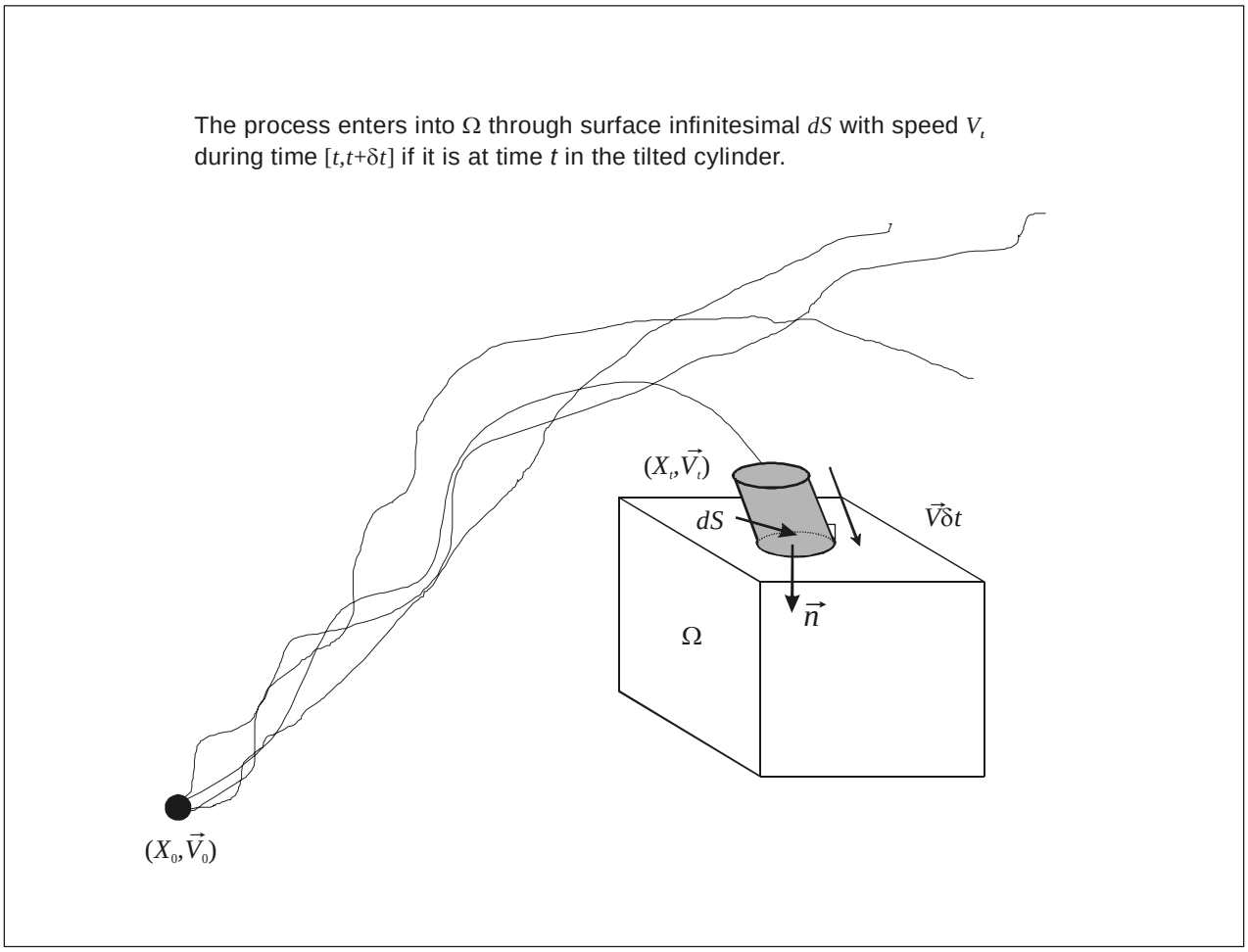

Figure 4-5. The probability of a three-dimensional stochastic process entering a three-dimensional volume Ω, seen in terms of the incoming rate of the trajectories

4.5.6 Performing this integration, it is found that the probability for this random process, outside of Ω at *t*, to enter Ω at position *X*, through *dS* between *t* and *t* + δ*t*, equals the triple integral $\iiint\left(f_t(X,V)\left(\vec{n}\bullet(\vec{V}\,\delta t)\right)^+ dS\right)dV$:

$$\Pr\left\{\text{outside } \Omega \text{ at } t \text{ and enters } \Omega \text{ through } dS \text{ during } [t,t+\delta t]\right\} = \delta t\, dS\left(\iiint f_t(X,V)(\vec{n}\bullet\vec{V})^+ dV\right). \tag{4-6}$$

4.5.7 Integrating over all positions on the boundary of Ω, the probability of entering into Ω during $[t,t+\delta t]$ is given by:

$$\Pr\left\{\text{outside } \Omega \text{ at } t \text{ and enters } \Omega \text{ during } [t,t+\delta t]\right\} = \delta t\iint_{\partial\Omega}\left(\iiint f_t(X,V)(\vec{n}\bullet\vec{V})^+ dV\right)dS. \tag{4-7}$$

This equation is known as the Rice formula (see Chapter 10, Reference 10, pages 145 to 160). It is sometimes used in the one-dimensional case for estimating a frequency of crossing through a certain threshold (see, Chapter 10, Reference 12,

"the level-crossing problem"). Recall that *dS* corresponds to the surface infinitesimal at *X* and that $\vec{n}$ corresponds to the inward normal at *X*. The symbol *dS* in Equation (4-7) is a two-dimensional surface element and *dV* represents a product of three infinitesimal speeds, so there are five integrals in total.

4.5.8 As seen in Chapter 2, Figures 2-2 and 2-3, a collision can be modelled by a particle entering a certain volume. If Ω denotes this volume, then Pr{outside Ω at t and enters Ω during $[t,t+\delta t]$} represents the probability that the two aircraft, geometrically separated at time *t*, enter into collision during the time interval $[t,t+\delta t]$. The modelling of a probability of collision using that representation was first published in 1993 (see Chapter 10, Reference 3).

4.5.9 Later is this document Equation (4-7) will be used in that context, with Ω denoting one of the two volumes of Figures 2-2 and 2-3 (depending on whether parallel routes or crossing routes are considered). In that context, Equation (4-7) becomes:

$$\begin{aligned}&\Pr\left\{\text{outside collision volume at } t \text{ and collision during } \left[t,t+\delta t\right]\right\}\\&= \delta t \iint_{\partial\Omega}\left(\iiint f_t(X,V)(\vec{n}\bullet\vec{V})^+ dV\right)dS.\end{aligned} \tag{4-8}$$

4.5.10 Note that f_t is a function of relative positions and velocities. It is therefore a density function formed by convolving the position and velocity densities for the two aircraft. This will be seen in more detail in later examples. In real cases, it is always possible to simplify Equation (4-8). Notice that the time variable in Equation (4-8) is in the t index of f_t. In order to make this time dependence more explicit, let $\Psi(t)$ be the integral term

$$\Psi(t) = \iint_{\partial\Omega}\left(\iiint f_t(X,V)(\vec{n}\bullet\vec{V})^+ dV\right)dS \tag{4-9}$$

so that Equation (4-8) is rewritten as:

$$\Pr\left\{\text{outside collision volume at } t \text{ and collision during } \left[t,t+\delta t\right]\right\} = \delta t\, \psi(t). \tag{4-10}$$

4.6 PROBABILITY OF THE PROCESS ENTERING Ω DURING $[t_a,t_b]$

4.6.1 The Rice formula in Equation (4-7) gives the probability of entering Ω during an infinitesimal time interval $[t,t+\delta t]$. From the Rice formula, it is possible to derive an upper bound for the probability of entering Ω over a time interval$[t_a,t_b]$. The time interval $[t_a,t_b]$ is divided into *N* consecutive subintervals of length $\delta t = (t_b,t_a)/N$, with *N* sufficiently large for δt to be considered as an infinitesimal. For $0 \le i \le N-1$, the consecutive time intervals are $[t_i,t_{i+1}]$, with $t_i = t_a + i \times \delta t$.

4.6.2 At t_a the stochastic process is assumed to be outside of Ω, and the time of first entrance into Ω is defined as follows: for all $N-1$ consecutive time intervals, an indicator variable F_i is defined which is equal to 1 if the following conditions are satisfied:

a) $F_k = 0$ for $0 \le k \le i-1$; and

b) the stochastic process is outside of Ω at t_i and it enters Ω during the time interval $[t_i,t_{i+1}]$.

4.6.3 If one of the two previous conditions is not satisfied, then $F_i = 0$. It follows from condition a) that at most one F_i is different from zero, since once a given F_i differs from zero all the successive F_j (with $j > i$) have to be zero. Furthermore, if $F_i = 1$, then the time when the stochastic process enters into Ω for the first time belongs to the subinterval $[t_i,t_{i+1}]$. The fact that $\sum_{i=0}^{n-1} F_i$ is either zero or one allows one to write $\Pr\left\{\sum_{i=0}^{n-1} F_i = 1\right\} = E\left\{\sum_{i=0}^{n-1} F_i\right\}$. Therefore,

$$\begin{aligned}\Pr\left\{\text{collision during } \left[t_a,t_b\right]\right\} &= \Pr\left\{\sum_{i=0}^{n-1} F_i = 1\right\} \\ &= E\left\{\sum_{i=0}^{n-1} F_i\right\} \\ &= \sum_{i=0}^{n-1} E\left\{F_i\right\}.\end{aligned} \tag{4-11}$$

4.6.4 Now, for $0 \le i \le N-1$, the following is obtained:

$$\begin{aligned}E\left\{F_i\right\} &= \Pr\left\{F_i = 1\right\} \\ &= \Pr\left\{\text{outside of } \Omega \text{ during } \left[t_a,t_i\right] \text{and enters } \Omega \text{ during } \left[t_i,t_{i+1}\right]\right\} \\ &\le \Pr\left\{\text{outside of } \Omega \text{ at } t_i \text{ and enters } \Omega \text{ during } \left[t_i,t_{i+1}\right]\right\}.\end{aligned} \tag{4-12}$$

The inequality in the last line follows from the fact that event A = {outside of Ω at t_i and enters Ω during $[t_i,t_{i+1}]$} is the sum of the two following disjoint events:

$$\begin{aligned}&A = A_1 \cup A_2 \text{ with} \\ &A_1 = \left\{\text{outside of } \Omega \text{ during } \left[t_a,t_i\right] \text{ and enters } \Omega \text{ during } \left[t_i,t_{i+1}\right]\right\} \\ &A_2 = \left\{\text{enters } \Omega \text{ during } \left[t_a,t_i\right[, \text{ outside of } \Omega \text{ at } t_i, \text{ and enters again } \Omega \text{ during } \left[t_i,t_{i+1}\right]\right\}.\end{aligned} \tag{4-13}$$

4.6.5 Since A_1 and A_2 are disjoint, $\Pr\{A\} = \Pr\{A_1\} + \Pr\{A_2\}$ which implies that $\Pr\{A_1\} \le \Pr\{A\}$. Furthermore, by Equation (4-10) Pr {outside of Ω at t_i and enters Ω during $[t_i,t_{i+1}]$} = $\psi(t_i)\,\delta t$. Putting together Equations (4-11) and (4-12) the following is obtained:

$$\begin{aligned}\Pr\left\{\text{collision during } \left[t_a,t_b\right]\right\} &\le \delta t \sum_{i=0}^{n-1} \psi\left(t_i\right) \\ &\le \int_{t_a}^{t_b} \psi\left(t\right) dt.\end{aligned} \tag{4-14}$$

4.6.6 Equation (4-14) provides an upper bound for the probability of collision during the time interval $[t_a,t_b]$. It is now possible to examine under which additional assumption the "$\le$" symbol in Equation (4-14) can be replaced by the "$=$" symbol. Actually, the "$\le$" symbol in Equation (4-14) comes from the inequality $\Pr\{A_1\} \le \Pr\{A\}$ in the bottom line of Equation (4-12), with A_1 and A_2 defined in Equation (4-13). Since A_1 and A_2 are disjoint, they can be replaced by an equality, provided it is assumed that $\Pr\{A_2\} = 0$. In other words, zero probability needs to be assigned to the events "enters Ω during $[t_a,t_i]$, outside of Ω at t_i, and enters again Ω during $[t_i,t_{i+1}]$" for all i. Neglecting the probabilities associated to all previous events for all i is the same as neglecting the probability of multiple collisions during $[t_a,t_b]$. In other words, if the probability of multiple collisions during $[t_a,t_b]$ is neglected, then the "$\le$" symbol can be replaced by the "=" symbol in Equation (4-14). Under this additional assumption, the following is obtained:

$$\Pr\left\{\text{collision during } \left[t_a,t_b\right]\right\} = \int_{t_a}^{t_b} \psi\left(t\right) dt. \tag{4-15}$$

4.6.7 The rationale for neglecting multiple collisions is a "rare event assumption": it is assumed that the probability of one collision during the time interval $[t_a,t_b]$ is so small that the occurrence of multiple collisions can be neglected. This assumption is often implicit and results from the choice of the metrics for the risk. As will be seen later

in this document, the usual metrics for risk is the number of fatal accidents per flying hour; however in practice, the risk assessment is done by estimating, for all proximate pairs of aircraft, the probability of collision. By doing so, the probability of multiple collisions for the same pair is implicitly neglected.

4.6.8 The collision risk models presented in Doc 9689 and Doc 9574 will be introduced in subsequent chapters, and an analytical derivation for each of them based on the Rice formula will be provided.

———————

Chapter 5

LATERAL COLLISION RISK MODELLING FOR AIRCRAFT ON PARALLEL ROUTES

5.1 INTRODUCTION

5.1.1 A collision risk model for aircraft on parallel routes was developed by P.G. Reich in the early 1960s (see Chapter 10, Reference 13). This model quickly became known as the Reich model and was subsequently adapted for the modelling of collision risk in the vertical dimension, i.e. for aircraft at adjacent flight levels either on the same route or on crossing routes.

5.1.2 This chapter introduces the original Reich model for the modelling of lateral collision risk for aircraft on parallel routes. Chapter 6 will model vertical risk using a similar approach.

5.1.3 The Reich model is used in Doc 9574 (without being introduced) in the derivation of the performance specifications for reduced vertical separation minimum (RVSM). It is introduced in detail (without being analytically derived) in the *Report of the Sixth Meeting of the Review of the General Concept of Separation Panel* (RGCSP/6, Doc 9536) and its associated appendices. It is implicitly used in Appendices 12 to 15 of Doc 9689 for deriving navigation performance specifications of aircraft with a predetermined lateral separation between adjacent parallel routes.

5.1.4 The Reich model mainly applies to the determination of strategic separation minima, i.e. lateral separations between parallel routes or vertical separation between adjacent flight levels. An important assumption in the Reich model is that aircraft are always assumed to have been flying sufficiently long on their routes to have reached a "steady state" in the lateral and vertical dimensions, where the distributions of the error terms no longer depend on time.

5.2 NOTATION AND ASSUMPTIONS

5.2.1 Consider two steady aircraft at the same altitude on two parallel routes nominally separated, and let S_y denote the lateral separation. Assume that the two aircraft will overlap in the longitudinal dimension during the flight time on their routes, and denote by t_{init} and t_{end} the beginning and the end of their longitudinal overlap. It is recalled that a longitudinal overlap corresponds to an overlap in the longitudinal dimension of the boxes associated with each aircraft (see Figure 5-1).

5.2.2 The objective is to determine the probability of collision for the two aircraft between t_{init} and t_{end}. If a reference frame centred on one of the aircraft is taken, a collision corresponds to the situation that the relative position between the aircraft belongs to the box shown in Figure 5-2 where the coordinates of the four top corners have been added. Following the notation of Chapter 4, 4.5, (X_t,V_t) denotes the couple made up of the relative position and the relative velocity (both of them being three-dimensional) for the pair of aircraft and f_t denotes the joint probability density function of this couple, conditioned on the pair being in longitudinal overlap. In what follows a velocity component will frequently be referred to as a speed (with the assumption that the speed could be negative).

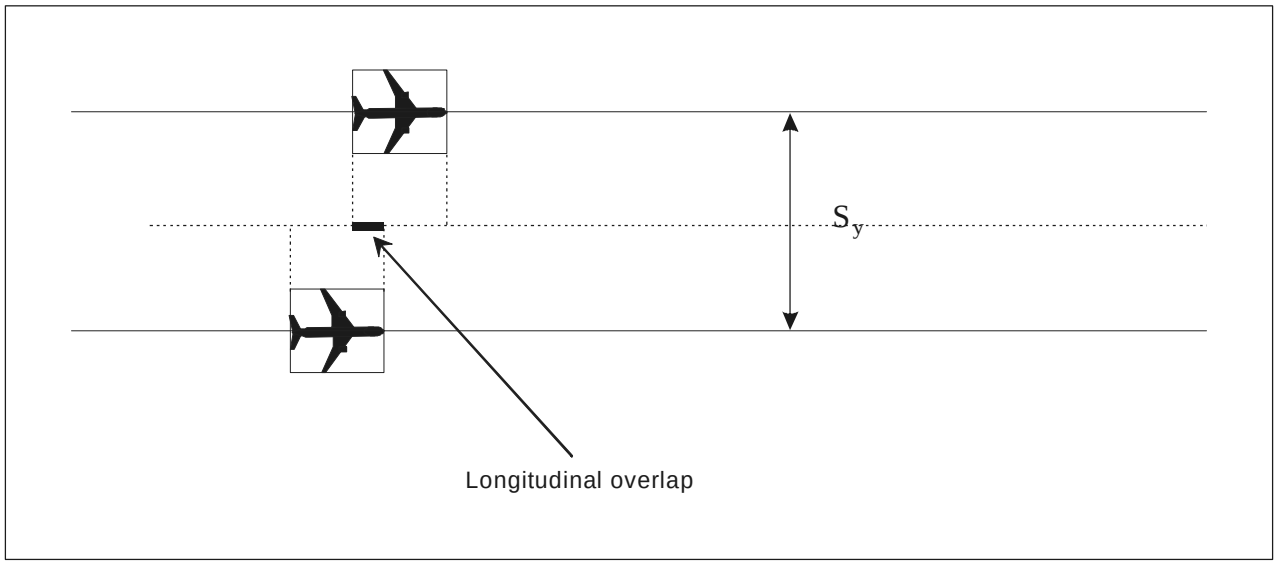

Figure 5-1. A longitudinal overlap

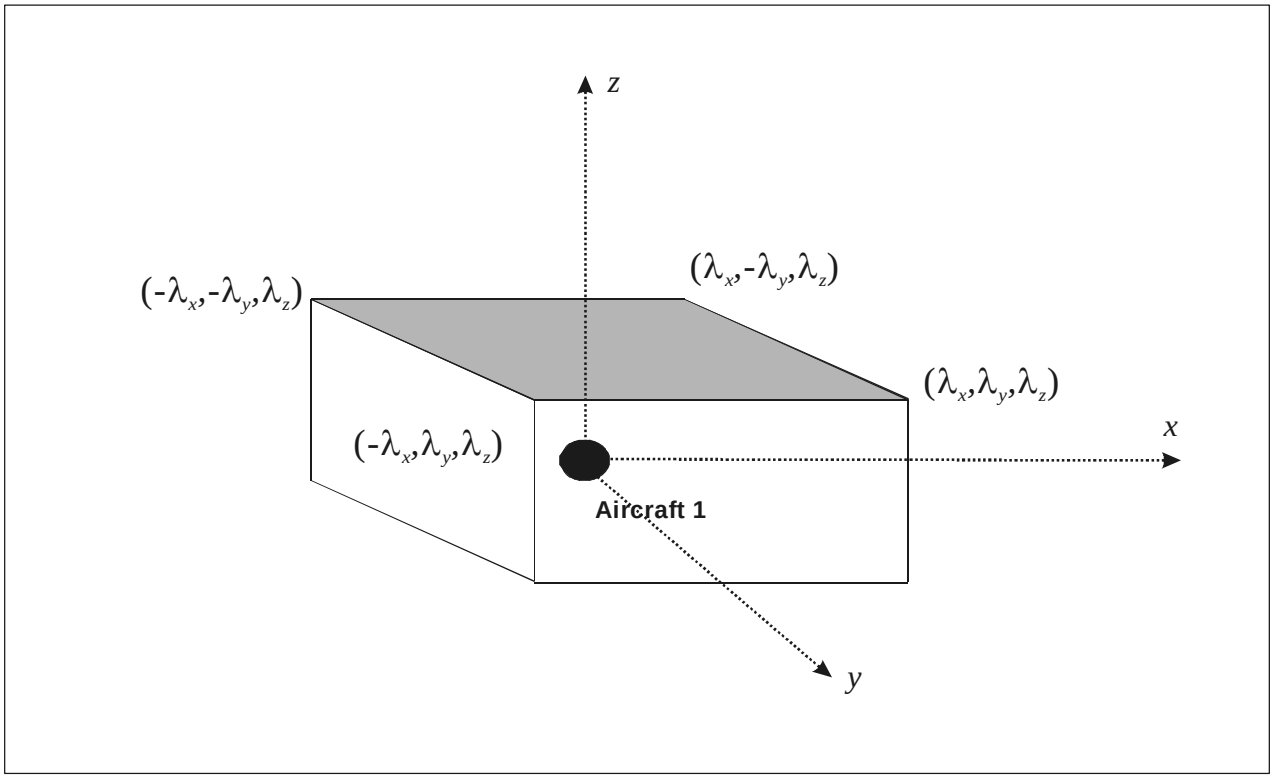

Figure 5-2. Aircraft reference frame

5.2.3 First, assume that the relative position and velocity terms can be decoupled in the three dimensions. For the longitudinal dimension this means that the longitudinal relative speed and position are independent of the relative speed and position in the two other dimensions. Similarly, the lateral relative speed and position are independent of those in the vertical dimension. This assumption does not take into account "directional perturbations" such as the wind, which are clearly not independent in the three dimensions. However, as per the next assumption, the Reich model applies to aircraft that are assumed to have reached a steady state, and it is the stationary distribution which is assumed to be independent in the lateral and vertical dimensions.

5.2.4 With $X = (x, y, z)$, the three components of the position error, and $V = (\dot{x}, \dot{y}, \dot{z})$, the three components of the velocity error, the joint probability density function $f_t(X,V)$ can be written as the product of three factors, each corresponding to the joint probability density function of the speed and position error in one dimension:

$$f_t(X,V) = f_{x,\dot{x},t}(x,\dot{x})\, f_{y,\dot{y},t}(y,\dot{y})\, f_{z,\dot{z},t}(z,\dot{z}). \tag{5-1}$$

5.2.5 Second, assume that both aircraft have been flying sufficiently long to have reached a steady state in the lateral and vertical dimensions. This means that the joint density of the relative lateral and vertical (position, speed) no longer depends on time. If the joint (position, speed) couple in each of the three dimensions is expressed as in Equation (5-2), this assumption means that the time index in the joint density for the relative vertical and lateral (position, speed) can be removed:

$$\begin{aligned} f_{x,\dot{x},t}(x,\dot{x}) &= f_{x_t}(x_t = x)\, f_{\dot{x}_t|x_t}(\dot{x}_t = \dot{x} \,|\, x_t = x) \\ f_{y,\dot{y},t}(y,\dot{y}) &= f_y(y)\, f_{\dot{y}|y}(\dot{y}_t = \dot{y} \,|\, y_t = y) \\ f_{z,\dot{z},t}(z,\dot{z}) &= f_z(z)\, f_{\dot{z}|z}(\dot{z}_t = \dot{z} \,|\, z_t = z). \end{aligned} \tag{5-2}$$

5.2.6 The probability density functions (pdfs) in Equation (5-2) have the following definitions:

a) $f_{x_t}(x_t = x)$ is the pdf of the relative longitudinal position at time t, and $f_{\dot{x}_t|x_t}\left(\dot{x}_t = \dot{x} \,|\, x_t = x\right)$ is the pdf of the relative longitudinal speed at time t conditional on the relative longitudinal position at time t;

b) $f_y(y)$ is the pdf of the relative lateral position at any time, and $f_{\dot{y}|y}\left(\dot{y}_t = \dot{y} \,|\, y_t = y\right)$ is the pdf of the relative lateral speed at any time t conditional on the relative lateral position at the same time t;

c) $f_z(z)$ is the pdf of the relative vertical position at any time, and $f_{\dot{z}|z}\left(\dot{z}_t = \dot{z} \,|\, z_t = z\right)$ is the pdf of the relative vertical speed at any time t conditional on the relative vertical position error at the same time t.

5.3 DERIVATION OF THE PROBABILITY OF COLLISION DURING A LONGITUDINAL OVERLAP

5.3.1 The key factor in the Reich model is the probability of collision during a longitudinal overlap, Pr, for example. Once this factor has been determined, the Reich model in the lateral dimension for aircraft at the same altitude on parallel routes is easy to determine and this will be done in sections 5.4 and 5.5.

5.3.2 In this section, the probability of collision during a longitudinal overlap is derived. In the Reich model, the expression for this probability is simplified with the help of several approximations. First, in 5.3.3 to 5.3.13, Pr is derived without any approximation. Then, in 5.3.14 to 5.3.18, it is shown how the expression for Pr can be simplified by applying additional approximations.

Analytical derivation of Pr

5.3.3 Pr represents the probability of collision during the time interval $[t_{init}, t_{end}]$ of a longitudinal overlap. In order to determine Pr, two cases must be distinguished:

a) At t_{init}, the two aircraft are in lateral and vertical overlap so that the collision corresponds to a "front-to-rear" collision.

b) At t_{init}, the two aircraft are not in simultaneous lateral and vertical overlap; this simultaneous overlap happens at some time during $[t_{init}, t_{end}]$. The collision is either a "top-to-bottom" or a "side-to-side" collision.

5.3.4 Let P_1 and P_2 be the probability of collision corresponding to the first and second case respectively. The first case is the easier to derive. The probability to be in lateral overlap at t_{init} is given by $\int_{y=-\lambda_y}^{\lambda_y} f_y(y)dy$ (recall that $f_y(y)$ is the pdf of the relative lateral position *y*, so that both aircraft are in lateral overlap when $-\lambda_y \le y \le \lambda_y$) and is usually denoted by $P_y(S_y)$, as seen before in Chapter 3, 3.4. Similarly, the probability to be in vertical overlap at t_{init} is given by $\int_{z=-\lambda_z}^{\lambda_z} f_z(z)dz$ and is usually denoted by $P_z(0)$. The probability of collision corresponding to the first case is given by:

$$P_1 = P_y(S_y)\, P_z(0)\,. \tag{5-3}$$

5.3.5 Figure 5-3 illustrates the two scenarios of "top-to-bottom" collision and "side-to-side" collision corresponding to the second case. Each of these two scenarios has two further subcases, corresponding to opposite sides of the box. The box dimensions shown in Figure 5-2 are now used. For the "top-to-bottom" scenario illustrated in the left diagram of Figure 5-3, the longitudinal relative position at t_{init} belongs to $[-\lambda_x, \lambda_x]$ (since both aircraft are in longitudinal overlap) but there is no simultaneous lateral and vertical overlap. During the time interval from t_{init} until the collision, the relative vertical position, which was initially greater than λ_z, reduces to the value λ_z, which corresponds to a "top-to-bottom" collision. Notice that from t_{init} until the collision, the longitudinal relative position remains inside $[-\lambda_x, \lambda_x]$ since both aircraft are in longitudinal overlap.

5.3.6 Equation (4-15) is now used to determine the probability of collision P_2 in the time interval $[t_{init}, t_{end}]$ as

$$\begin{aligned} P_2 &= \Pr\left\{\text{collision during } [t_{init}, t_{end}]\right\} \\ &= \int_{t_{init}}^{t_{end}} \Psi(u)\,du \text{ with } \Psi(t) = \iint_{\partial\Omega}\left(\iiint f_t(X,V)(\vec{n}\bullet\vec{V})^+ dV\right)dS \end{aligned} \tag{5-4}$$

where the volume boundary $\partial\Omega$ corresponds to the left, right, top and bottom sides of the box. Following the notation of Figure 5-3, indices 1 and 1' are assigned to the top and bottom sides of the box, as well as indices 2 and 2' to the two lateral sides, such that $\partial\Omega$ corresponds to the union of the four sides 1, 1', 2 and 2'. The integral $\Psi(t)$ in Equation (5-4) is the sum of four integrals, one for each side:

$$\begin{aligned} \Psi(t) &= \iint_{\partial\Omega}\left(\iiint f_t(X,V)(\vec{n}\bullet\vec{V})^+ dV\right)dS \\ &= \Psi_1(t) + \Psi_{1'}(t) + \Psi_2(t) + \Psi_{2'}(t). \end{aligned} \tag{5-5}$$

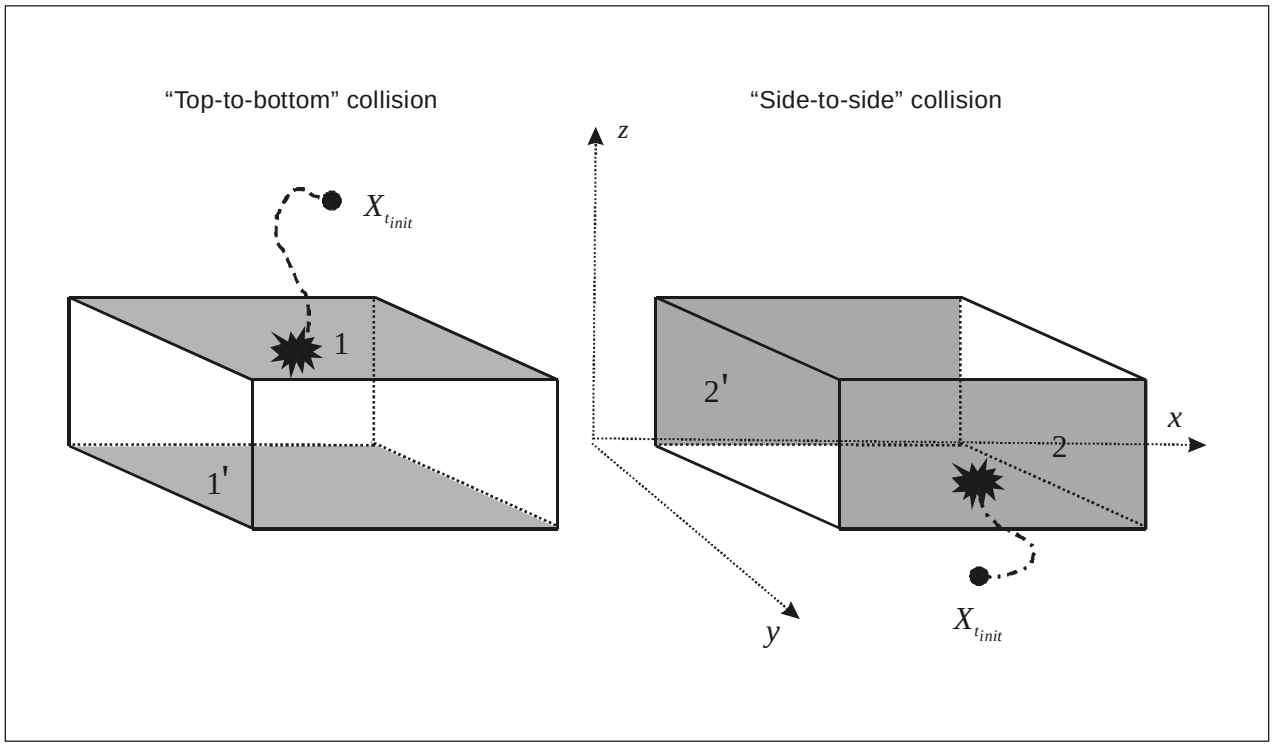

Figure 5-3. Top-to-bottom and side-to-side collisions

5.3.7 All four integrals will now be determined. The computations are developed in detail for the first integral only, since the three remaining integrals can be derived similarly. Starting with the first integral over the top of the box, represented in grey in Figure 5-2, the inward normal vector is directed downward so that the dot product $\left(\vec{n} \bullet \vec{V}\right)^{+}$ corresponds to $\dot{z}^{-}$ and

$$\Psi_1(t) = \int_{x=-\lambda_x}^{x=\lambda_x} \int_{y=-\lambda_y}^{y=\lambda_y} \iiint_{\dot{x}\,\dot{y}\,\dot{z}} \dot{z}^{-} f \, d\dot{z}\, d\dot{y}\, d\dot{x} dy dx \tag{5-6}$$

where

$$f = f_{x_t}(x)\; f_{\dot{x}_t|x_t}(\dot{x}_t = \dot{x}|x_t = x)\; f_y(y)\; f_{\dot{y}|y}(\dot{y}_t = \dot{y}|y_t = y)\; f_z(\lambda_z)\; f_{\dot{z}|z}(\dot{z}_t = \dot{z}|z_t = \lambda_z).$$

5.3.8 The following simplifications are now applied to Equation (5-6):

a) $\int_{\dot{y}=-\infty}^{\infty} f_{\dot{y}|y}(\dot{y}_t = \dot{y}|y_t = y)d\dot{y} = 1$ for all y.

b) $\int_{\dot{x}=-\infty}^{\infty} f_{\dot{x}_t|x_t}(\dot{x}_t = \dot{x}|x_t = x)d\dot{x} = 1$ for all x.

c) $\int_{y=-\lambda_y}^{\lambda_y} f_y(y)dy = P_y(S_y)$ represents the probability for the pair of aircraft to be in lateral overlap.

d) Since for all t in $[t_{init}, t_{end}]$ the pair of aircraft are in longitudinal overlap, $\int_{x=-\lambda_x}^{\lambda_x} f_{x_t}(x)dx = 1$.

e) $\int_{\dot{z}} \dot{z}^- f_{\dot{z}|z}(\dot{z}_t = \dot{z} | z_t = \lambda_z) d\dot{z} = E\left\{\dot{z}_t^- | z_t = \lambda_z\right\}$.

Thus, the following is obtained:

$$\Psi_1(t) = P_y(S_y)\, E\left\{\dot{z}_t^- | z_t = \lambda_z\right\}\, f_z(\lambda_z). \tag{5-7}$$

5.3.9 For the bottom face 1', the computation is similar to that for the top, except that the term $f_z(\lambda_z)$ is replaced by $f_z(-\lambda_z)$ and the inner product $\left(\vec{n} \bullet \vec{V}\right)^+$ now corresponds to $\dot{z}^+$. Therefore,

$$\Psi_{1'}(t) = P_y(S_y)\, E\left\{\dot{z}_t^+ | z_t = -\lambda_z\right\}\, f_z(-\lambda_z). \tag{5-8}$$

5.3.10 The lateral faces 2 and 2' are similar to the top and bottom, except that the y and z indices are swapped. Without showing the calculations, the following equations are obtained:

$$\Psi_2(t) = P_z(0)\, E\left\{\dot{y}_t^- | y_t = \lambda_y\right\}\, f_y(\lambda_y) \tag{5-9}$$

and

$$\Psi_{2'}(t) = P_z(0)\, E\left\{\dot{y}_t^+ | y_t = -\lambda_y\right\}\, f_y(-\lambda_y). \tag{5-10}$$

5.3.11 None of the terms $\Psi_1(t)$, $\Psi_2(t)$, $\Psi_{1'}(t)$ and $\Psi_{2'}(t)$ depend on time *t*, since the densities $f_{\dot{y}|y}\left(\dot{y}_t = \dot{y} | y_t = y\right)$ and $f_{\dot{z}|z}\left(\dot{z}_t = \dot{z} | z_t = z\right)$ are assumed to be time-independent. Using Equations (5-4), (5-5) and (5-7) to (5-10),

$$P_2 = \left(t_{end} - t_{init}\right)\Psi \tag{5-11}$$

with

$$\begin{aligned}\Psi = \; & P_y(S_y)\left(E\left\{\dot{z}_t^- | z_t = \lambda_z\right\}\, f_z(\lambda_z) + E\left\{\dot{z}_t^+ | z_t = -\lambda_z\right\}\, f_z(-\lambda_z)\right) \\ & + P_z(0)\left(E\left\{\dot{y}_t^- | y_t = \lambda_y\right\}\, f_y(\lambda_y) + E\left\{\dot{y}_t^+ | y_t = -\lambda_y\right\}\, f_y(-\lambda_y)\right).\end{aligned} \tag{5-12}$$

5.3.12 Since the probability Pr of collision during the time interval $[t_{init}, t_{end}]$ equals the sum of P_1 and P_2 the following equation is finally obtained:

$$\Pr = P_1 + P_2 = P_y\left(S_y\right) P_z\left(0\right) + \left(t_{end} - t_{init}\right)\Psi \tag{5-13}$$

with Ψ given by equation (5-12).

5.3.13 Equation (5-13) gives an analytical expression for the probability of collision during a longitudinal overlap, with a minimum of simplifications. Paragraphs 5.3.14 to 5.3.18 show how this expression can be simplified by the use of additional approximations.

Simplification of Pr using additional approximations

5.3.14 A first approximation in Equation (5-13) is to replace λ_y and λ_z by zero. This approximation is justified by the fact that λ_y and λ_z, which represent the width and height of an aircraft, are usually very small in comparison to the lateral and vertical navigational performance. Hence $f_z(\lambda_z)$ and $f_z(-\lambda_z)$ can be approximated by $f_z(0)$, and similarly $f_y(\lambda_y)$ and $f_y(-\lambda_y)$ can be approximated by $f_y(0)$. Using this first approximation, Ψ in Equation (5-13) becomes:

$$\begin{aligned}\Psi = \quad & P_y(S_y)\, f_z(0)\left(E\left\{\dot{z}_t^- \,|z_t = 0\right\} + E\left\{\dot{z}_t^+ \,|z_t = 0\right\}\right) \\ & + P_z(0)\, f_y(0)\left(E\left\{\dot{y}_t^- \,|y_t = 0\right\} + E\left\{\dot{y}_t^+ \,|y_t = 0\right\}\right).\end{aligned}$$

Then, since $E\left\{v^+\right\} + E\left\{v^-\right\} = E\left\{|v|\right\}$ for any real random variable v,

$$\Psi = P_y(S_y)\, f_z(0)\, E\left\{\left|\dot{z}_t\right| \middle| z_t = 0\right\} + P_z(0)\, f_y(0) E\left\{\left|\dot{y}_t\right| \middle| y_t = 0\right\}.$$

Finally, a consequence of approximating $f_z(\lambda_z)$ and $f_z(-\lambda_z)$ by $f_z(0)$ is that $\int_{y=-\lambda_y}^{\lambda_y} f_y(y)dy = P_y(S_y)$ can be rewritten as $P_y(S_y) = \int_{y=-\lambda_y}^{\lambda_y} f_y(y)dy \approx 2\lambda_y f_y(0)$ and similarly $P_z(0) \approx 2\lambda_z f_z(0)$. Using the above, the following is obtained for Equation (5-12):

$$\Psi = P_y(S_y)\, P_z(0)\left(\frac{E\left\{\left|\dot{z}_t\right| \middle| z_t = 0\right\}}{2\lambda_z} + \frac{E\left\{\left|\dot{y}_t\right| \middle| y_t = 0\right\}}{2\lambda_y}\right). \tag{5-14}$$

5.3.15 It has already been observed that the two terms $E\left\{\left|\dot{y}_t\right| \middle| y_t = 0\right\}$ and $E\left\{\left|\dot{z}_t\right| \middle| z_t = 0\right\}$ do not depend on time due to the stationarity assumption. $E\left\{\left|\dot{z}_t\right| \middle| z_t = 0\right\}$ can be seen as the expectation of the absolute value of the relative vertical speed conditional on a vertical overlap at *t* and the same holds for $E\left\{\left|\dot{y}_t\right| \middle| y_t = 0\right\}$ (expected absolute value of the relative lateral speed at *t* conditional on a lateral overlap at *t*).

5.3.16 The same notation as in Doc 9689 is now applied and $E\left\{\left|\dot{z}_t\right| \middle| z_t = 0\right\}$ and $E\left\{\left|\dot{y}_t\right| \middle| y_t = 0\right\}$ are represented as $\overline{|\dot{z}|}$ and $\overline{|\dot{y}|}$ respectively. Similarly, later in this document, the quantity $E\left\{\left|\dot{x}_t\right| \middle| x_t = 0\right\}$ (expected absolute value of the relative longitudinal speed at *t* conditional on a longitudinal overlap at *t*) will be denoted as $\overline{|\dot{x}|}$. However, the reader should keep in mind that these expected quantities are conditional on an overlap in the corresponding dimension and that they correspond to absolute values of relative speed "at the time of an overlap"**.** The following is thus obtained:

$$\mathrm{Pr} = P_1 + P_2 = P_y\left(S_y\right) P_z\left(0\right) + \left(t_{end} - t_{init}\right)\Psi \tag{5-15}$$

with

$$\Psi = P_y(S_y)\, P_z(0)\left(\frac{\overline{|\dot{z}|}}{2\lambda_z} + \frac{\overline{|\dot{y}|}}{2\lambda_y}\right). \tag{5-16}$$

5.3.17 Aggregating Equations (5-15) and (5-16) gives:

$$\Pr = P_y\left(S_y\right)P_z\left(0\right)\left(1+\left(t_{end}-t_{init}\right)\left(\frac{\overline{|\dot{y}|}}{2\lambda_y}+\frac{\overline{|\dot{z}|}}{2\lambda_z}\right)\right). \tag{5-17}$$

Equation (5-17) gives the value of the probability of collision during a longitudinal overlap as a function of the duration of the longitudinal overlap, $\left(t_{end}-t_{init}\right)$. When the relative speed between the two aircraft is large enough, this duration can be approximated by $t_{end}-t_{init}\approx\frac{2\lambda_x}{\overline{|\dot{x}|}}$, so that Equation (5-17) becomes:

$$\Pr = P_y\left(S_y\right)P_z\left(0\right)\left(1+\frac{\lambda_x}{\lambda_y}\frac{\overline{|\dot{y}|}}{\overline{|\dot{x}|}}+\frac{\lambda_x}{\lambda_z}\frac{\overline{|\dot{z}|}}{\overline{|\dot{x}|}}\right). \tag{5-18}$$

5.3.18 Equation (5-18) is the final expression for the probability of collision during a longitudinal overlap, which will be used later in this document. The intermediate equations (5-14) to (5-17) are given only for information, showing how to update the model in order to account for "atypical" cases (such as a pair of aircraft flying at nearly the same speed, with a prolonged duration of longitudinal overlap). In 5.4 and 5.5 the approximations given above will be used implicitly, and particularly the duration of a longitudinal overlap will always be approximated by $t_{end}-t_{init}\approx\frac{2\lambda_x}{\overline{|\dot{x}|}}$.

5.4 RISK ASSESSMENT BASED ON THE PROPORTION OF TIME IN LONGITUDINAL OVERLAP

5.4.1 The usual metric for collision risk is an expected number of fatal accidents per flying hour, where one collision counts for two fatal accidents. In order to perform the risk assessment one has to collect a sample of air traffic during an observation period and to count the number of longitudinal overlaps in the same and in the opposite direction. The reason why one distinguishes between same and opposite direction will be explained later in this document. It results from the very different values of the relative speeds.

5.4.2 For each pair of aircraft in longitudinal overlap, the corresponding probability of collision is given by Equation (5-18); the value of the total risk corresponds to the sum of all the probabilities of collision multiplied by two to convert from collisions to accidents. The risk per flying hour is then the ratio of the total risk divided by the total flight time.

5.4.3 Assuming that a sample of the air traffic has been collected during an observation period, F is used to denote the total flight time during the observation period, and nb_{same} and nb_{opp} the number of longitudinal overlaps in the same direction and in the opposite direction during the observation period.

5.4.4 The expected absolute value of the relative longitudinal speed conditional on a longitudinal overlap is still denoted by $\overline{|\dot{x}|}$ for two aircraft in the same direction. For two aircraft in the opposite direction, this expectation equals $2\overline{V}$, where $\overline{V}$ denotes the average speed of the aircraft.

5.4.5 Then, applying Equation (5-18), each of the nb_{same} longitudinal overlaps in the same direction has the same associated probability of collision, determined by:

$$P_{same} = P_y\left(S_y\right)P_z\left(0\right)\left(1+\frac{\lambda_x}{\lambda_y}\frac{\overline{|\dot{y}|}}{\overline{|\dot{x}|}}+\frac{\lambda_x}{\lambda_z}\frac{\overline{|\dot{z}|}}{\overline{|\dot{x}|}}\right) \tag{5-19}$$

and similarly each of the nb_{opp} longitudinal overlaps in the opposite direction have the same associated probability of collision, determined by:

$$P_{opp} = P_y\left(S_y\right)P_z\left(0\right)\left(1+\frac{\lambda_x}{\lambda_y}\frac{\overline{|\dot{y}|}}{2\overline{V}}+\frac{\lambda_x}{\lambda_z}\frac{\overline{|\dot{z}|}}{2\overline{V}}\right). \tag{5-20}$$

5.4.6 The expected number of collisions in the same direction can be seen as the sum of nb_{same} Bernoulli random variables, with parameter P_{same}. In other words, the number of collisions is a binomial random variable, whose expectation corresponds to the product $nb_{same}\,P_{same}$. Therefore, the expected number of collisions in the same direction, $E\{Nb_{same}\}$, is given by:

$$E\left\{Nb_{same}\right\} = nb_{same}P_y\left(S_y\right)P_z\left(0\right)\left(1+\frac{\lambda_x}{\lambda_y}\frac{\overline{|\dot{y}|}}{\overline{|\dot{x}|}}+\frac{\lambda_x}{\lambda_z}\frac{\overline{|\dot{z}|}}{\overline{|\dot{x}|}}\right) \tag{5-21}$$

and similarly

$$E\left\{Nb_{opp}\right\} = nb_{opp}P_y\left(S_y\right)P_z\left(0\right)\left(1+\frac{\lambda_x}{\lambda_y}\frac{\overline{|\dot{y}|}}{2\overline{V}}+\frac{\lambda_x}{\lambda_z}\frac{\overline{|\dot{z}|}}{2\overline{V}}\right). \tag{5-22}$$

5.4.7 The usual metric of collision risk is an expected number of fatal accidents per flying hour, where one collision accounts for two fatal accidents. Since one collision corresponds to two fatal accidents, the expected number of fatal accidents per flying hour for aircraft in the same direction, $N_{ac,same}$, is given by:

$$N_{ac,same} = \frac{2nb_{same}}{F}P_y\left(S_y\right)P_z\left(0\right)\left(1+\frac{\lambda_x}{\lambda_y}\frac{\overline{|\dot{y}|}}{\overline{|\dot{x}|}}+\frac{\lambda_x}{\lambda_z}\frac{\overline{|\dot{z}|}}{\overline{|\dot{x}|}}\right) \tag{5-23}$$

and similarly, for aircraft in the opposite direction:

$$N_{ac,opp} = \frac{2nb_{opp}}{F}P_y\left(S_y\right)P_z\left(0\right)\left(1+\frac{\lambda_x}{\lambda_y}\frac{\overline{|\dot{y}|}}{2\overline{V}}+\frac{\lambda_x}{\lambda_z}\frac{\overline{|\dot{z}|}}{2\overline{V}}\right). \tag{5-24}$$

5.4.8 Let $\Pi_x(same)$ denote the probability that one aircraft is in longitudinal overlap with another aircraft in the same direction at any time. Then $\Pi_x(same)$ can be estimated as the ratio of the total time spent by all aircraft in longitudinal overlap in the same direction, divided by the total flight time. The total flight time spent by all aircraft in longitudinal overlap in the same direction is estimated as $2nb_{same}\times\frac{2\lambda_x}{\overline{|\dot{x}|}}$ (recall that all longitudinal overlaps in the same direction are assigned the same duration $\frac{2\lambda_x}{\overline{|\dot{x}|}}$) so that:

$$\Pi_x(same) = \frac{2nb_{same}\times\frac{2\lambda_x}{\overline{|\dot{x}|}}}{F} \tag{5-25}$$

and similarly

$$\Pi_x(opp) = \frac{2\, nb_{opp} \times \frac{\lambda_x}{\bar{V}}}{F}. \tag{5-26}$$

5.4.9 Inserting Equation (5-25) into Equation (5-23) the following is finally obtained:

$$N_{ac,same} = \Pi_x(same)\, P_y\left(S_y\right) P_z(0) \left(\frac{\overline{|\dot{x}|}}{2\lambda_x} + \frac{\overline{|\dot{y}|}}{2\lambda_y} + \frac{\overline{|\dot{z}|}}{2\lambda_z} \right) \tag{5-27}$$

and similarly

$$N_{ac,opp} = \Pi_x(opp)\, P_y\left(S_y\right) P_z(0) \left(\frac{\bar{V}}{\lambda_x} + \frac{\overline{|\dot{y}|}}{2\lambda_y} + \frac{\overline{|\dot{z}|}}{2\lambda_z} \right). \tag{5-28}$$

5.4.10 These are the fundamental equations of the Reich model for same- and opposite-direction parallel routes respectively, expressed in terms of proportion of time in longitudinal overlap. In practice the only available data for estimating $\Pi_x(same)$ and $\Pi_x(opp)$ consists of flight plan archives. Instead of counting events involving longitudinal overlap, it is more convenient to count proximate events, which correspond to pairs of aircraft which are longitudinally within S_x (set at 120 NM in Chapter 10, Reference 11). Assuming that the longitudinal distance between the aircraft in a pair is uniformly distributed within the interval $\left[-S_x, S_x\right]$, the probability of longitudinal overlap conditioned on a proximate event equals $\frac{2\lambda_x}{2S_x} = \frac{\lambda_x}{S_x}$.

5.4.11 Therefore, if $\Pi_{prox}(same)$ and $\Pi_{prox}(opp)$ denote the probability for a pair of aircraft to be longitudinally within S_x, then $\Pi_x(same) = \frac{\lambda_x}{S_x}\Pi_{prox}(same)$ and $\Pi_x(opp) = \frac{\lambda_x}{S_x}\Pi_{prox}(opp)$ are obtained such that Equations (5-27) and (5-28) become:

$$N_{ac,same} = \Pi_{proxx}(same)\, P_y\left(S_y\right) P_z(0) \frac{\lambda_x}{S_x} \left(\frac{\overline{|\dot{x}|}}{2\lambda_x} + \frac{\overline{|\dot{y}|}}{2\lambda_y} + \frac{\overline{|\dot{z}|}}{2\lambda_z} \right) \tag{5-29}$$

and

$$N_{ac,opp} = \Pi_{prox}(opp)\, P_y\left(S_y\right) P_z(0) \frac{\lambda_x}{S_x} \left(\frac{\bar{V}}{\lambda_x} + \frac{\overline{|\dot{y}|}}{2\lambda_y} + \frac{\overline{|\dot{z}|}}{2\lambda_z} \right). \tag{5-30}$$

5.4.12 In Chapter 10, References 8 and 11, the estimation of $\Pi_{prox}(same)$ and $\Pi_{prox}(opp)$ is made by counting in a flight plan data sample twice the number of "proximate pairs" and dividing by the overall number of aircraft. This approximate value is referred to as the occupancy and is denoted as E_s for the same direction and E_o for the opposite direction. Aggregating Equations (5-29) and (5-30) into a combined risk estimate, the following is obtained:

$$N_{ac} = P_y\left(S_y\right) P_z(0) \frac{\lambda_x}{S_x} \left\{ E_s \left(\frac{\overline{|\dot{x}|}}{2\lambda_x} + \frac{\overline{|\dot{y}|}}{2\lambda_y} + \frac{\overline{|\dot{z}|}}{2\lambda_z} \right) + E_o \left(\frac{\bar{V}}{\lambda_x} + \frac{\overline{|\dot{y}|}}{2\lambda_y} + \frac{\overline{|\dot{z}|}}{2\lambda_z} \right) \right\}. \tag{5-31}$$

5.5 RISK ASSESSMENT BASED ON THE FREQUENCY OF PASSING EVENTS

5.5.1 Equations (5-27) and (5-28) have an equivalent formulation in terms of the frequency of passing events. A passing frequency is an expected number of longitudinal overlaps experienced by an aircraft during one flying hour. Denoting by $N_x(same)$ and $N_x(opp)$ the passing frequency in the same direction and opposite direction, respectively and keeping the same notation as in 5.4, $N_x(same)$ can be estimated as the ratio of the overall number of longitudinal overlaps experienced by all aircraft in the same direction (one overlap being experienced by two aircraft) divided by the total flight time. This gives:

$$N_x(same) = \frac{2nb_{same}}{F} \tag{5-32}$$

and

$$N_x(opp) = \frac{2nb_{opp}}{F}. \tag{5-33}$$

5.5.2 By inserting Equation (5-32) into Equation (5-23), the following is obtained:

$$N_{ac,same} = N_x(same)\, P_y\left(S_y\right) P_z(0)\left(1 + \frac{\lambda_x}{\lambda_y}\frac{\overline{|\dot{y}|}}{\overline{|\dot{x}|}} + \frac{\lambda_x}{\lambda_z}\frac{\overline{|\dot{z}|}}{\overline{|\dot{x}|}}\right) \tag{5-34}$$

and similarly

$$N_{ac,opp} = N_x(opp)\, P_y\left(S_y\right) P_z(0)\left(1 + \frac{\lambda_x}{\lambda_y}\frac{\overline{|\dot{y}|}}{2\overline{V}} + \frac{\lambda_x}{\lambda_z}\frac{\overline{|\dot{z}|}}{2\overline{V}}\right). \tag{5-35}$$

These are the fundamental equations of the Reich model for same- and opposite-direction parallel routes, expressed in terms of passing frequency.

———————

Chapter 6

VERTICAL COLLISION RISK MODELLING

6.1 VERTICAL CRM FOR AIRCRAFT ON THE SAME ROUTE AT ADJACENT FLIGHT LEVELS

6.1.1 This case is completely similar to the lateral collision risk for aircraft on parallel routes developed in Chapter 5 except that the lateral and the vertical axis are now permuted. For example, the lateral separation term S_y is replaced by a vertical separation term S_z, and the term $P_y(S_y)$ which represented the probability for two aircraft laterally separated by S_y to be in lateral overlap is now replaced by $P_z(S_z)$ which represents the probability for two aircraft vertically separated by S_z to be in vertical overlap. Similarly $P_z(0)$ is replaced by $P_y(0)$ and more generally the indices z and y are permuted. Equation (5-18) which accounted for the probability of collision for a pair of aircraft in longitudinal overlap is now replaced by:

$$\Pr = P_y(0)P_z(S_z)\left(1+\frac{\lambda_x}{\lambda_y}\frac{\overline{|\dot{y}|}}{\overline{|\dot{x}|}}+\frac{\lambda_x}{\lambda_z}\frac{\overline{|\dot{z}|}}{\overline{|\dot{x}|}}\right). \tag{6-1}$$

6.1.2 Similarly, Equations (5-29) and (5-30) which give the risk estimate as a function of the occupancy for the same and opposite directions are replaced by:

$$N_{ac,same} = E(same)P_y(0)P_z(S_z)\frac{\lambda_x}{S_x}\left(\frac{\overline{|\dot{x}|}}{2\lambda_x}+\frac{\overline{|\dot{y}|}}{2\lambda_y}+\frac{\overline{|\dot{z}|}}{2\lambda_z}\right) \tag{6-2}$$

and

$$N_{ac,opp} = E(opp)P_y(0)P_z(S_z)\frac{\lambda_x}{S_x}\left(\frac{\bar{V}}{\lambda_x}+\frac{\overline{|\dot{y}|}}{2\lambda_y}+\frac{\overline{|\dot{z}|}}{2\lambda_z}\right). \tag{6-3}$$

6.1.3 In addition, Equations (5-34) and (5-35) which give the risk estimate as a function of the frequency of passing events for the same and opposite directions are now replaced by:

$$N_{ac,same} = N_x(same)P_y(0)P_z(S_z)\left(1+\frac{\lambda_x}{\lambda_y}\frac{\overline{|\dot{y}|}}{\overline{|\dot{x}|}}+\frac{\lambda_x}{\lambda_z}\frac{\overline{|\dot{z}|}}{\overline{|\dot{x}|}}\right) \tag{6-4}$$

and

$$N_{ac,opp} = N_x(opp)P_y(0)P_z(S_z)\left(1+\frac{\lambda_x}{\lambda_y}\frac{\overline{|\dot{y}|}}{2\bar{V}}+\frac{\lambda_x}{\lambda_z}\frac{\overline{|\dot{z}|}}{2\bar{V}}\right). \tag{6-5}$$

6.1.4 Equations (6-2) to (6-5) give the analytical expressions of the Reich model for vertical collision risk in the same and opposite directions. Next the crossing routes case is considered.

6.2 NOTATION AND ASSUMPTIONS FOR CROSSING ROUTES

6.2.1 The main difference with the parallel routes model is that the error terms are no longer decoupled in the three dimensions, but only in the vertical and horizontal. Two steady aircraft on two crossing routes are considered. S_z denotes the vertical separation of the two routes. It is assumed that the two aircraft will overlap in the horizontal plane during the flight time on their routes, and t_{init} and t_{end} denote the beginning and the end of their horizontal overlap. Recall (see Figure 6-1) that a horizontal overlap corresponds to an overlap in the horizontal plane of the two cylinders associated with each aircraft.

6.2.2 To determine the probability of collision for the two aircraft between t_{init} and t_{end}, as in the parallel routes case of Chapter 4, a reference frame centred on one of the aircraft is taken, such that a collision corresponds to the situation that the relative position between the aircraft belongs to the cylinder shown in Figure 6-2. (X_t,V_t) continues to denote the couple made up of the relative position and the relative speed (both of them being three-dimensional) for the pair of aircraft, and f_t denotes the joint probability density function of this couple, conditioned on the pair being in horizontal overlap.

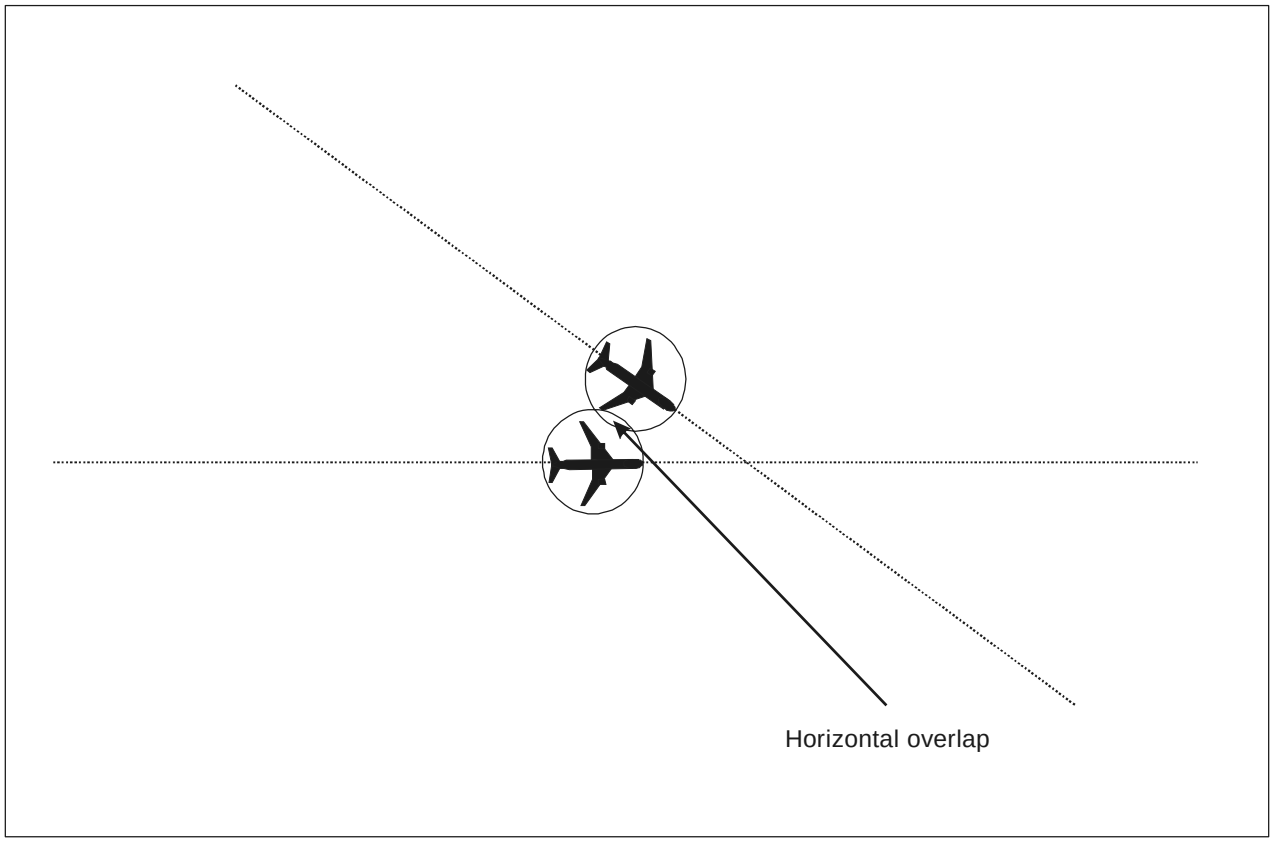

Figure 6-1. Horizontal overlap

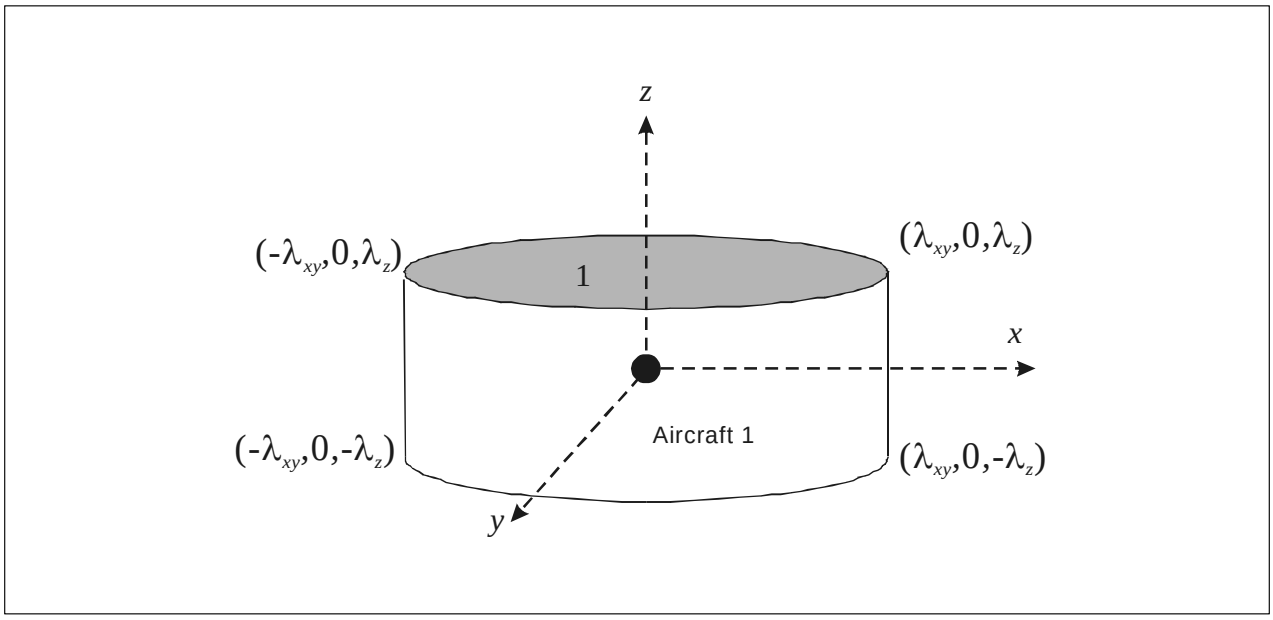

Figure 6-2. Reference frame centred on one aircraft

6.2.3 The assumptions are the same as for the parallel routes case, but when considering the distributions of the horizontal terms, there is no decoupling into the longitudinal and lateral dimensions. Rather they are kept together in the joint distribution. First, it is assumed that the relative speeds and positions are independent in the horizontal and vertical dimensions. If $X = (x, y, z)$ denotes the three components of the relative position and $V = (\dot{x}, \dot{y}, \dot{z})$ denotes the three components of the relative speed, the joint probability density function $f_t(X, V)$ can be written as the product of two factors:

$$f_t(X, V) = f_{x,y,\dot{x},\dot{y},t}(x, y, \dot{x}, \dot{y})\, f_{z,\dot{z},t}(z, \dot{z}). \tag{6-6}$$

6.2.4 Secondly, as for the same/parallel routes case, it is assumed that the relative speed and position in the vertical dimension correspond to a "steady state" independent of the time. This means that when the (position, speed) densities are decoupled as:

$$\begin{aligned} f_{x,\dot{x},y,\dot{y},t}(x, y, \dot{x}, \dot{y}) &= f_{x_t,y_t}\left((x_t, y_t) = (x, y)\right)\, f_{\dot{x}_t,\dot{y}_t|x_t,y_t}\left((\dot{x}_t, \dot{y}_t) = (\dot{x}, \dot{y}) \middle| (x_t, y_t) = (x, y)\right) \\ f_{z,\dot{z},t}(z, \dot{z}) &= f_z(z)\, f_{\dot{z}|z}(\dot{z}_t = \dot{z} \,|\, z_t = z) \end{aligned} \tag{6-7}$$

the densities $f_z(z)$ and $f_{\dot{z}|z}(\dot{z}_t = \dot{z} \,|\, z_t = z)$ no longer depend on the time.

6.2.5 The probability density functions defined in Equation (6-7) are:

a) $f_{x_t,y_t}\left((x_t, y_t) = (x, y)\right)$ is the probability density function of the relative horizontal position at time *t*, and $f_{\dot{x}_t,\dot{y}_t|x_t,y_t}\left((\dot{x}_t, \dot{y}_t) = (\dot{x}, \dot{y}) \middle| (x_t, y_t) = (x, y)\right)$ is the probability density function of the relative horizontal speed at time *t* conditional on the relative horizontal position at time *t*.

b) f_z is the probability density function of the relative vertical position at any time, and $f_{\dot{z}|z}\left(\dot{z}_t = \dot{z} \,|\, z_t = z\right)$ is the probability density function of the relative vertical speed at any time *t* conditional on the relative vertical position at the same time *t*.

6.2.6 As for the same/parallel routes case, the key term in the Reich model is the probability of collision during a horizontal overlap. First this term is determined, which is denoted as Pr. Again two steps are followed: first an analytical expression is derived for Pr and then that expression is simplified with the help of additional approximations.

Analytical derivation of Pr

6.2.7 Pr represents the probability of collision during the time interval $[t_{init},t_{end}]$ of a horizontal overlap. Here also two cases are distinguished:

a) At t_{init}, the two aircraft are in vertical overlap so that the collision corresponds to a "side-to-side" collision.

b) At t_{init}, the two aircraft are not in vertical overlap, but this overlap happens at some time during $[t_{init},t_{end}]$. The collision is then a "top-to-bottom" type of collision.

6.2.8 P_1 and P_2 denote the probability of collision corresponding to the first and second case respectively. The first case is the easier to derive. The probability to be in vertical overlap at time t_{init}, $\int_{z=-\lambda_z}^{\lambda_z} f_z(z)dz$, is again denoted by $P_z(S_z)$. The probability of collision corresponding to the first case is therefore given by:

$$P_1 = P_z(S_z). \tag{6-8}$$

6.2.9 Figure 6-3 illustrates the two possibilities for a scenario of "top-to-bottom" collision corresponding to the second case. The cylinder is similar to the one represented in Figure 6-2. Notice that for the two possibilities the horizontal component of X_t remains within λ_{xy} from the centre of the cylinder since the pair of aircraft is assumed to be in horizontal overlap.

6.2.10 The probability of collision P_2 is then determined by using Equation (4-15) on the time interval $[t_{init},t_{end}]$:

$$\begin{aligned} P_2 &= \Pr\left\{\text{collision during } \left[t_{init}, t_{end}\right]\right\} \\ &= \int_{t_{init}}^{t_{end}} \Psi(u)\,du \text{ with } \Psi(t) = \iint_{\partial\Omega}\left(\iiint f_t(X,V)(\vec{n}\bullet\vec{V})^+ dV\right)dS \end{aligned} \tag{6-9}$$

where the volume boundary $\partial\Omega$ corresponds to the top and bottom sides. Following the notation of Figure 6-3, indices 1 and 1' are assigned to the top and bottom of the cylinder such that $\partial\Omega$ corresponds to the union of the top and bottom 1 and 1'. The integral $\Psi(t)$ in Equation (6-9) is the sum of two integrals, one for the top and one for the bottom:

$$\begin{aligned} \Psi(t) &= \iint_{\partial\Omega}\left(\iiint f_t(X,V)(\vec{n}\bullet\vec{V})^+ dV\right)dS \\ &= \Psi_1(t) + \Psi_{1'}(t). \end{aligned} \tag{6-10}$$

6.2.11 Starting with the first integral over the top of the cylinder, represented in grey in Figure 6-2, the inward normal vector is directed downward so that the dot product $\left(\vec{n}\bullet\vec{V}\right)^+$ corresponds to $\dot{z}^-$. The following is obtained:

$$\Psi_1(t) = \iint_{x^2+y^2\le\lambda_{xy}^2} \iint_{(\dot{x},\dot{y})} \int_{\dot{z}} \dot{z}^-(\ldots)\,d\ldots \tag{6-11}$$

where $d\ldots$ represents the product of the five infinitesimals $dx\ dy\ d\dot{x}\ d\dot{y}\ d\dot{z}$ and the symbol (…) represents to the product:

$$f_{x_t,y_t}\left((x,y)\right) f_{\dot{x}_t,\dot{y}_t|x_t,y_t}\left((\dot{x},\dot{y})\middle|(x,y)\right) f_z(\lambda_z)\, f_{\dot{z}|z}(\dot{z}\,|\lambda_z).$$

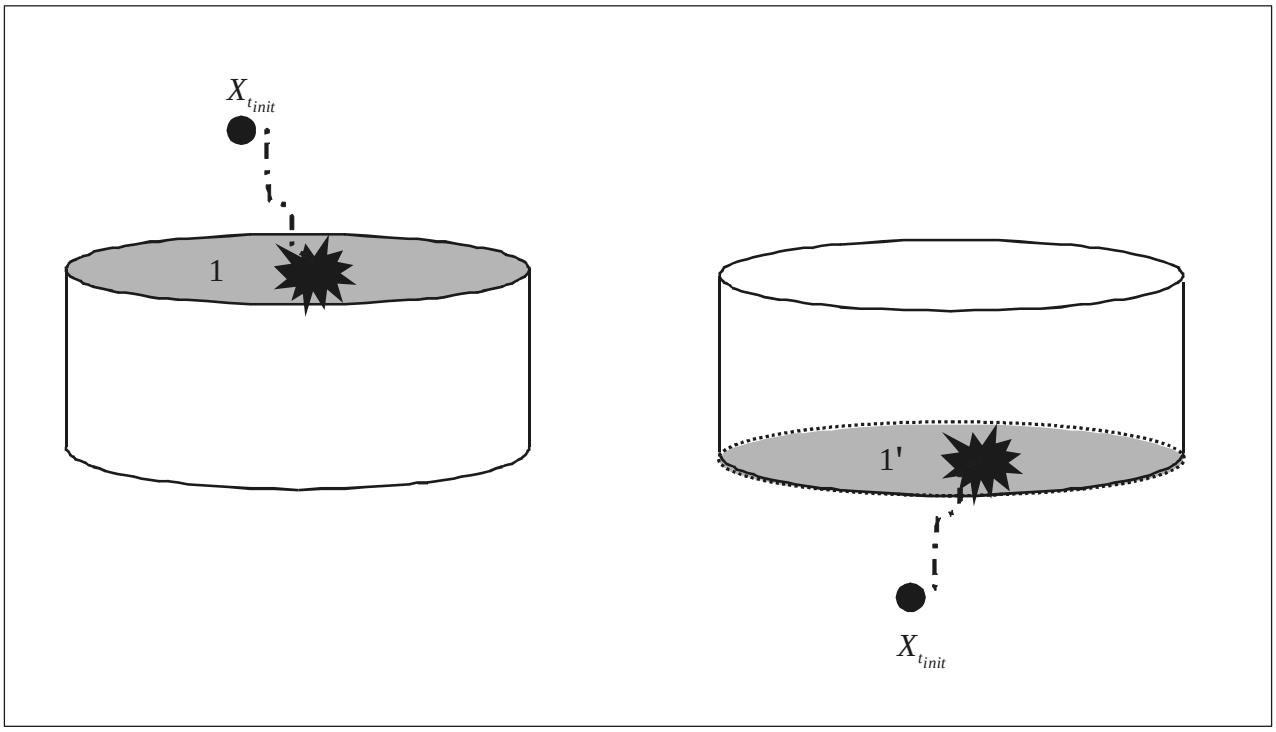

Figure 6-3. Two top-to-bottom collision possibilities

6.2.12 The following simplifications are then applied to Equation (6-11):

a) $\iint\limits_{\dot{x},\dot{y}} f_{\dot{x}_t,\dot{y}_t|x_t,y_t}\left((\dot{x},\dot{y})|(x,y)\right)d\dot{x}d\dot{y}=1$ for all (x,y);

b) $\iint\limits_{x^2+y^2\le\lambda_{xy}^2} f_{x_t,y_t}(x,y)\,dxdy=1$ (since for all t within $[t_{init},t_{end}]$ the pair is in horizontal overlap);

c) $\int\limits_{\dot{z}} \dot{z}^{-} f_{\dot{z}|z}(\dot{z}_t=\dot{z}|z_t=\lambda_z)d\dot{z}=E\left\{\dot{z}_t^{-}|z_t=\lambda_z\right\}$.

6.2.13 Thus, the following is obtained:

$$\Psi_1(t)=E\left\{\dot{z}_t^{-}|z_t=\lambda_z\right\}\,f_z(\lambda_z) \tag{6-12}$$

and similarly

$$\Psi_{1'}(t)=E\left\{\dot{z}_t^{+}|z_t=-\lambda_z\right\}\,f_z(-\lambda_z). \tag{6-13}$$

6.2.14 As for the same/parallel routes case, notice that $\Psi_1(t)$ and $\Psi_{1'}(t)$ do not depend on the time t since the conditional density $f_{\dot{z}|z}(\dot{z}_t=\dot{z}|z_t=\lambda_z)$ is assumed to be time-independent. It can be concluded that:

$$P_2=(t_{end}-t_{init})\Psi \tag{6-14}$$

with

$$\Psi = E\left\{\dot{z}_t^- \middle| z_t = \lambda_z\right\} f_z(\lambda_z) + E\left\{\dot{z}_t^+ \middle| z_t = -\lambda_z\right\} f_z(-\lambda_z) \tag{6-15}$$

and

$$\Pr = P_1 + P_2 = P_z(S_z) + \left(t_{end} - t_{init}\right)\Psi \tag{6-16}$$

with Ψ given by Equation (6-16). Equation (6-16) is the analytical expression for the probability of collision during a horizontal overlap based on a minimum of simplifications. This expression can then be simplified by applying additional approximations.

Simplification of Pr using additional approximations

6.2.15 As in Chapter 5, 5.3.14 to 5.3.18, a first approximation in Equation (6-16) consists of replacing λ_z by zero such that $f_z(\lambda_z)$ and $f_z(-\lambda_z)$ can be approximated by $f_z(0)$, and $f_z(0)$ can be approximated by $f_z(0) \approx \frac{P_z(S_z)}{2\lambda_z}$. Using the equality $E\left\{v^+\right\} + E\left\{v^-\right\} = E\left\{|v|\right\}$, Equation (6-15) becomes:

$$\Psi = E\left\{\left|\dot{z}_t\right| \middle| z_t = 0\right\} \frac{P_z(S_z)}{2\lambda_z} = \overline{|\dot{z}|} \frac{P_z(S_z)}{2\lambda_z}. \tag{6-17}$$

Once more the attention of the reader is drawn to the fact that $\overline{|\dot{z}|}$ represents the conditional expectation of the absolute value of the vertical speed at a fixed time, conditional on a vertical overlap happening at the same time.

6.2.16 The average duration of a horizontal overlap is then estimated, which is the value that will be used for [$t_{end} - t_{init}$]. v_{rel} denotes the relative horizontal speed of the two aircraft.

6.2.17 Figure 6-4 shows the trajectory of aircraft A_2 in a reference frame fixed to aircraft A_1 and oriented so as to make A_2 move along the vertical axis. Denoting by u the lateral offset of A_2 relative to A_1, it can be seen that a necessary and sufficient condition for a horizontal overlap to take place in the course of time is that u has to belong to the interval [$-\lambda_{xy}$, λ_{xy}]. For a given u in this interval, the portion of the trajectory of A_2 in horizontal overlap with A_1 has length $d = 2\sqrt{\lambda_{xy}^2 - u^2}$.

6.2.18 Assuming that the lateral offset of A_2 relative to A_1 can take any value uniformly in the range [$-\lambda_{xy}$, λ_{xy}], it can be seen that the average duration of an overlap is given by:

$$\begin{aligned} E\left\{t_{end} - t_{init}\right\} &= \frac{1}{2\lambda_{xy}} \int_{-\lambda_{xy}}^{\lambda_{xy}} \frac{2\sqrt{\lambda_{xy}^2 - u^2}}{v_{rel}} du \\ &= \frac{1}{v_{rel}} \int_{-\lambda_{xy}}^{\lambda_{xy}} \sqrt{1 - \left(\frac{u}{\lambda_{xy}}\right)^2}\, du \\ &= \frac{\pi}{2} \frac{\lambda_{xy}}{v_{rel}}. \end{aligned} \tag{6-18}$$

The fact that $\int_{-t}^{t} \sqrt{1 - \left(\frac{u}{t}\right)^2}\, du = \frac{t\pi}{2}$ has been used.

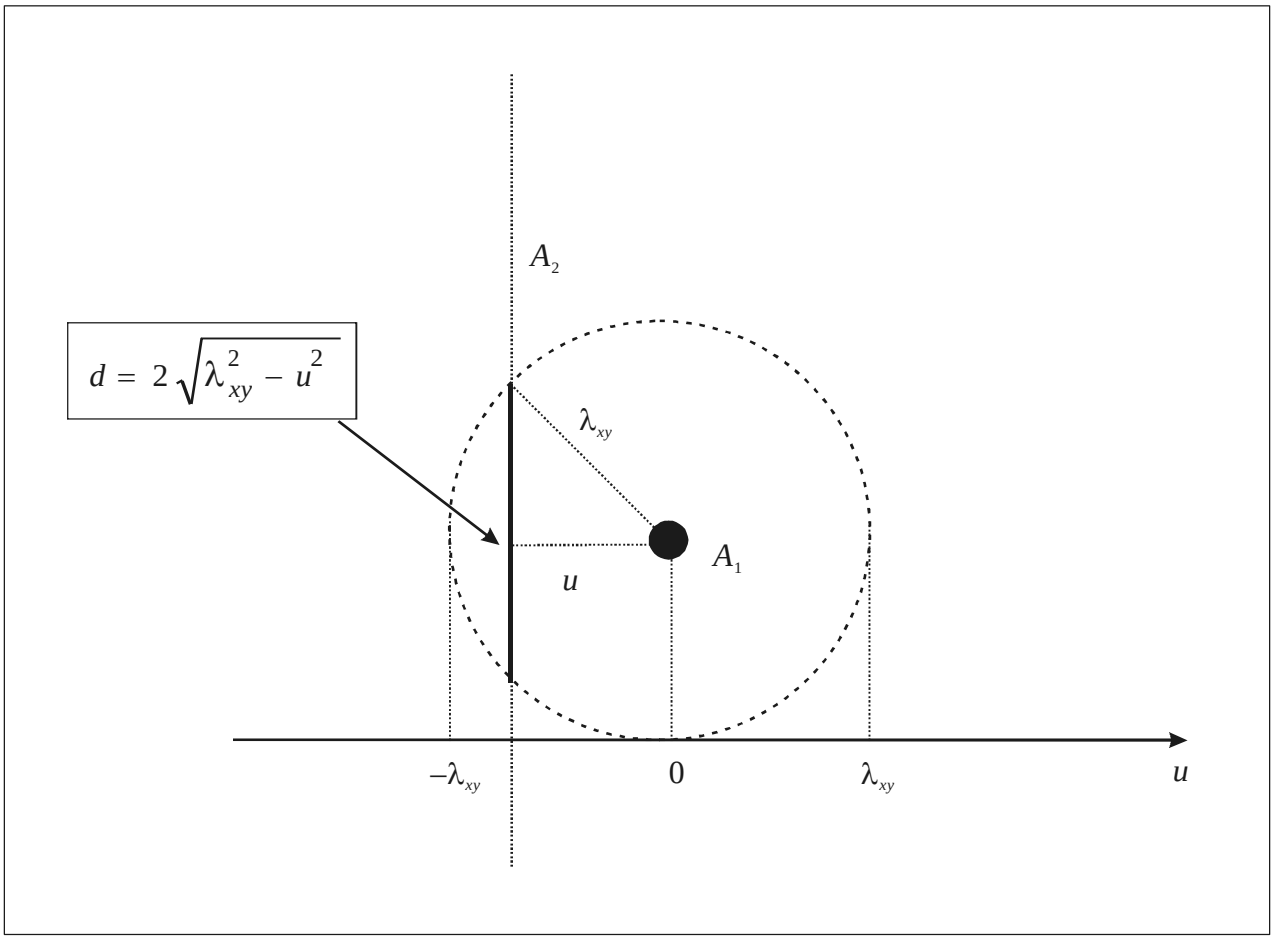

Figure 6-4. The trajectory of aircraft A_2 in a reference frame fixed to aircraft A_1 and oriented so as to make A_2 move along the vertical axis

6.2.19 Replacing ($t_{end} - t_{init}$) by its expectation in Equation (6-16) and using Equation (6-17), the following is finally obtained:

$$\Pr\{\text{collision during a horizontal overlap}\} = P_z(S_z)\left(1+\frac{\pi}{4}\frac{\overline{|\dot{z}|}}{v_{rel}}\frac{\lambda_{xy}}{\lambda_z}\right). \qquad (6\text{-}19)$$

Equation (6-19) gives the final value for the probability of collision during a horizontal overlap which will be used in the Reich model for crossing routes in 6.3.

6.3 RISK ASSESSMENT BASED ON PASSING FREQUENCY OR PROPORTION OF TIME IN HORIZONTAL OVERLAP

6.3.1 Let *N*(*cross*) be the passing frequency, i.e. the expected number of horizontal overlaps (one overlap being experienced by two aircraft) divided by the total flight time. It is given by:

$$N(cross) = \frac{2\,nb_{cross}}{F} \tag{6-20}$$

where nb_{cross} is the number of crossing events.

6.3.2 By following the same approach as in Equation (5-23), the expected number of fatal accidents per flying hour, $N_{acc,cross}$, is given by:

$$\begin{aligned} N_{ac,cross} &= \frac{2\,nb_{cross}\,\Pr\{\text{collision during a horizontal overlap}\}}{F} \\ &= N(cross)\,\Pr\{\text{collision during a horizontal overlap}\} \\ &= N(cross)P_z(S_z)\left(1+\frac{\pi}{4}\frac{\overline{|\dot{z}|}}{v_{rel}}\frac{\lambda_{xy}}{\lambda_z}\right) \end{aligned} \tag{6-21}$$

where Equations (6-20) and (6-19) have been used. The bottom line of Equation (6-21) is the fundamental equation of the Reich model for vertical collision risk on crossing routes, based on the passing frequency.

6.3.3 Similarly, $\Pi(cross)$ denotes the probability, taken over all aircraft pairs, of two aircraft having experienced horizontal overlap, i.e. the proportion of flight time when an aircraft is in horizontal overlap with another aircraft. It is given by:

$$\begin{aligned} \Pi(cross) &= \frac{2nb_{cross}E\{t_{end}-t_{init}\}}{F} \\ &= 2nb_{cross}\frac{\frac{\pi}{2}\frac{\lambda_{xy}}{v_{rel}}}{F}. \end{aligned} \tag{6-22}$$

6.3.4 Using this time Equations (6-19) and (6-22), $N_{acc,cross}$ is expressed in terms of $\Pi(cross)$ by:

$$\begin{aligned} \Pi(cross) &= \frac{2nb_{cross}E\{t_{end}-t_{init}\}}{F} \\ &= 2nb_{cross}\frac{\frac{\pi}{2}\frac{\lambda_{xy}}{v_{rel}}}{F}. \end{aligned} \tag{6-23}$$

The bottom line of Equation (6-23) is the fundamental equation of the Reich model for vertical collision risk on crossing routes, based on the proportion of time in horizontal overlap.

———————————

Chapter 7

LONGITUDINAL COLLISION RISK MODELLING FOR AIRCRAFT ON THE SAME ROUTE: DISTANCE-BASED SEPARATION

7.1 INTRODUCTION

7.1.1 This collision risk model is introduced in Attachment A to Appendix 5 of Doc 9689. The model considers a flow of consecutive aircraft on the same route at the same altitude in the same direction. The reporting period is denoted by T. τ is the communication and controller intervention buffer. τ corresponds to the overall duration required by the controller to successfully issue a collision avoidance instruction. It includes the communication delay, the duration for issuing the ATC instruction and the duration necessary for the pilot to execute the manoeuvre.

7.1.2 The difficulty with this collision risk model is estimating the probability of a pair of consecutive aircraft being in longitudinal overlap during their flight time. This probability is determined by reasoning as follows. For a pair of consecutive aircraft, the flight time is decomposed into consecutive time intervals of duration T. During each interval, the probability of longitudinal overlap is maximized if the two aircraft have simultaneously sent their position reports at the beginning of the time interval, at $t = 0$. This is because the position error is mainly due to the extrapolated speed error, so that it increases in the course of time. The probability is maximal if both aircraft send their reports simultaneously, since in that time the controller has to wait for T before receiving the next position report and deciding to issue a conflict avoidance clearance. This clearance will require an extra τ for being applied. Therefore, if a longitudinal overlap happens during the time interval $[0, T + \tau]$, it cannot be avoided by the controller.

7.2 NOTATION AND ASSUMPTIONS

This "worst-case" scenario is the one which is conservatively assumed for estimating the probability of longitudinal overlap during a time interval of duration $T + \tau$. $U(s)$ denotes the probability that a longitudinal overlap will occur between $t = 0$ and $t = T + \tau$ in this "worst-case scenario", given that the initial separation between the aircraft is s. The assumptions are the same as for the same/opposite-direction Reich model. $w(s)$ denotes the probability density function of the separation s between consecutive aircraft. Finally, the separation standard in use in the airspace is denoted by S_x. It follows from our "worst-case scenario" that for each time interval of duration $T + \tau$, the probability for a pair of consecutive aircraft to experience a longitudinal overlap during this time interval is bounded by $\int U(s)w(s)ds$.

7.3 DERIVATION OF THE COLLISION RISK

7.3.1 The application is similar to the same-direction Reich model, based on the proportion of time in longitudinal overlap. In the current case, the lateral and vertical separation minima S_y and S_z are zero, since the two aircraft are on the same route and at the same altitude. Equation (5-27) becomes:

$$N_{ac,x} = \Pi_x(same)\, P_y(0)\, P_z(0) \left(\frac{\overline{|\dot{x}|}}{2\lambda_x} + \frac{\overline{|\dot{y}|}}{2\lambda_y} + \frac{\overline{|\dot{z}|}}{2\lambda_z} \right). \tag{7-1}$$

7.3.2 Here, Π_x (*same*) corresponds to the proportion of time that a typical aircraft is in longitudinal overlap with another aircraft on the same track and flight level, summed over all aircraft pairs. In order to estimate Π_x (*same*), a fixed route is considered and *D* denotes the average flying time to traverse the entire route. It is assumed that at any time there are *N* aircraft on the track, with aircraft constantly entering at one end and leaving at the other. As a period of observation, a sufficiently large time period for *K N* aircraft to have completed their flight on the route is considered, which represents a total number of flight hours of *K N D*.

7.3.3 The *K N* consecutive aircraft can be seen as *K N* – 1 pairs of consecutive aircraft. For each such pair, the probability for the pair to have experienced a longitudinal overlap is determined as follows. For a pair of consecutive aircraft, the flight time *D* is split into consecutive time intervals of duration $T + \tau$, and the probability of longitudinal overlap during each time interval is bounded by $\int U(s)w(s)ds$. Using the inequality $\Pr\{A_1 \cup A_1 \ldots \cup A_k\} \le \Pr\{A_1\} + \Pr\{A_2\} + \ldots + \Pr\{A_k\}$, it can be seen that the probability for a pair to experience a longitudinal overlap during their flight time on the route is conservatively approximated as $\frac{D}{T}$ times $\int U(s)w(s)ds$:

$$\begin{aligned} P &= \Pr\{\text{longitudinal overlap for a pair}\} \\ &\le \frac{D}{T}\Pr\{\text{longitudinal overlap for a pair during } [0,\mathrm{T}+\tau]\} \\ &\le \frac{D}{T}\int U(s)w(s)ds. \end{aligned} \tag{7-2}$$

7.3.4 During the period of observation, the total flight time for the aircraft is equal to *K N D*, the total number of pairs of consecutive aircraft is *K N* – 1, and the expected time spent by all aircraft pairs in longitudinal overlap is given by $2\delta t\,(K\,N - 1)$ (Pr {longitudinal overlap for the pair}). As in the same/opposite-direction Reich model, the duration of a longitudinal overlap is approximated as $\delta t \approx \frac{2\lambda_x}{\overline{|\dot{x}|}}$. Here, it is possible to obtain an upper bound for δt, by noticing that the longitudinal overlap occurs between time $t = 0$ and $t = T + \tau$ for a pair of aircraft initially separated by *s*. Then, assuming that $s \ge S_x$, $\overline{|\dot{x}|} \ge \frac{S_x}{T+\tau}$ (since $|\dot{x}|$ corresponds to the expected relative longitudinal speed conditional on a longitudinal overlap), which implies that $\delta t \le (T+\tau)\frac{2\lambda_x}{S_x}$.

7.3.5 It can be concluded that the proportion of time in longitudinal overlap is given by:

$$\begin{aligned} \Pi_x(same) &= \frac{2\delta t\,(K\,N-1)\Pr\{\text{longitudinal overlap for a pair}\}}{K\,N\,D} \\ &= 2\delta t\,\frac{K\,N-1}{K\,N\,D}\left(\frac{D}{T+\tau}\int U(s)w(s)ds\right) \\ &\le \frac{4\lambda_x}{S_x}(T+\tau)\frac{1}{D}\left(\frac{D}{T+\tau}\int U(s)w(s)ds\right) \\ &\le \frac{4\lambda_x}{S_x}\int U(s)w(s)ds. \end{aligned} \tag{7-3}$$

Thus, a conservative estimate of the occupancy Π_x (*same*) is given by $\frac{4\lambda_x}{S_x}\int U(s)w(s)ds$.

7.3.6 As a conclusion, the expected number of fatal accidents per flying hour is given by:

$$N_{ac,x} = \left(\frac{4\lambda_x}{S_x} \int U(s)w(s)ds \right) P_y(0) P_z(0) \left(\frac{\overline{|\dot{x}|}}{2\lambda_x} + \frac{\overline{|\dot{y}|}}{2\lambda_y} + \frac{\overline{|\dot{z}|}}{2\lambda_z} \right). \tag{7-4}$$

This is the fundamental equation of the distance-based longitudinal collision risk model that can be found in Attachment A to Appendix 5 of Doc 9689.

7.4 AN ANALYTICAL ESTIMATION OF $\overline{|\dot{x}|}$

7.4.1 In this section a method for analytically determining $\overline{|\dot{x}|}$ is presented, which can be found in Appendix 1 of Doc 9689. The scenario is unchanged from the previous case. Let $\hat{d}_1^0$ and $\hat{d}_2^0$ be the nominal initial positions of the two aircraft, d_1^0 and d_2^0 their true initial positions, and $\varepsilon_1^A = d_1^0 - \hat{d}_1^0$ and $\varepsilon_2^A = d_2^0 - \hat{d}_2^0$ the initial along-track errors (see Figure 7-1).

7.4.2 Also let $\hat{V}_1$ and $\hat{V}_2$ be the nominal ground speeds of the two aircraft, V_1 and V_2 their true ground speeds, and $v_1 = V_1 - \hat{V}_1$ and $v_2 = V_2 - \hat{V}_2$ the difference between the true and the nominal ground speed. The true separation at time $t = T + \tau$ is given by:

$$\begin{aligned} sep &= \hat{d}_1^0 + \varepsilon_1^A + \left(\hat{V}_1 + v_1\right)(T+\tau) - \hat{d}_2^0 - \varepsilon_2^A - \left(\hat{V}_2 + v_2\right)(T+\tau) \\ &= \left[\hat{d}_1^0 - \hat{d}_2^0 + \left(\hat{V}_1 - \hat{V}_2\right)(T+\tau)\right] + \left[\varepsilon_1^A - \varepsilon_2^A + \left(v_1 - v_2\right)(T+\tau)\right] \end{aligned} \tag{7-5}$$

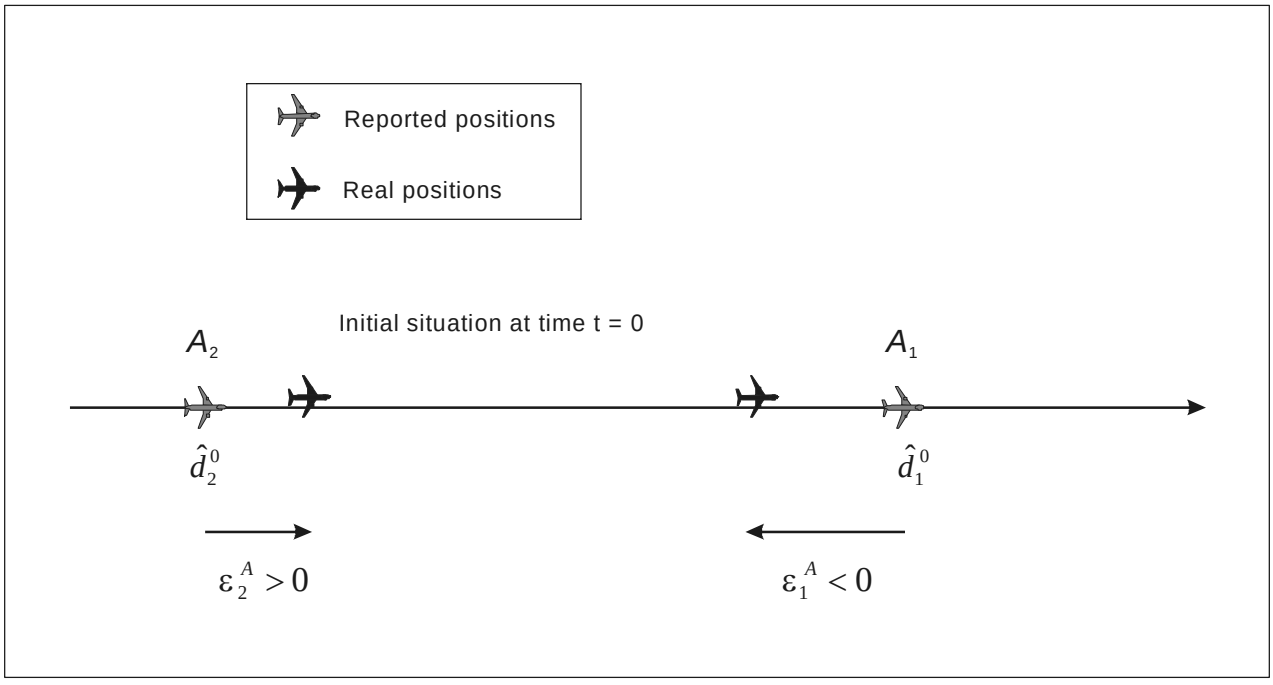

Figure 7-1. A method for analytically determining $\overline{|\dot{x}|}$

where the deterministic terms and the non-deterministic terms have been grouped inside square brackets. The condition for a longitudinal overlap to have happened before $t = T + \tau$ is that $sep \leq \lambda_x$ and the absolute value of the relative speed is given by $\left|\left(\hat{V}_1 - \hat{V}_2\right) + \left(v_1 - v_2\right)\right|$. Therefore, the expectation of the absolute value of the longitudinal relative speed conditional on a longitudinal overlap is given by:

$$\left|\dot{x}\right| = E\left\{ \left|\left(\hat{V}_1 - \hat{V}_2\right) + \left(v_1 - v_2\right)\right| \;\middle|\; \varepsilon_1^A - \varepsilon_2^A + \left(v_1 - v_2\right)\left(T + \tau\right) \leq \lambda_x - \left[\hat{d}_1^0 - \hat{d}_2^0 + \left(\hat{V}_1 - \hat{V}_2\right)\left(T + \tau\right)\right]\right\}. \qquad (7\text{-}6)$$

7.4.3 Equation (7-6) allows $\left|\dot{x}\right|$ to be determined analytically once the probability distributions of the error terms ε_1^A, ε_2^A, v_1 and v_2 are known.

Chapter 8

NON-STATIONARY COLLISION RISK MODELLING IN THE SAME AND OPPOSITE DIRECTIONS

8.1 GENERAL INTRODUCTION TO NON-STATIONARY COLLISION RISK MODELS (CRMS)

8.1.1 The CRMs introduced so far share some similarities in the sense that, for all of them, it is possible to derive a frequency of fatal accidents per flying hour as the product of two independent quantities:

a) one depending solely on the navigational performance in all three dimensions; and

b) one representing a frequency of horizontal overlaps per flying hour (or equivalently a probability for an individual aircraft to be in horizontal overlap).

8.1.2 The first quantity can be seen as the "average collision risk" for a given pair of aircraft in horizontal overlap. It is remarkable that for all these CRMs, the risk of collision can be averaged in such a way. The reason why this is possible is that, for all these CRMs, the aircraft are assumed to have reached a "steady-state" distribution of position errors in the vertical dimension, and also in the lateral dimension for parallel routes. In other words, it is possible to simplify the expression of the collision risk as an average risk per overlap times a frequency of overlap because the assumptions used require that the distribution of the position errors in one or two dimensions be independent of time.

8.1.3 In this chapter and in Chapter 9, two collision risk models (one for the same/opposite-direction case and one for the crossing case) are introduced, which apply to a pair of aircraft and which do not require any assumption on the time independence of the individual aircraft position or speed errors. In mathematical terminology the stochastic process of the relative position or speed is not required to be stationary in any dimension. Therefore, the two collision risk models can model any operational situation: aircraft are allowed to have vertical evolution, to execute manoeuvres, etc.

8.1.4 The benefit of these two collision risk models is that they can be applied to any operational scenario. The drawback is that, instead of returning a global risk estimate in terms of frequency of fatal accidents per flying hour, they return a probability of collision for an individual pair of aircraft in a predetermined scenario. Put differently, our two CRMs are more adapted to the risk assessment for one given hazard scenario rather than to the aggregation of all possible scenarios of error into a global distribution of position errors, as was done in the previous CRMs.

8.1.5 In this chapter the collision risk model for a pair of aircraft in the same or opposite direction is introduced. The collision risk model for crossing routes will be introduced in Chapter 9. First the model for the most general application, making as few assumptions as possible, is presented and then it is shown how this general model can be simplified by adding further assumptions.

8.2 NOTATION AND ASSUMPTIONS FOR THE SAME/PARALLEL ROUTES CRM

8.2.1 The configuration of the routes is the same as in Chapter 5. As in Chapter 5, Figure 5-4, S_y is the lateral separation between two routes, and $S_y = 0$ corresponds to both aircraft on the same route. The aim is to determine the risk of collision between the two aircraft during a given time interval $[t_0,t_1]$. As in the parallel routes Reich model, a

reference frame centred on one of the aircraft is taken so that a collision corresponds to both aircraft inside the box shown in Chapter 5, Figure 5-2. Again (X_t,V_t) is the couple of the relative position and the relative speed (both of them being three-dimensional) for the pair of aircraft, and f_t is the joint probability density function of this couple. It is assumed again that the relative position and speed components are independent in all three dimensions, such that:

$$f_t(X,V) = f_{x,\dot{x},t}(x,\dot{x})\, f_{y,\dot{y},t}(y,\dot{y})\, f_{z,\dot{z},t}(z,\dot{z}). \tag{8-1}$$

8.2.2 However, here no assumption is made on a steady-state distribution of the lateral and vertical relative position so that the distributions of the components are now given by:

$$\begin{aligned} f_{x,\dot{x},t}(x,\dot{x}) &= f_{x_t}(x_t = x)\, f_{\dot{x}_t|x_t}(\dot{x}_t = \dot{x} \,|\, x_t = x) \\ f_{y,\dot{y},t}(y,\dot{y}) &= f_{y_t}(y_t = y)\, f_{\dot{y}_t|y_t}(\dot{y}_t = \dot{y} \,|\, y_t = y) \\ f_{z,\dot{z},t}(z,\dot{z}) &= f_{z_t}(z_t = z)\, f_{\dot{z}_t|z_t}(\dot{z}_t = \dot{z} \,|\, z_t = z). \end{aligned} \tag{8-2}$$

The probability density functions defined in Equation (8-2) are the same as in Equation (5-2) for the parallel routes Reich model, except for $f_{z_t}(z_t = z)$ and $f_{y_t}(y_t = y)$ which now depend on time t.

8.3 DERIVATION OF THE COLLISION RISK MODEL

8.3.1 The main approximation made in this non-stationary collision risk model is that the box Ω is sufficiently small to justify that, when X_t is inside $\partial\Omega$ (the boundary of Ω), X_t can be approximated by the zero vector (0,0,0).

8.3.2 It is assumed that at the initial time t_0 the two aircraft are not in collision, so X_{t_0} is outside **Ω,** this being a necessary assumption for the application of Equation (4-15). By approximating the components of X_t by zero when X_t is inside Ω, Equation (4-15) becomes:

$$\begin{aligned} &\Pr\{\text{collision during } [t_0,t_1]\} = \int_{t_0}^{t_1} \Psi(t)\, dt \\ &\text{with } \Psi(t) = \iint_{\partial\Omega} \left(\iiint f_t(X,V)(\vec{n}\bullet\vec{V})^+ dV \right) dS \\ &\qquad = \iint_{(x,y,z)\in\partial\Omega} \left(\iiint_{\dot{x},\dot{y},\dot{z}} (\vec{n}\bullet\vec{V})^+ f_{x_t}(x)\, f_{\dot{x}_t|x_t}(\dot{x}|x)\, f_{y_t}(y)\, f_{\dot{y}_t|y_t}(\dot{y}|y) d\ldots \right) dS \\ &\qquad \approx \iint_{(x,y,z)\in\partial\Omega} \left(\iiint_{\dot{x},\dot{y},\dot{z}} (\vec{n}\bullet\vec{V})^+ f_{x_t}(0)\, f_{\dot{x}_t|x_t}(\dot{x}|0)\, f_{y_t}(0)\, f_{\dot{y}_t|y_t}(\dot{y}|0) d\ldots \right) dS. \end{aligned} \tag{8-3}$$

8.3.3 The boundary, $\partial\Omega$, is composed of the six faces of the box. $\Psi(t)$ in Equation (8-3) is decomposed as the sum of six integrals, one for each side. As in Chapter 5, Figure 5-3, indices 1 and 1' are assigned to the top and bottom sides, and 2 and 2' to the right and left sides. Finally indices 3 and 3' are assigned to the rear and front sides, and I_1, $I_{1'}$, I_2, $I_{2'}$, I_3, and $I_{3'}$ are the six integrals.

8.3.4 For the top of the box one obtains:

$$\begin{aligned} I_1(t) &= f_{z_t}(0) \left(\int_{x=-\lambda_x}^{x=\lambda_x} f_{x_t}(0) dx \right) \left(\int_{y=-\lambda_y}^{y=\lambda_y} f_{y_t}(0) dy \right) \left(\int_{\dot{x}} f_{\dot{x}_t|x_t}(\dot{x}|0) d\dot{x} \right) \left(\int_{\dot{y}} f_{\dot{y}_t|y_t}(\dot{y}|0) d\dot{y} \right) \left(\int_{\dot{z}} \dot{z}^- f_{\dot{z}_t|z_t}(\dot{z}|0) d\dot{z} \right) \\ &\approx \frac{\Pr\{|z_t| \le \lambda_z\}}{2\lambda_z} \Pr\{|x_t| \le \lambda_x\} \Pr\{|y_t| \le \lambda_y\} E\{\dot{z}_t^- \,|\, z_t = 0\} \end{aligned} \tag{8-4}$$

where $\left(\int_{\dot{x}} f_{\dot{x}_t|x_t}(\dot{x}|0)d\dot{x}\right)=1$, $\left(\int_{\dot{y}} f_{\dot{y}_t|y_t}(\dot{y}|0)d\dot{y}\right)=1$ and the approximation $f_{z_t}(0)\approx\dfrac{\Pr\{|z_t|\le\lambda_z\}}{2\lambda_z}$ have been used.

8.3.5 Similarly, one finds that:

$$I_{1'}=\frac{\Pr\{|z_t|\le\lambda_z\}}{2\lambda_z}\Pr\{|x_t|\le\lambda_x\}\Pr\{|y_t|\le\lambda_y\}E\{\dot{z}_t^{+}\,|z_t=0\}$$

and thus

$$I_1(t)+I_{1'}(t)=\frac{\Pr\{|z_t|\le\lambda_z\}}{2\lambda_z}\Pr\{|x_t|\le\lambda_x\}\Pr\{|y_t|\le\lambda_y\}E\{|\dot{z}_t||z_t=0\}. \tag{8-5}$$

8.3.6 In a similar way, one finds that:

$$I_2(t)+I_{2'}(t)=\frac{\Pr\{|y_t|\le\lambda_y\}}{2\lambda_y}\Pr\{|x_t|\le\lambda_x\}\Pr\{|z_t|\le\lambda_z\}E\{|\dot{y}_t||y_t=0\} \tag{8-6}$$

and

$$I_3(t)+I_{3'}(t)=\frac{\Pr\{|x_t|\le\lambda_x\}}{2\lambda_x}\Pr\{|y_t|\le\lambda_y\}\Pr\{|z_t|\le\lambda_z\}E\{|\dot{x}_t||x_t=0\}. \tag{8-7}$$

8.3.7 In conclusion, the probability of collision in the time interval $[t_0,t_1]$ is given by:

$$\begin{aligned}&\Pr\{\text{collision during }[t_0,t_1]\}=\int_{t_0}^{t_1}\Psi(t)\,dt \text{ with}\\ &\Psi(t)=\Pr\{|x_t|\le\lambda_x\}\Pr\{|y_t|\le\lambda_y\}\Pr\{|z_t|\le\lambda_z\}\left(\frac{E\{|\dot{x}_t||x_t=0\}}{2\lambda_x}+\frac{E\{|\dot{y}_t||y_t=0\}}{2\lambda_y}+\frac{E\{|\dot{z}_t||z_t=0\}}{2\lambda_z}\right).\end{aligned} \tag{8-8}$$

8.4 A SIMPLIFIED VERSION OF THE COLLISION RISK MODEL FOR PARALLEL ROUTES

Equation (8-8) gives the most general form of the non-stationary collision risk model, where no assumption is made on a "steady-state" distribution of any quantity. If, as in the Reich model for parallel routes, it is assumed that both the speed terms and the lateral and vertical position components have reached their steady-state distribution, Equation (8-8) simplifies to:

$$\begin{aligned}&\Pr\{\text{collision during }[t_0,t_1]\}=\int_{t_0}^{t_1}\Psi(t)\,dt\\ &\text{with }\Psi(t)=\Pr\{|x_t|\le\lambda_x\}P_y(S_y)P_z(0)\left(\frac{\overline{|\dot{x}|}}{2\lambda_x}+\frac{\overline{|\dot{y}|}}{2\lambda_y}+\frac{\overline{|\dot{z}|}}{2\lambda_z}\right)\end{aligned} \tag{8-9}$$

where the quantities $\overline{|\dot{z}|}$, $\overline{|\dot{y}|}$ and $\overline{|\dot{x}|}$ are defined as in Chapter 5, 5.3.14 to 5.3.18. This equation is more tractable if the factor $\Pr\{|x_t| \le \lambda_x\}$ is replaced by $2\lambda_x f_{x_t}(0)$, so that:

$$\Pr\{\text{collision during } [t_0, t_1]\} = \int_{t_0}^{t_1} \Psi(t)\, dt$$

$$\text{with } \Psi(t) = f_{x_t}(0) P_y(S_y) P_z(S_z) \left(\overline{|\dot{x}|} + \frac{\lambda_x}{\lambda_y} \overline{|\dot{y}|} + \frac{\lambda_x}{\lambda_z} \overline{|\dot{z}|} \right). \tag{8-10}$$

Chapter 9

NON-STATIONARY COLLISION RISK MODELLING FOR CROSSING ROUTES

9.1 NOTATION AND ASSUMPTIONS

9.1.1 Two aircraft with assigned crossing routes are considered with the aim of determining the risk of collision between the two aircraft during a given time interval $[t_0,t_1]$. As in the crossing routes Reich model, a reference frame centred on one of the aircraft is taken such that the collision corresponds to the situation where the relative position between the aircraft is inside the cylinder shown in Chapter 6, Figure 6-2. Again (X_t,V_t) is the couple made up of the relative position and the relative speed (both of them being three-dimensional) for the pair of aircraft, and f_t is the joint probability density function of this couple. It is also assumed that the relative speeds and positions are again independent in the horizontal and vertical dimensions, i.e.:

$$f_t\left(X,V\right) = f_{x,y,\dot{x},\dot{y},t}(x,y,\dot{x},\dot{y})\, f_{z,\dot{z},t}(z,\dot{z})\,. \tag{9-1}$$

9.1.2 However, here no assumption is made on a steady-state distribution of the vertical relative position. The joint distributions of the relative position and speed are given by:

$$\begin{aligned} f_{x,y,\dot{x},\dot{y},t}(x,y,\dot{x},\dot{y}) &= f_{x_t,y_t}\left((x_t,y_t)=(x,y)\right)\times f_{\dot{x}_t,\dot{y}_t|x_t,y_t}\left((\dot{x}_t,\dot{y}_t)=(\dot{x},\dot{y})\middle|(x_t,y_t)=(x,y)\right) \\ f_{z,\dot{z},t}(z,\dot{z}) &= f_{z_t}(z_t=z)\, f_{\dot{z}_t|z_t}(\dot{z}_t=\dot{z}\,|\,z_t=z). \end{aligned} \tag{9-2}$$

The probability density functions defined in Equation (9-2) are the same as for the crossing routes Reich model, except for $f_{z_t}(z_t = z)$ which is the probability density function of the relative vertical position error at time t.

9.2 DERIVATION OF THE COLLISION RISK MODEL

9.2.1 As for the previous non-stationary case in Chapter 8, 8.2, the main approximation made in this non-stationary collision risk model is that cylinder Ω is sufficiently small to justify that, when X_t is inside Ω, X_t can be approximated by the zero vector (0,0,0).

9.2.2 It is again assumed that at the initial time t_0 the two aircraft are not in collision, so that X_{t_0} is outside Ω. By approximating the components of X_t by zero when X_t is inside Ω, Equation (4-15) becomes:

$$
\begin{aligned}
&\Pr\{\text{collision during } [t_0,t_1]\} = \int_{t_0}^{t_1} \Psi(t)\,dt \\
&\text{with } \Psi(t) = \iint_{\partial\Omega}\left(\iiint f_t(X,V)(\vec{n}\bullet\vec{V})^+\,dV\right)dS \\
&\qquad = \iint_{(x,y,z)\in\partial\Omega}\left(\iiint_{\dot{x},\dot{y},\dot{z}}\left(\vec{n}\bullet\vec{V}\right)^+ f_{x_t,y_t}(x,y)\, f_{\dot{x}_t,\dot{y}_t|x_t,y_t}\left(\dot{x},\dot{y}\middle|x,y\right)\ldots\right)dS \\
&\qquad \approx \iint_{(x,y,z)\in\partial\Omega}\left(\iiint_{\dot{x},\dot{y},\dot{z}}\left(\vec{n}\bullet\vec{V}\right)^+ f_{x_t,y_t}(0,0)\, f_{\dot{x}_t,\dot{y}_t|x_t,y_t}\left(\dot{x},\dot{y}\middle|0,0\right)\ldots\right)dS.
\end{aligned}
\tag{9-3}
$$

9.2.3 The boundary surface of Ω, $\partial\Omega$, is decomposed into three parts: the top (having index 1), the bottom (having index 1') and the side (having index 2). $\Psi(t)$ in Equation (9-3) is decomposed as the sum of three integrals, one for each part. I_1, $I_{1'}$ and I_2 are these three integrals.

9.2.4 For the top of the cylinder,

$$
\begin{aligned}
I_1(t) &= \iint_{x^2+y^2\le\lambda_{xy}^2} f_{x_t,y_t}((0,0))\left(\iint_{\dot{x},\dot{y}} f_{\dot{x}_t,\dot{y}_t|x_t,y_t}\left((\dot{x},\dot{y})\middle|(0,0)\right)d\dot{x}d\dot{y}\right)\left(\int_{\dot{z}} \dot{z}^-\, f_{z_t}(0)\, f_{\dot{z}_t|z_t}(\dot{z}|0)d\dot{z}\right)dxdy \\
&= \pi\lambda_{xy}^2\; f_{x_t,y_t}((0,0))\, f_{z_t}(0)\, E\left\{\dot{z}_t^-\middle|z_t=0\right\} \\
&\approx \pi\lambda_{xy}^2\; f_{x_t,y_t}((0,0))\frac{\Pr\{|z_t|\le\lambda_z\}}{2\lambda_z} E\left\{\dot{z}_t^-\middle|z_t=0\right\}
\end{aligned}
\tag{9-4}
$$

where $\int_{\dot{x}}\int_{\dot{y}} f_{\dot{x}_t,\dot{y}_t|x_t,y_t}((\dot{x},\dot{y})\,|\,(0,0))d\dot{x}d\dot{y} = 1$ has been used, and $f_{z_t}(0)$ has been approximated by $f_{z_t}(0) \approx \dfrac{\Pr\{|z_t|\le\lambda_z\}}{2\lambda_z}$.

9.2.5 Similarly,

$$
I_{1'}(t) \approx \pi\lambda_{xy}^2\; f_{x_t,y_t}((0,0))\frac{\Pr\{|z_t|\le\lambda_z\}}{2\lambda_z} E\left\{\dot{z}_t^+\middle|z_t=0\right\} \tag{9-5}
$$

so that

$$
\begin{aligned}
I_1(t)+I_{1'}(t) &\approx \pi\lambda_{xy}^2\; f_{x_t,y_t}((0,0))\frac{\Pr\{|z_t|\le\lambda_z\}}{2\lambda_z}\left(E\left\{\dot{z}_t^+\middle|z_t=0\right\}+E\left\{\dot{z}_t^-\middle|z_t=0\right\}\right) \\
&\approx \pi\lambda_{xy}^2\; f_{x_t,y_t}((0,0))\frac{\Pr\{|z_t|\le\lambda_z\}}{2\lambda_z} E\left\{|\dot{z}_t|\middle|z_t=0\right\}.
\end{aligned}
\tag{9-6}
$$

9.2.6 For the integral over the side of the cylinder,

$$
I_2(t) = \left(\int_{\dot{z}} f_{\dot{z}_t|z_t}(\dot{z}|0)d\dot{z}\right)\left(\int_{z=-\lambda_z}^{z=\lambda_z} f_{z_t}(0)dz\right)\iint_{\dot{x},\dot{y}}\left(f_{x_t,y_t}((0,0))\oint_{x^2+y^2=\lambda_{xy}^2}\left(\vec{n}*\vec{V}\right)^+ dl\right) f_{\dot{x}_t,\dot{y}_t|x_t,y_t}\left((\dot{x},\dot{y})\middle|(0,0)\right)d\dot{x}d\dot{y}. \tag{9-7}
$$

First the quantity $\oint_{x^2+y^2=\lambda_{xy}^2} \left(\vec{n}\bullet\vec{V}\right)^+ dl$, which appears inside the integral $\iint_{\dot{x},\dot{y}} (\cdots) d\dot{x}d\dot{y}$, is determined. Denoting by C the two-dimensional circle: $C=\left\{(x,y); x^2+y^2=\lambda_{xy}^2\right\}$, and choosing for C an angular parameterization θ between $(\dot{x},\dot{y})$ and $\vec{n}$, it can be seen that (Figure 9-1) $\vec{n}\bullet\vec{V}=\sqrt{\dot{x}^2+\dot{y}^2}\cos(\pi+\theta)$ and thus $\left(\vec{n}\bullet\vec{V}\right)^+=0$ for θ in $\left[-\frac{\pi}{2},\frac{\pi}{2}\right]$ and $\left(\vec{n}*\vec{V}\right)^+=-\sqrt{\dot{x}^2+\dot{y}^2}\cos(\theta)$ for θ in $\left[\frac{\pi}{2},\frac{3\pi}{2}\right]$. Therefore:

$$\begin{aligned}\oint_{(x,y)\in C}\left(\vec{n}\bullet\vec{V}\right)^+ dl &= -\int_{\frac{\pi}{2}}^{\frac{3\pi}{2}} \sqrt{\dot{x}^2+\dot{y}^2}\,\lambda_{xy}\cos\theta\, d\theta \\ &= 2\sqrt{\dot{x}^2+\dot{y}^2}\,\lambda_{xy}.\end{aligned} \tag{9-8}$$

9.2.7 Returning to Equation (9-7) and using the result of Equation (9-8) the following is obtained:

$$\begin{aligned}I_2(t) &= \left(\int_{\dot{z}} f_{\dot{z}_t|z_t}(\dot{z}|0)d\dot{z}\right)\left(\int_{z=-\lambda_z}^{z=\lambda_z} f_{z_t}(0)dz\right)\iint_{\dot{x},\dot{y}}\left(f_{x_t,y_t}((0,0))\oint_{x^2+y^2=\lambda_{xy}^2}\left(\vec{n}*\vec{V}\right)^+ dl\right) f_{\dot{x}_t,\dot{y}_t|x_t,y_t}\left((\dot{x},\dot{y})|(0,0)\right)d\dot{x}d\dot{y} \\ &\approx 1\times \Pr\left\{|z_t|\le\lambda_z\right\}\times f_{x_t,y_t}((0,0))\iint_{\dot{x},\dot{y}} 2\lambda_{xy}\sqrt{\dot{x}^2+\dot{y}^2}\, f_{\dot{x}_t,\dot{y}_t|x_t,y_t}\left((\dot{x},\dot{y})|(0,0)\right)d\dot{x}d\dot{y} \\ &\approx 2\lambda_{xy}\Pr\left\{|z_t|\le\lambda_z\right\} f_{x_t,y_t}((0,0))E\left\{\sqrt{\dot{x}_t^2+\dot{y}_t^2}\,|(x_t,y_t)=(0,0)\right\}.\end{aligned} \tag{9-9}$$

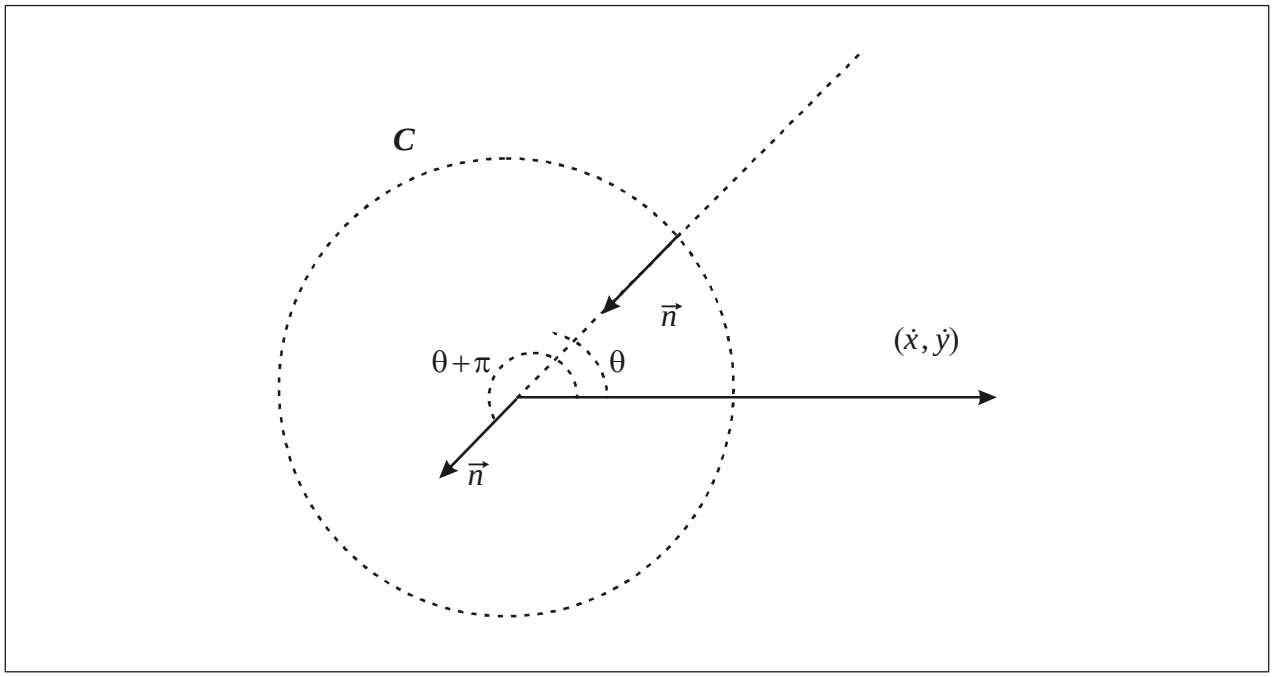

Figure 9-1. Integral over the side of the cylinder

9.2.8 Combining Equations (9-4), (9-5) and (9-7), it is found that:

$$\begin{aligned}\Psi(t) &= I_1(t) + I_{1'}(t) + I_2(t)\\ &= 2\lambda_{xy}\, f_{x_t,y_t}((0,0))\Pr\{|z_t| \le \lambda_z\}\, E\left\{\sqrt{\dot{x}_t^2 + \dot{y}_t^2}\,|(x_t, y_t) = (0,0)\right\} +\\ &\quad \pi\lambda_{xy}^2\, f_{x_t,y_t}((0,0))\frac{\Pr\{|z_t| \le \lambda_z\}}{2\lambda_z} E\{|\dot{z}_t| \mid z_t = 0\}\\ &= \pi\lambda_{xy}^2\, f_{x_t,y_t}((0,0))\Pr\{|z_t| \le \lambda_z\}\left(\frac{2}{\pi}\frac{E\left\{\sqrt{\dot{x}_t^2 + \dot{y}_t^2}\,|(x_t, y_t) = (0,0)\right\}}{\lambda_{xy}} + \frac{1}{2}\frac{E\{|\dot{z}_t| \mid z_t = 0\}}{\lambda_z}\right).\end{aligned} \tag{9-10}$$

9.2.9 $v_{rel,t}$ denotes the quantity $E\left\{\sqrt{\dot{x}_t^2 + \dot{y}_t^2}\,|(x_t, y_t) = (0,0)\right\}$ and $\overline{|\dot{z}_t|}$ the quantity $E\{|\dot{z}_t| \mid z_t = 0\}$. Using Equation (9-10), the following is obtained for the probability of collision during the time interval $[t_0, t_1]$:

$$P = \int_{t_0}^{t_1} \psi(t)\,dt \text{ with } \Psi(t) = \pi\lambda_{xy}^2\, f_{x_t,y_t}((0,0))\Pr\{|z_t| \le \lambda_z\}\left(\frac{2}{\pi}\frac{v_{rel,t}}{\lambda_{xy}} + \frac{1}{2}\frac{\overline{|\dot{z}_t|}}{\lambda_z}\right). \tag{9-11}$$

9.2.10 The index t in $v_{rel,t}$ and $\overline{|\dot{z}_t|}$ refers to the fact that these two quantities represent expectations at time t conditional on the fact that an overlap happens at time *t* in the corresponding dimension.

9.2.11 Equation (9-11) gives the probability of collision in the most general case. How the equation can be simplified if some further approximations are applied to the model will now be examined.

9.3 SIMPLIFIED VERSIONS OF THE NON-STATIONARY COLLISION RISK MODEL

9.3.1 The term $v_{rel,t}$ is the expectation of the relative horizontal speed at time *t* conditional on a horizontal overlap at *t*. It can be approximated by the relative horizontal speed for the aircraft pair, denoted by v_{rel}. Similarly, the term $\overline{|\dot{z}_t|}$ can be approximated by the absolute value of the vertical relative speed for the aircraft pair, denoted by $\overline{|\dot{z}|}$.

9.3.2 If none of the aircraft are in vertical motion, the term $\Pr\{|z_t| \le \lambda_z\}$ simplifies to $P_z(S_z)$, where S_z is the vertical separation between the aircraft. Finally, if all the previous approximations are combined:

$$P = \pi\lambda_{xy}^2\, P_z(S_z)\left(\frac{2}{\pi}\frac{v_{rel}}{\lambda_{xy}} + \frac{1}{2}\frac{\overline{|\dot{z}|}}{\lambda_z}\right)\int_{t_0}^{t_1} f_{x_t,y_t}((0,0))\,dt. \tag{9-12}$$

This is the usual expression for the non-stationary collision risk model for crossing routes.

9.4 APPLICATION TO A COLLISION RISK MODEL IN AN ADS-C ENVIRONMENT

9.4.1 The application presented in this section comes from the safety assessment performed in the context of the distance-based lateral separation for RNP k aircraft as specified in the *Procedures for Air Navigation Services — Air Traffic Management* (PANS-ATM, Doc 4444), 5.4.1.2.1.5.1:

> "For intersecting tracks, the entry points to and the exit points from the area in which the lateral distance between the tracks is less than the required minimum are termed lateral separation points. The area bounded by the lateral separation points is termed the area of conflict". (See Figure 9-2.)

The pertinent CRM is presented in Chapter 10, Reference 1.

9.4.2 Proceeding as in the case of the distance-based longitudinal collision risk model, the risk of collision during a time interval that consists of the reporting period plus the communication and controller intervention buffer is estimated. This time interval is denoted by $[t_0,t_1]$.

9.4.3 $\hat{d}_1^0$ and $\hat{d}_2^0$ denote the nominal distances before the intersection at time $t = t_0$ of aircraft 1 and 2. ε_1^A and ε_2^A denote the along-track errors and ε_1^C and ε_2^C the cross-track errors of the two aircraft. $f_A(x)$ denotes the probability density functions of ε_1^A and ε_2^A (assumed to have the same distribution) and $f_C(x)$ the probability density functions of ε_1^C and ε_2^C (also assumed to have the same distribution). It is assumed that the horizontal speeds of the two aircraft, denoted by V_1 and V_2, are constant during the time interval $[t_0,t_1]$. The coordinates of the actual positions of the two aircraft at time t are then given by:

$$\begin{aligned} x_1(t) &= -\hat{d}_1^0 + \varepsilon_1^A + V_1(t - t_0) \\ y_1(t) &= \varepsilon_1^C \end{aligned} \tag{9-13}$$

and

$$\begin{aligned} x_2(t) &= -\left(\hat{d}_2^0 - \varepsilon_2^A\right)\cos\theta - \varepsilon_2^C \sin\theta + V_2(t - t_0)\cos\theta \\ y_2(t) &= -\left(\hat{d}_2^0 - \varepsilon_2^A\right)\sin\theta + \varepsilon_2^C \cos\theta + V_2(t - t_0)\sin\theta. \end{aligned} \tag{9-14}$$

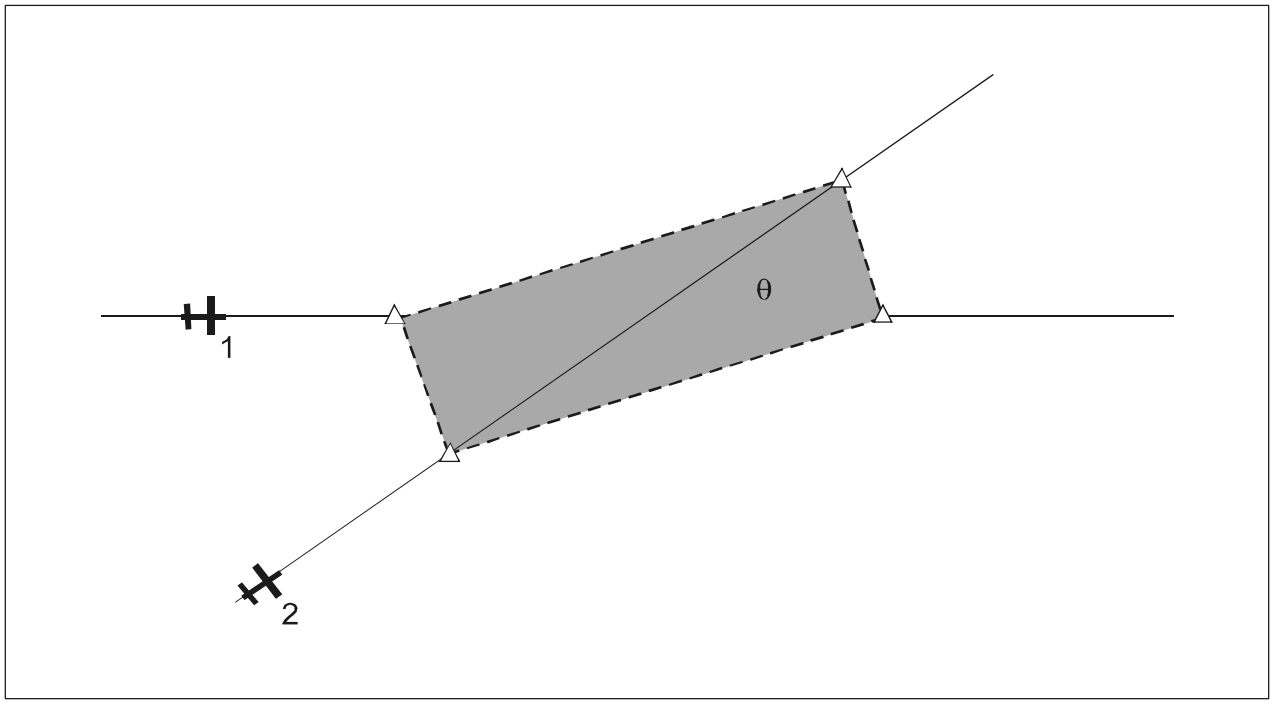

Figure 9-2. Area of conflict

Note that the along-track and cross-track errors are assumed to be constant during the time interval $[t_0,t_1]$, and positive, except for ε_2^A which is negative in the configuration shown in Figure 9-3.

9.4.4 The true difference in *x*-coordinates at time *t* is thus given by:

$$\begin{aligned}\Delta x(t) &\equiv x_1(t) - x_2(t) \\ &= (V_1 - V_2\cos\theta)(t - t_0) - \hat{d}_1^0 + \hat{d}_2^0\cos\theta + \varepsilon_1^A - \varepsilon_2^A\cos\theta + \varepsilon_2^C\sin\theta \\ &= D_x(t) + \varepsilon_1^A - \varepsilon_2^A\cos\theta + \varepsilon_2^C\sin\theta\end{aligned} \tag{9-15}$$

where $D_x(t) = (V_1 - V_2\cos\theta)(t - t_0) - \hat{d}_1^0 + \hat{d}_2^0\cos\theta$ is the nominal difference in *x*-coordinates at time *t*, given V_1 and V_2.

9.4.5 Similarly, the true difference in *y*-coordinates at time *t* is given by:

$$\begin{aligned}\Delta y(t) &\equiv y_1(t) - y_2(t) \\ &= -V_2(t - t_0)\sin\theta + \hat{d}_2^0\sin\theta + \varepsilon_1^C - \varepsilon_2^A\sin\theta - \varepsilon_2^C\cos\theta \\ &= D_y(t) + \varepsilon_1^C - \varepsilon_2^A\sin\theta - \varepsilon_2^C\cos\theta\end{aligned} \tag{9-16}$$

where

$$D_y(t) = -V_2(t - t_0)\sin\theta + \hat{d}_2^0\sin\theta.$$

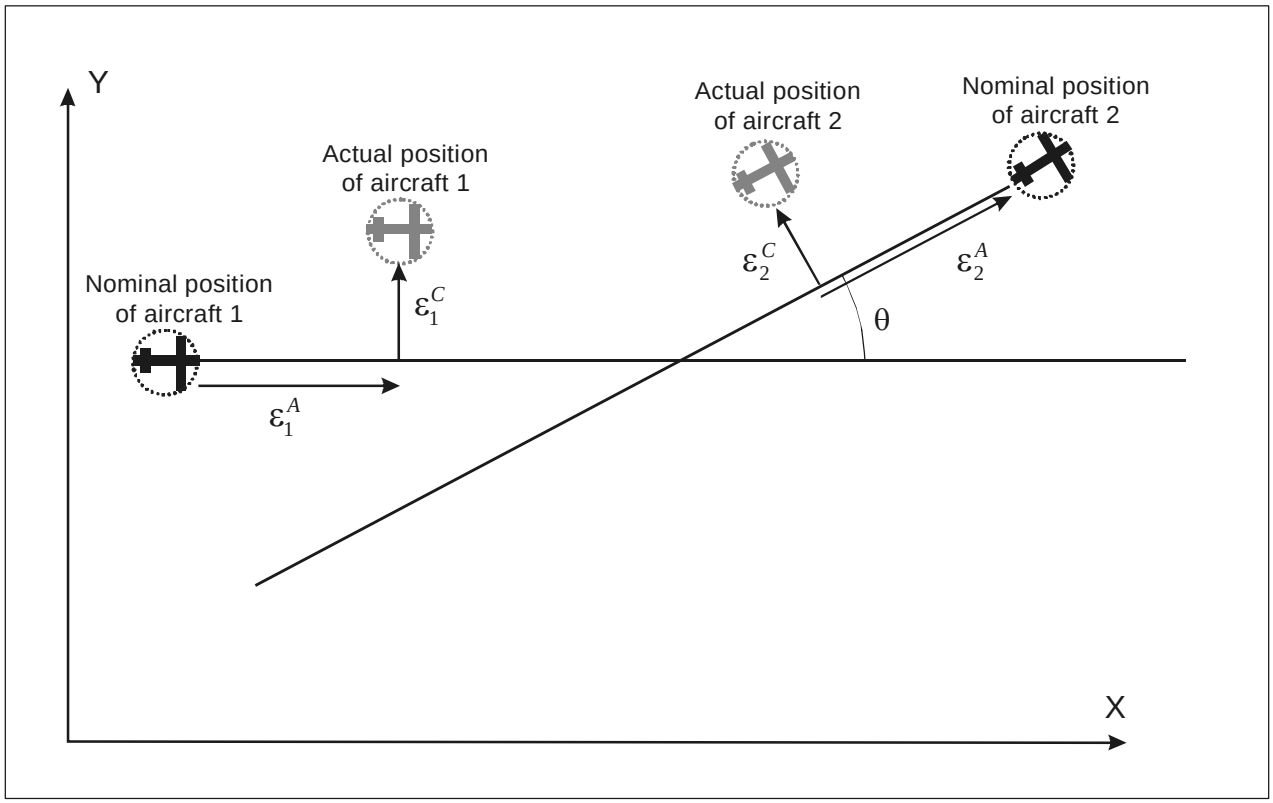

Figure 9-3. Depiction of along-track errors

9.4.6 In order to determine the quantity $f_{x_t,y_t}((0,0))$ of Equation (9-12) (which is the value of the probability density function associated with the two-dimensional relative position at (0,0)), the probability for the two-dimensional relative position $(\Delta x(t), \Delta y(t))$ is now estimated to be in a small square of size $2h \times 2h$:

$$
\begin{aligned}
P &= \Pr\left\{-h \le \Delta y(t) \le h \text{ and } -h \le \Delta x(t) \le h\right\} \\
&= \int_{\varepsilon_2^A} f_A\left(\varepsilon_2^A\right) \int_{\varepsilon_2^C} f_C\left(\varepsilon_2^C\right) \left(\int_{\varepsilon_1^A=\varepsilon_2^A\cos\theta-\varepsilon_2^C\sin\theta-D_x(t)-h}^{\varepsilon_1^A=\varepsilon_2^A\cos\theta-\varepsilon_2^C\sin\theta-D_x(t)+h} f_A\left(\varepsilon_1^A\right) \right) \left(\int_{\varepsilon_1^C=\varepsilon_2^A\sin\theta+\varepsilon_2^C\cos\theta-D_y(t)-h}^{\varepsilon_1^C=\varepsilon_2^A\sin\theta+\varepsilon_2^C\cos\theta-D_y(t)+h} f_C\left(\varepsilon_1^C\right) \right) \mathrm{d}\varepsilon_2^C \mathrm{d}\varepsilon_1^C \mathrm{d}\varepsilon_2^A \mathrm{d}\varepsilon_1^A \\
&\approx 4h^2 \iint_{\varepsilon_2^A,\varepsilon_2^C} f_A\left(\varepsilon_2^A\right) f_C\left(\varepsilon_2^C\right) f_A\left(\varepsilon_2^A\cos\theta-\varepsilon_2^C\sin\theta-D_x(t)\right) f_C\left(\varepsilon_2^A\sin\theta+\varepsilon_2^C\cos\theta-D_y(t)\right) \mathrm{d}\varepsilon_2^A \mathrm{d}\varepsilon_2^C .
\end{aligned}
$$

9.4.7 This probability can also be approximated by $4h^2\, f_{x_t,y_t}((0,0))$ for very small values of *h*. By identification, it can be concluded that:

$$
f_{x_t,y_t}((0,0)) = \iint_{\varepsilon_2^A,\varepsilon_2^C} f_A\left(\varepsilon_2^A\right) f_C\left(\varepsilon_2^C\right) f_A\left(\varepsilon_2^A\cos\theta-\varepsilon_2^C\sin\theta-D_x(t)\right) f_C\left(\varepsilon_2^A\sin\theta+\varepsilon_2^C\cos\theta-D_y(t)\right) \mathrm{d}\varepsilon_2^A \mathrm{d}\varepsilon_2^C .
$$

9.4.8 Following Equation (9-12), the risk of collision for a pair of aircraft during the time interval $[t_0,t_1]$ is then given by:

$$
\begin{aligned}
&P = \pi\lambda_{xy}^2 P_z(S_z)\left(\frac{2}{\pi}\frac{v_{rel}}{\lambda_{xy}} + \frac{1}{2}\frac{\overline{|\dot{z}|}}{\lambda_z}\right)\int_{t_0}^{t_1} f_{x_t,y_t}((0,0))\,dt \text{ with} \\
&f_{x_t,y_t}(0) = \iint_{\varepsilon_2^A,\varepsilon_2^C} f_A\left(\varepsilon_2^A\right) f_C\left(\varepsilon_2^C\right) f_A\left(\varepsilon_2^A\cos\theta-\varepsilon_2^C\sin\theta-D_x(t)\right) f_C\left(\varepsilon_2^A\sin\theta+\varepsilon_2^C\cos\theta-D_y(t)\right) \mathrm{d}\varepsilon_2^A \mathrm{d}\varepsilon_2^C .
\end{aligned}
\tag{9-17}
$$

Chapter 10

REFERENCES

1. Aldous, D., *Probability Approximations via the Poisson Clumping Heuristic*, Volume 77 of Applied Mathematical Sciences, Springer Verlag, 1989.

2. Anderson, D., *A General Distance-Based Collision Risk Model Based on Reliability Theory*, SASP-WG/WHL/4-WP/9.

3. Bakker, G. J. and H. Blom, *Air Traffic Collision Risk Modelling, Proceedings of the 32nd IEEE Conference on Decision and Control*, San Antonio, Texas, December 1993.

4. Billingsley, P., *Probability and Measure*, Wiley Series in Probability and Mathematical Statistics, Third Edition, 1995.

5. Dacre, M., *Estimating Collision Risk for UK RVSM*, SASP-WG/WHL/1-WP/24.

6. Embrechts, P., C. Klüppelberg, and T. Mikosch, *Modelling Extremal Events for Insurance and Finance*, Springer, 1997.

7. Flax, B., *Navigational Requirements for the Implementation of 50-NM Route Spacing in Oceanic Airspace*, RGCSP-WG/A/17-WP/4.

8. ICAO, *Manual on Airspace Planning Methodology for the Determination of Separation Minima* (Doc 9689), First Edition, 1988.

9. ICAO, *Manual on Implementation of a 1 000 ft Vertical Separation Between FL 290 and FL 410 Inclusive* (Doc 9574), Second Edition, 2002.

10. Leadbetter, M.R., G. Lindgren, and H. Rootzen, *Extremes and Related Properties of Random Sequences of Processes*, Springer, April 1983.

11. *North Atlantic MNPS Risk Quick Reference Guide*, NAT SPG, June 2006.

12. Papoulis, A., *Probability, Random Variables and Stochastic Processes*, McGraw-Hill.

13. Reich, P.G., *Analysis of Long Range Air Traffic Systems-Separation Standards I to III*, Journal of Navigation, 1966.

— END —

ISBN 978-92-9231-428-6